An Integrated Robotic and Virtual Mirror Therapy System for Stroke Rehabilitation

A thesis presented in partial fulfilment of the requirements for the degree of

Doctor of Philosophy

In

Engineering

at Massey University, Albany

New Zealand

Iain Emerson

2014

Abstract

Stroke affects approximately 2% of the population, and with advances in modern technology, more patients are surviving the event and requiring rehabilitation, placing further demand on already stretched medical systems. Because of this, an emergent area of research has arisen, investigating the use of robotics as a means to aid in the rehabilitation of patients affected by stroke. Projects such as the MIT Manus have provided evidence of the efficacy of robotic rehabilitation for stroke patients, but further research is required to provide ongoing improvements to this approach.

Further to this, mirror therapy, a treatment initially found to be useful in the treatment of phantom pain syndrome in amputees, has also shown promise in the rehabilitation of stroke, though further research into the mechanisms behind mirror therapy need further investigation.

A novel prototype robotic rehabilitation system was developed to investigate the integration of these two emergent approaches to stroke rehabilitation as a more comprehensive approach to stroke rehabilitation. This system was developed around a small industrial robot, utilising motion capture and force feedback for control of the robot with a virtual mirror therapy system to provide visual stimulation for the patient.

The operation of the prototype was verified, however further development is required to produce a system suitable for patient trials. Areas that require further investigation include the virtual mirror therapy system, and an improved approach to achieving real time operation of the system.

Acknowledgement

I'd like to thank my primary supervisor, Professor Peter Xu, for his support, advice and guidance through the PhD process. I would also like to state my appreciation to Professor Xu for giving me the opportunity to enter the PhD program.

I'd also like to thank my secondary supervisors, Professor Subhas Mukhopadhyay & Professor Jen-Yuan (James) Chang, for their advice and guidance through the process of the PhD program.

I'd like to state my appreciation for the financial support for this research provided under a grant provided by the Ministry of Science and Innovation (MSI) (formerly Foundation for Research, Science and Technology) under contract MAUX0809 "Novel Enabling Technologies for Wearable Assistive Devices and Humanoid Machines".

Finally, I'd like to acknowledge the support of my family throughout my studies. My parents, Alastair and Judy, who have encouraged me to achieve my goals, my partner, Charlotte, for her support, encouragement to keep focused, and her patience with the time required in my dedication to my studies. I'd also like to state my appreciation to Azaria, Kaytlyn and Keagan for their patience, and understanding when they had to miss out due to my study commitments.

Related Publications

I. Emerson, W.L. Xu, S.C. Mukhopadhyay, J.Y. Chang, O. Diegel, “Robotic Rehabilitation System for Stroke in Combination with Mirror Therapy: A Research Proposal” In 25th International Conference of Cad/Cam, Robotics & Factories of the Future, Conference Proceedings, 2010

Contents

List of Figures

List of Tables

List of Code Snippets

1 Introduction

1.1 Background

The field of robotic assistive devices is currently a very active field of research. It includes projects in the areas of robotic exoskeletons, rehabilitation robotics, and virtual reality.

Robotic therapy is proving to be a useful tool in the treatment of hemiparesis due to stroke. Although there are many other noteworthy robotic rehabilitation projects, for both upper and lower limb rehabilitation, that have been developed since the introduction of this rehabilitation approach, the MIT Manus and MIME had the highest relevance to the development of this research. It was intended to combine aspects of both of these robotic rehabilitation approaches and integrate them with a virtual mirror visual feedback system.

The development of this system was intended to investigate the hypothesis that combining robotic rehabilitation with mirror therapy would improve the outcome for the patient. It was proposed that the mirror therapy component will enhance the motor function improvements already being achieved by robotic therapy, while the lack of effect on spasticity observed in mirror therapy trials will be addressed by the robotic therapy component.

Stroke patients were selected because there was already an emergent body of work in this area using either robotic assisted therapy or mirror therapy, giving a good basis for comparisons with the combined approach. Most of this work has been focused on upper limb hemiparetic patients, so it further follows that an investigation in that area would be more readily able to be placed in context against other research findings.

The motivation to advance research into the effectiveness of robotic assisted therapy in this area came from the patient who was reported to have stated that having restored mobility is great, but what they really wanted was to be able to feed themselves.

1.2 **Research Question**

"Is it feasible to develop a robotic/mirror therapy hybrid system for future use in the investigation as to whether using mirror therapy as an adjunct to robotic assisted therapy will improve the quality of rehabilitation for patients with hemiparetic upper limbs due to stroke?"

To achieve the research aim, a prototype system was developed that would utilise the bilateral movement capabilities demonstrated by the MIME system design, while integrating this with the video game interface demonstrated in the MIT Manus. Figure 1.1 - System Overview shows the conceptual overview of the system developed.

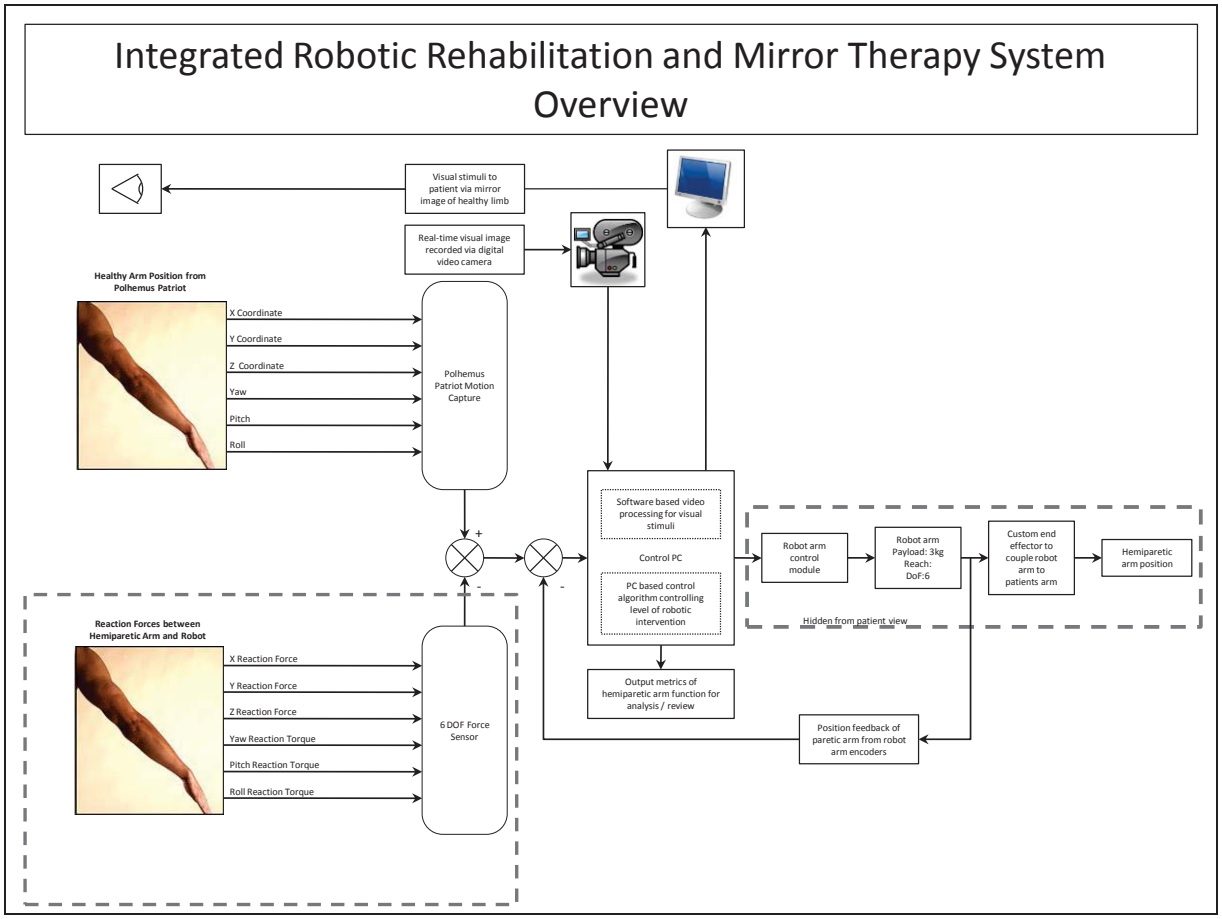

Figure 1.1 - System Overview

1.3 **Aim**

The aim of this research was the development of a robotic rehabilitation system combined with a virtual mirror therapy system, as a means for further research into the effects of combining these two emergent rehabilitation approaches on the success of rehabilitating patients affected by stroke.

1.4 **Major Objectives**

This was a multi-faceted project, requiring aspects of robotics, mechanical design and computer science to successfully develop the rehabilitation system. Considering the different aspects required for the development of the system, it was necessary to set a

number of objectives to be completed individually to develop the complete system as discussed below.

1.4.1 **Robot**

A suitable robotic arm was required to achieve the rehabilitation exercises required of the system. Once selected, it was crucial to develop a suitable control system for the robot to ensure the safe operation of the system. This involved the development and verification of the closed form solution of the robot for use in the system control algorithms. The robot control also included integrated solutions for singularity conditions, and determining whether or not the robot targets required for the rehabilitation exercises will be within the robot's working envelope.

1.4.2 **Motion Capture**

As the system control was dependent upon the motion of the patient's healthy arm, to perform the mirror image motion of the devised rehabilitation approach, it was necessary to develop a system for capturing the motion of the healthy arm for use as the main control for the robot.

Due to the complexity of the overall system, the development of the motion capture system involved the selection of a suitable commercially available motion capture device, and developing the software to capture the data from the device and translate it into a suitable data form for use with the robot control. This also required verification of the operation of the completed motion capture system, with respect to the application requirements.

1.4.3 **Force Feedback System**

For the compliance of the system, the ability of the robot to follow the motion of the patient's hemiparetic arm when necessary, it was essential for force feedback to be integrated into the system. The force feedback element of the system was integrated as part of the robot-patient coupling, monitoring the forces and torques between the patient and robot end effector, effectively measuring the loadings being exerted on the patient's arm.

As with the motion capture system, due to the complexity of the final system, a commercial force sensor was selected in favour of developing custom force sensor for the application. Software was developed to read the force and torque loadings from the sensor for use both as the input for compliance control, and to monitor for force overload conditions as part of the safety systems of the final rehabilitation system.

1.4.4 **Robot-Patient Connection**

To connect the robot to the patients arm, it was necessary to develop a custom made, novel coupling system. As safety of the patient was an important factor in the development of the final system, it was considered that this coupling must be rigid so as to achieve the safe manipulation of the patient's hemiparetic arm during rehabilitation exercises, while being able to safely disconnect the patients arm from the robot in the case of force overload. It was also considered that this coupling should be re-useable without the need for replacing components, to simplify the use of the system in clinical situations. Due to the mode of operation of the system being in three dimensions, this coupling was designed to disconnect when loads were applied about any of the three main axes relative to the coupling, unlike common couplings that tend to be designed to operate as torque limiters about one axis.

1.4.5 **Visual Feedback**

As the intended purpose of the final system was a tool for investigating the effect of combining robotic therapy with mirror therapy, it was necessary to develop a means of providing visual feedback to the patient. The visual feedback system was developed in the form of a virtual mirror, displaying a mirror image of the patient for them to observe while performing the rehabilitation exercises.

1.4.6 **System Integration**

Once the individual components of the system had been developed and validated for fitness for purpose in the case of the system being developed, the final objective of the project was to integrate the separate components into a single system. This required the physical assembly of the mechanical components, and integration of the separate components' software into a single control system to take the inputs from the sensors, process this data and use it for control of the robot.

1.5 **Outline**

This thesis describes the process undertaken in the design, development and validation process of a novel robotic rehabilitation system, integrating a mirror therapy component for use as a research tool into the effects on patient recovery of combining the two approaches. Chapter 2 includes a literature review, exploring the fields of robotic rehabilitation, mirror therapy, and their prospective areas of application, while providing insight into the state of the art in robotic rehabilitation. Chapter 3 outlines the initial concept of the system, and discusses the equipment requirements for the main components required to develop the system. Chapter 4 introduces the approach taken to develop the mirror therapy visual stimulation for the patient. Chapter 5 discusses the equipment selection and validation

processes undertaken to obtain suitable equipment for the system, and prove the suitability of the equipment, as well as the design and validation of a novel re-useable break-away coupling system for connecting the robot to the patient safely. Chapter 6 discusses the implementation of the control systems in software, including issues encountered. Chapter 7 details trials of the system with able bodied individuals for system evaluation. The thesis is concluded in chapter 0 with conclusions and recommendations based on the findings throughout this research project.

1.6 **Contribution**

The main contribution produced by this project is a prototype mechatronic system for investigating the effects of mirror therapy and other visual stimuli on the outcomes of robotic therapy approaches. This is the first research investigation into the combination of robotic rehabilitation and mirror therapy.

The development of this project has also provided new knowledge into the use of industrial robots for this type of application, requiring real time response. This has also illustrated some of the potential flaws and given enlightenment into possible considerations that future research could be mindful of when planning to use machines designed and developed for industrial applications in this type of project.

A novel passive re-usable breakaway coupling system was developed for use in this project to provide an added safety feature to the system. The design concepts employed for the development of this coupling have also shown promise as a means for integrating passive compliance into couplings for this type of application in future developments.

2 Literature Review

The following literature review will introduce a myriad of possible applications for robotic assistive devices. Attempting to cover the relevant research projects in the field, the topics of powered exoskeletons, robotic rehabilitation and the use of virtual reality as applied to rehabilitation will be introduced. The concept of mirror therapy, an emergent simple passive therapy for phantom pain syndrome in stroke and amputees, will also be introduced including recent research utilising this approach for the rehabilitation of hemiparesis in stroke.

The following is a discussion of the potential areas of application for assistive robotic devices, and recent developments in this field of research.

2.1 Robotic Assistive Devices – Overview

The term "robotic assistive device" can be interpreted to encompass a wide range of devices, basically any automated device that is intended to assist humans in tasks, making the task easier, or even the impossible possible (such as lifting weights far beyond normal human capacity). For the sake of the current work, it is intended that the term "robotic assistive device" be limited to areas of rehabilitation and the augmentation of human ability. These devices are intended to operate in contact with the operator (i.e. will have some form of physical connection with the operator) and are designed to improve the ability of the user, by increasing strength or assisting the user with tasks that they are unable to achieve alone, for example, or to assist in physical rehabilitation of patients.

There are many groups around the world performing the research and development of these systems, ranging from exoskeleton devices for application to a single joint of the human body, to full body exoskeletons intended to improve strength and endurance of the

user and rehabilitation robotic devices intended to aid patients in their recovery from devastating ailments which cause major disability. In many of the rehabilitation projects, they overlap with the exoskeleton field, as the devices are developed as exoskeletons but with therapeutic intentions.

2.2 Potential Areas of Application

Robotic assistive devices are intended to be used to improve or amplify human function. There is a range of potential applications for robotic assistive devices, from exoskeletons designed to amplify the strength or abilities of the user, to rehabilitation robotics used for aiding patient recovery. This section will introduce some of these areas of application.

2.2.1 Stroke

Stroke is a major cause of disability in all world populations as a consequence of the damage inflicted on the neural pathways in the brain. Damage to the brain is caused by a sudden disruption of the blood flow in the brain which causes a permanent lesion. There are two forms of stroke: The most common is an ischemic stroke, which is the result of a blood clot forming in the brain, while haemorrhagic stroke is the result of a haemorrhage (or bleeding) in the brain.

The 2008 New Zealand Health survey reports that stroke affects 1.8% of the New Zealand population, which equates to approximately 57,700 adults [1].

In simple terms a stroke is caused by a lack of blood supply resulting in damage to or destruction of brain cells; the disruption of blood supply being caused by either a clot or a haemorrhage as described above. However, it is probably more useful to consider the underlying causes which predispose an individual to the possibility of stroke. The most

common of these, according to The Stroke Source Book are High Blood Pressure, Heart Disease, Smoking, Diabetes and High Cholesterol levels, all conditions for which some level of physical activity, as a source of or accompaniment to weight loss is indicated [2].

The symptoms of a stroke, as presented in the Stroke Sourcebook [2], are:

- Numbness or weakness of the face, arm or leg, usually on one side of the body,
- Abrupt confusion, accompanied by trouble speaking or understanding words
- Rapid onset visual problems affecting one or both eyes
- Sudden difficulty in walking, dizziness, loss of balance or coordination.
- Sudden severe headache for no obvious cause.

The current rehabilitation regimes for stroke survivors are exercise based, engaging patients in physiotherapy, speech therapy and occupational therapy interventions in an attempt to recover, or relearn, as much of their previous function as possible. In some cases patients make a full recovery. Henrik et al. comment that the majority of neurological and functional recovery from stroke occurs in the first 6 months, with the general impression of clinicians suggesting that most of the motor recovery occurs in the first 6 weeks [3]. To achieve the best possible results for each patient however, requires a large amount of mainly human resources which are unfortunately, not readily available due to the limited number of rehabilitation therapists. As a result, the exploring of alternative approaches to stroke therapy has become a very active field of research worldwide involving many different disciplines.

Many researches are trialling differing approaches to robotic assisted therapy in this field, with positive results. The present study intends to explore a novel approach in this field and is aimed to further explore potential additional applications that my result.

2.2.2 **Cerebral Palsy**

This is a disorder that affects an individual from infancy. It encompasses a wide range of physical difficulties due to damage to the brain [4]. This damage is considered to originate from a non-progressive lesion leading to variable degrees of deficits in muscle action coordination. These deficits prohibit the afflicted individual from maintaining normal movements [5].

Cerebral Palsy is generally considered not to be genetic, with a prevalence of 2.5 in every 1000 births [5]. This is a non-infectious disorder, resulting from injury to the brain during pregnancy, birth or infancy. This injury can have a myriad of causes, including the contraction of infections such as rubella during pregnancy, lack of oxygen to the baby during birth or infections, such as meningitis, during infancy [4, 5].

Cerebral palsy is considered to be divided into three different types: Spastic, Athetoid and Ataxic.

Spastic Cerebral palsy is the most common manifestation of the disorder. As with stroke, the lesion in the brain affects the neural pathways between the brain and muscles, causing antagonistic muscle groups to tighten making movement difficult or impossible [4]. Related difficulties include hemiplegia, diplegia and quadriplegia. Hemiplegia relates to either the left or right side of the body being affected by muscle spasticity, diplegia relates to the legs being affected by spasticity but with little or no affect on the arms, and quadriplegia relates to all limbs being affected.

Athetoid cerebral palsy is a syndrome in which the muscles change from a rigid state to a limp state causing uncontrollable movements. This can also affect the tongue and vocal cords, causing speech problems.

Ataxic cerebral palsy shows as affected balance and possibly shaky hand movements. Spatial awareness and speech may also be affected in individuals afflicted by this form of cerebral palsy [5].

Although there are three main types of cerebral palsy, diagnoses can often include a several of these. This case is termed “mixed” [4].

There are many treatments to help improve the symptoms of cerebral palsy, although at this stage it is an incurable condition. More conventional treatments include speech language therapy, physiotherapy, medication and surgery. Less conventional treatment modalities include Hippotherapy (horseback riding), hydrotherapy (performed in water), and alternative medicine [4, 6].

There would appear to be potential for some forms of Robotic Assisted Therapy in relation to this condition, as the symptoms of cerebral palsy is similar to that of stroke, namely hemiparesis, it is viable that rehabilitation as applied to stroke, could have a similar effect with cerebral palsy.

2.2.3 **Parkinson’s Disease**

Parkinson’s disease is considered to be a progressive, degenerative neurological disorder that currently has no cure, although treatment is available. This condition is a resultant of a lack of dopamine in the brain. It is a disorder of the basal ganglia [7] where a significant neuronal depletion has been observed in recent studies investigating the density of dopamine D2 receptors [8]. Parkinson’s disease has a relatively low prevalence

of less than 0.3% of the adult New Zealand population (aged 15 years and over) being diagnosed [1], while it is estimated that in the United Kingdom 2 people per 1000 are affected by this condition [9]. However, the rate of Parkinson's disease in the population increases with age [7-9].

The causes of Parkinson's disease remain yet unknown. Factors that have been proposed as possible causes include ageing, genetic factors and substances that are either endogenous or exogenous to the individual which are toxic to the dopaminergic cells [7]. Interestingly, the substance MPTP (which is related to MPPP, a synthetic drug similar to morphine and pethidine) is a neurotoxin that has been shown to selectively damage the dopaminergic neurons in the basal ganglia, giving rise to a Parkinsonian condition very similar to Parkinson's disease. This gives strength to the argument that exposure to a "yet to be discovered" endogenous or exogenous substance may be the cause [7].

Generally the first symptom of Parkinson's disease manifests as a resting tremor in the hand of the affected side of the body. This tremor will tend to reduce during activity, but some patients may also present with and action tremor. Patients may also have a tremor in the lower lip or chin, but are less likely to have a tremor in the leg.

Rigidity is another symptom of this condition, evident as a continuous resistance to passive motion of the limb. It is usually expressed by patients as a feeling of stiffness. Parkinson's patients also experience bradykinesia, a term that refers to the slowing of movement or the impairment of the ability to initiate movements, and akinesia which refers to the deficiency or lack of movement of the patient.

Later stages of the disorder will include postural instability. The patient will show difficulties moving from a seated to a standing position, and may start to spontaneously lose their balance.

Literature provides differing models for the progression of Parkinson's disease, Kernohan et al. [9] present a four stage model for the progression of the condition:

Diagnosis - Symptoms of Parkinson's disease can often take a long time to emerge, and therefore affecting the time frame for diagnosis of this condition. In early stages it can often be misdiagnosed as other neurodegenerative disorders.

Maintenance - The goal in this stage is to maintain the patient's standard of living to the best possible degree. This is achieved by managing symptoms and any possible complication with medication (this also requires a multidisciplinary approach to treatment).

Complex - At this stage the effectiveness of the medications start to reduce, with the patient experiencing an increase of disabilities and complications. Various members of the multidisciplinary team will increase their involvement, while the patient becomes more dependent on their carer. A specialist Parkinson's disease team may be advantageous to care at this stage, if available.

Advanced disease - This final stage of Parkinson's disease can be defined by dopaminergic therapy becoming unbearable, the patient is no longer fit for surgical procedures, and co-morbidity is becoming more apparent in presentation of the patient's condition. This stage averages approximately 2.2 years and by now the medical focus is on the patient's quality of life.

Whereas Starkstein & Merello [8] offer a modified 5 stage model of illness severity, originally devised by Hoehn & Yahr in 1967, as follows:

Stage 0	No signs of disease
Stage 1	Unilateral disease (only one side of the body)
Stage 1.5	Unilateral disease plus axial involvement (back, neck and head)
Stage 2	Bilateral disease, without impaired balance
Stage 2.5	Bilateral disease, with recovery on pull test (examiner stands behind the patient and pulls them backward, observing the patients balance recovery)
Stage 3	Mild to moderate bilateral disease; some postural instability; physically independent
Stage 4	Severe disability; still able to walk or stand unassisted
Stage 5	Wheelchair-bound or bedridden unless aided

As noted above, there is currently no cure for Parkinson's disease. The patient is likely to live with the ongoing degeneration for approximately 14 years [7]. The current practice in the treatment of Parkinson's disease is the utilisation of medication to control the symptoms, and maintain the best level of function and comfort for the patient. There could be a possible use of robotic assisted devices for these patients in assisting to maintain motor function and control for longer periods, or providing assistance when such functions have become extensively deteriorated. To this end, a recent study has been

undertaken to investigate the use of robotic rehabilitation with Parkinson's disease patients, which reported promising results [10].

A further advantage of using robotic devices is alluded to by Krebs et al in their discussion of the ability to gather precise quantitative data on the patients during treatment, and eliminating the necessarily subjective nature of relying on clinicians' judgements. Very precise measurement in several dimensions can be recorded during therapy, giving a more accurate picture of progress than is currently available [11].

2.2.4 **Osteoarthritis**

Of the different forms of arthritis, Osteoarthritis is the most prevalent. It tends to present in greater prevalence in populations with increased age. With current statistics showing an ageing population in many countries, it is likely that the reported cases of osteoarthritis will increase. This is a condition defined by the progressive degradation of articular cartilage (which cushions forces and acts as a wear resistant smooth surface to aid the motion of the joint) in the joints, appositional surfaces of the joint having new bone formation, and bone spurs (called osteophytes) forming at the joint margins [12]. As these conditions develop in the joint, they cause intense pain to the afflicted person.

Osteoarthritis does not manifest in a systemic manner, and usually effects only a few joints. Weight bearing joints such as the hip, knee or spine are the most common joints to be affected by the syndrome, although it can also occur in the smaller joints of the hands and feet.

Osteoarthritis has two types, primary and secondary. Primary osteoarthritis is the more common of the two. In this manifestation, there appears to be no obvious initiating reason for the onset of cartilage degeneration in the joints. Secondary osteoarthritis is

often observed in younger patients under the age of 50, with the degenerative onset linked to factors such as joint injury, chronic overuse, metabolic diseases, or increased mechanical joint stresses caused by obesity [12]. Desmeules et al. [13] report on studies that link the Body Mass Index (BMI) to detrimental effects of osteoarthritis in the knee joint, with weight loss programs improving patient outcomes for pain symptoms and rehabilitation. They suggest that weight loss therapy may be an important component for pre-rehabilitation programs.

The main symptom of osteoarthritis is joint pain in the affected joint. This pain becomes more intense during exercise, and eases when resting.

The symptoms of osteoporosis are managed by medication for pain relief, and physical therapy regimes aimed at strengthening the supporting muscles of the affected joint, but ultimately the condition may deteriorate to a level where surgery is required. Unfortunately waiting lists for surgery are up to 6 months long. Figures for 2008 report 6,993 hip and 5,595 knee replacements [14] There is a possibility that robotic assisted therapy could be useful in maintaining and enhancing pain free movement at all stages of this disease.

2.2.5 **Motor Neurone Disease**

This is a condition that affects the neurones of the brain and spinal cord destroying motor function. In this disease the upper and lower motor neurones experience progressive deterioration, causing the afflicted patient to slowly lose motor control [15]. Patients lose bodily functions including movement, speech, swallowing and breathing. The cause of this disease is at present unknown, and a cure is yet to be discovered. The average onset age of this disorder has been shown in population based studies to be approximately sixty five years, with an average duration of three years from clinical

diagnosis, although the timeframe can vary from only months after diagnosis to a mortality rate of 80% at five years' post diagnosis [15].

Approximately 200-250 New Zealanders suffer from this disease [16]

Muscle weakness is a symptom caused by degeneration of the lower motor neurons. These neurons are situated in the brain stem and spinal cord, making direct contact with the muscles by extending to the outer nerves. Other symptoms of lower motor neurone degeneration are muscle wasting and a twitching sensation observed as ripples under the skin, known as fasciculation. Symptoms of the degeneration of the upper motor neurones are spasticity of the muscles and exaggeration of deep tendon reflexes. The upper motor neurons are located within the motor cortex of the brain, extending down to activate the lower motor neurons. Patients may present with Degeneration of either the lower (this is called progressive muscular atrophy) or upper (this is called primary lateral sclerosis) motor neurons, or both. Progressive muscular atrophy and primary lateral sclerosis case progress more slowly, with a longer survival time, than cases presenting with degeneration of both sets of motor neurons.

Patients frequently defer medical attention with this disease because initial symptoms can be vague and intermittent. Because the initial symptoms are so vague, diagnosis can be complicated, with the patient being referred to many specialists such as ear, nose and throat, rheumatology or orthopaedics before finally seeing a neurology specialist [15].

As there is currently no cure for motor neuron disease, the current practice in treatment is to manage the symptoms, focusing on maintain quality of life to the best standard possible. Drug therapy is offered to most patients, but there is only one drug shown to have an effect on the condition. This drug is called Riluzole, which after being administered for 18 months has been shown to increasing survival by 3 months, but

evidence suggests that it may even have an effect of 4-19 months of extended life expectancy [15]. As with the other motor related conditions, the possibility of robotic assisted therapy having a therapeutic role should be explored.

2.2.6 **Multiple Sclerosis (MS)**

This is a continual demyelinating disease that disrupts the central nervous system through the brain and spinal cord [17]. A demyelinating disease is one in which the myelin sheath that surrounds the neurone axons is damaged, resulting in the axons no longer being able to transmit signals from the motor neurons in the brain to the muscles. Demyelinating diseases can be caused by infection, genetics or autoimmune response. Although the cause of multiple sclerosis is as yet unknown, Martin et al. [18] report that an autoimmune reaction attacking the myelin antigens is a contributing factor to the pathogenesis, or development, of the syndrome.

Prevalence of MS in New Zealand ranges from 50.8/100,000 people in Northland to 134.6/100,000 people in [19].

The symptoms of Multiple Sclerosis are generally not condition specific, creating some difficulty with early diagnosis. Symptoms may present over a broad range of categories, including bladder and bowel dysfunction, sexual dysfunction, fatigue, impaired cognitive function, impaired speech, difficulty in swallowing, visual disturbances, motor related symptoms including spasticity and weakness, impaired coordination and balance. The symptoms are frequently manifested as relapsing, particularly in early onset Multiple Sclerosis, before changing to a progressive degenerative pattern.

Since Multiple Sclerosis is a chronic, gradually degenerative disease with no known cure, the focus of treatment is on assisting with the maintenance as far as possible of quality of life, and the treatment of conditions arising from complications brought about by the main disease. There is thought to be an auto-immune dimension to the disease [18] resulting in the administering of immunosuppressant drugs. Richard Warner cites Burgess (2002) as proposing that death as a direct result of Multiple Sclerosis is extremely rare. This in turn leads to the proposal that Multiple Sclerosis is not itself a terminal condition, though death from complications arising is common. Physiotherapy is recommended as an important care intervention by Martin Hohfield and McFarland as well as the recommendation of the maintenance of regular daily activity. There is a likelihood that Robotic Assisted Therapy could be of significance in assisting in both these areas.

2.2.7 **Paralysed and Mobility Impaired Individuals**

The 2006 Disability Survey conducted by Statistics New Zealand found that twelve percent of adults aged 15 years and over had a physical disability (an estimated 383,500 adults). The term "Physical Disability" represented an agglomeration of those recorded as having either a mobility or agility disability, these terms being defined as follows:
Mobility – includes people who have difficulty with or cannot walk about 350 metres without resting; walk up or down a flight of stairs; carry an object as heavy as five kilograms for a 10 metre distance; move from room to room; or stand for periods longer than 20 minutes.

Agility – includes people who have difficulty with or cannot bend over to pick something up off the floor; dress or undress themselves; cut their own toe-nails; grasp or

handle small objects like scissors; reach in any direction; cut their own food; or get themselves in or out of bed.

Whilst these figures represent many more than those with a loss or gross inhibition of motor function, they do indicate the probability of a significant section of the population being able to benefit from the development of either Robotic Assisted Therapy devices, or Exoskeleton devices as aids to mobility.

Current rehabilitation of spinal accident victims involves extensive and intensive use of physiotherapy, delivered through specialist inpatient Health Units with extensive outpatient after care. Rehabilitation for other paralysis conditions is similar, and like stroke rehabilitation, requires extensive use of human resources which may not be readily available. It may be assumed that an exploration of Robotic Assisted Therapy in relation to stroke rehabilitation could have some relevance to this area of rehabilitation as well.

2.2.8 **Elderly, Weak and Infirm**

Figures taken from the Statistics New Zealand website [20] gives an estimated total of 535,390 people who may be assumed to have some degree of mobility and/or agility ability decreased for age related reasons, with the severity and need for rehabilitative therapy increasing with age. This is possibly another area where Robotic Assisted Therapy of the sort envisaged in this study could be beneficial to improve the quality of life of the patients through maintaining and enhancing their ability to remain independent.

2.2.9 **Able Bodied Individuals**

There are many projects currently being developed to aid able bodied people. These are generally exoskeleton type devices designed to amplify natural human abilities such as strength and endurance. This area of application tends to be of most interest military

use, aiding soldiers with heavy payloads, but there is also suggestion that these devices would be beneficial for search and rescue applications. Another use for exoskeletons is in hospitals to aid nursing staff in lifting patients.

2.2.10 **Summary**

It can be seen from this review that there are many feasible applications for robotic assistive devices. The development of well-designed equipment to aid in the rehabilitation of patients for syndromes such as stroke or cerebral palsy, or as assistive devices to patients, or their carer's, for syndromes such as Parkinson's disease, motor neurone disease, or multiple sclerosis have the potential to make vast improvements on the quality of life for the people who have to live with these debilitating afflictions. Alternatively, research in this area could focus on mobility aids for patients suffering from osteoarthritis and the elderly, weak or infirm. Robotic exoskeleton devices would be well suited to this purpose, as well as for able bodied people, to amplify human ability, improving efficiency in applications where heavy lifting for long durations are required, such as soldiers or search and rescue teams carrying heavy equipment in the field.

Of the illnesses presented above, the most active field of research is that of rehabilitation for stroke patients. One reason for this is the high prevalence of this syndrome in comparison to the others mentioned. Another is the proven success of rehabilitation for stroke through the fields of physiotherapy and occupational therapy, although there is potential room for improvement on these conventional approaches. Robotic rehabilitation devices are able to build on the knowledge already developed through manual therapy for stroke, automating these techniques and providing aid to an already stretched resource by potentially allowing a single therapist to treat multiple patients at a time (provided the equipment is made available).

2.3 **Current Research Areas**

2.3.1 **Exoskeletons**

Research and development in the area of exoskeletons, either partial or full body, is well represented in literature. Early development of powered human exoskeletons started in the late 1960s. These early projects were undertaken by groups in the USA, Generally intended for able bodied users to augment their abilities in applications such as the military, while groups from the former Yugoslavia developed devices for the physically challenged [21]. The general focus of the research and development of exoskeletons has had minimal change since the first developments with the prominent recent projects in this field still being developed for amplifying the abilities of able bodied persons, substantially increasing the carrying capacity and range of the user. While many of these exoskeletons are intended for use by military personnel and search and rescue teams [22, 23], others are being developed to help the elderly and infirm, or the nursing staff who care for these people [24].

This section will discuss the exoskeleton projects presented in literature that are targeted for amplifying human ability, while exoskeleton type devices intended for rehabilitation of patients, who have lost some of their function due to sickness or injury, will be discussed in the following robotic rehabilitation section.

Figure 2.1 - The HAL-5 (Hybrid Assistive Limb) [25]

HAL (Hybrid Assistive Limb) is an exoskeleton device developed by a team at the University of Tsukuba in Japan and is the first to be released commercially by Cyberdyne Inc. [24-26]. An initial development model, the HAL 3 was designed as a lower body exoskeleton, with its successor, the HAL 5 (which is the first commercialised design) including upper body assistance in its development, is a full body exoskeleton. The HAL suit uses the myoelectric signals from the operator's muscles to anticipate the intentions of the user, and produce appropriate torque at the joints to achieve this motion [27]. The intended purpose of the HAL suit is to aid the elderly, weak and disabled by increasing their mobility when they are too weak to support their own weight, it is also proposed that this exoskeleton will be useful for carers of these people, such as nurses.

This exoskeleton has an estimated battery life of 5 hours between charges and can increase the strength of the user by a magnitude of between 2 and 10 times their own strength [25]. By comparison, the HAL suit has the most aesthetically refined designed of any of the current exoskeletons in development.

Figure 2.2 - The Ratheon Sarcos XOS exoskeleton [28]

The XOS, developed by Ratheon Sarcos with funding from DARPA (Defence Advanced Research Projects Agency) [24, 28], future developments this exoskeleton are intended for use by the American defence force in the future. The current model of this project is electrically powered, with the exoskeleton currently tethered to its power supply via a cable, which can be seen in Figure 2.2.

Another full body exoskeleton is the Kanagawa Power Suit developed at the Kanagawa Institute of Technology in Japan [29]. The suit is pneumatically powered, with the pneumatic supply provided by battery operated air compressors mounted within the suit. It is intended for use by nurses caring for patients [30]. This suit is able to assist nurses to lift patients weighing up to 85kg with ease.

Figure 2.3 - The HULC exoskeleton - a development from the BLEEX exoskeleton [24]

Initially developed as a project at Berkeley University, which later commercialised through Berkeley Bionics, the BLEEX (Berkeley Lower Extremity Exoskeleton) is an exoskeleton for the lower limbs designed to augment human abilities, namely strength and endurance [23, 31]. It was developed under DARPA funding, and became the first load carrying lower extremity exoskeleton in the world [24]. Berkeley Bionics went on to develop this technology further in the HULC (Human Universal Load Carrier), the ExoHiker and ExoClimber) [24].

MIT have developed an exoskeleton based assistive device for carrying heavy loads over uneven terrain. This project is also DARPA funded [24], and the exoskeleton is similar in appearance to the BLEEX exoskeleton. As with the BLEEX, this exoskeleton was developed for military and emergency services use. Whilst it improves carrying capacity by 80%, there is some extra energy required on the part of the pilot due to alteration in gait because of the suit. This increases oxygen usage by 10% as compared to normal walking [22, 32].

The RoboKnee is a developmental exoskeleton device worn at the knee, and designed to enhance strength and endurance, particularly when climbing stairs or lifting heavy

loads. The device uses an innovative elastic actuator to add compliance to the system and achieve a low impedance actuator. This is a relatively light device that enhances performance while not hindering natural walking gait on a steady surface or ascending stairs. However the device causes the user to employ unnatural muscle groups when descending stairs, therefore hindering natural motion. The current design is cumbersome to put on and take off, requiring up to ten minutes, and prevents the user from sitting due to the location of the actuator [33].

The projects discussed above are representative of the current developments in exoskeleton technologies for non-therapeutic applications.

2.3.2 **Robotic Rehabilitation**

Research into the use of robots for therapeutic rehabilitation, especially in regard to the recovery of motor function after stroke, began in the early 1990's [34, 35]. The introduction of robotic therapy is intended to improve the therapeutic benefit for patients while reducing burden on over-stretched health resources by allowing therapists to treat more than one patient at a time.

Added benefits of robots, as used in therapeutic applications, are the continuity and consistency of treatment. Where a human therapist may become physically tired during a therapy session of continuous manipulation of the patients limb, robots are designed to perform for thousands of hours of laborious repetitive tasks with a high degree of accuracy, making them perfectly suited to provide consistent manipulation forces and trajectories throughout an entire therapy session. Objective, quantifiable and accurate evaluation tools are essential for optimised result, but difficult to obtain through conventional therapy [36]. Assuming a well-designed system, robotic therapy also provides the opportunity to collect quantitative data in regards to the patient's current

abilities during a therapy session and their progress throughout the course of rehabilitation therapy. This accurate objective data acquisition can then be used to provide an adaptive therapy regime ensuring that the patient is continuously encouraged to improve their abilities as they progress.

Pioneering projects in this field include the MIT Manus (developed by the Mechanical Engineering Department, MIT and commercialised as the InMotion2) [37], and the Mirror Image Motion Enabler (MIME) developed by the Rehabilitation Research Development Centre of Excellence on mobility (RRDC) at Stanford University [34].

2.3.3 **Lower Limb Systems**

Robotic rehabilitation as applied to the lower limb is mostly concerned with gait training and analysis. The focus on gait training is intended to aid in the recovery of mobility for patients afflicted with syndromes like stroke, cerebral palsy or spinal injuries [38].

Arguably, the most successful device in this field is the Lokomat, initially developed for gait training at the University Hospital, Balgrist, Zurich [39]. This is a treadmill based exoskeleton device for the lower limbs in which the patient's body weight is supported by the machine. The exoskeleton moves the legs of the patient as they walk on the treadmill, helping to rebuild muscle strength and regain motor control. The Lokomat has also proven useful in analysing gait and patient participation during rehabilitation exercises [38, 40].

Three devices for gait training have been developed at the University of Delaware, Newark. These are also exoskeleton devices designed for therapeutic means. Firstly the GBO (Gravity Balanced un-motorised Orthosis) was developed as to act on the hip and

knee joints during the swing of the limb. The device changes the level of gravity acting on these joints [41, 42]. The second of these exoskeleton devices is the ALEX (Active Leg Exoskeleton). This is a motorised exoskeleton device intended to provide support and maximise human-motor learning during gait. This is achieved in a similar manner to the MIT Manus, by guiding the foot if it is not successfully following the required trajectories [43]. Lastly, SUE (Swing-assist Un-motorised Exoskeleton) is a bilateral device that is designed to drive the legs while walking on a treadmill [41]

The LOPES is another treadmill based gait trainer [44]. This system differs from the Lokomat though as it is not a passive gait trainer. The LOPES is designed to only aid the patient during certain aspects of the gait cycle that they are known to have difficulty with (if the patient has trouble lifting the foot, the machine will support the patients gait only during the lift phase).Based on the literature available, it is understood that the LOPES still requires clinical trials to prove the efficacy of this approach.

Rehabilitation of the ankle is usually achieved using parallel robots. This robot form is well suited to ankle rehabilitation as the range of motion closely resembles that of an ankle joint if it were placed on the planar surface of the robot. One such example of this type of robot is the Reutgers Ankle robot. This is a Stewart platform robot with six degrees of freedom [45]. This system has been trialled in a case study with a patient 9 months post stroke. Preliminary results were promising [46]. Similar parallel robot devices have also been developed in China and Korea [47, 48]

2.3.4 **Upper Limb Systems**

The MIT Manus is a purpose built device developed for robotic therapy of the upper limb in stroke patients. The approach used in this system is that of unimanual activity, where by the patient uses their hemi-paretic arm to move the end effector of the robot,

much like a computer joystick, through a series of tasks displayed on the screen of the device, giving an interactive interface similar to a video game. If the patient is unable to complete the required movement the robot guides them by moving the end effector to the correct position. This system has had extensive clinical trials for more than 4 years to prove its efficacy [49], with the majority of participants achieving significant improvements in rehabilitation as compared with the control groups [50-52]. Another group in Italy has backed up these results with recent trials using the commercialised version of the MIT Manus, the InMotion2.0 [53, 54].

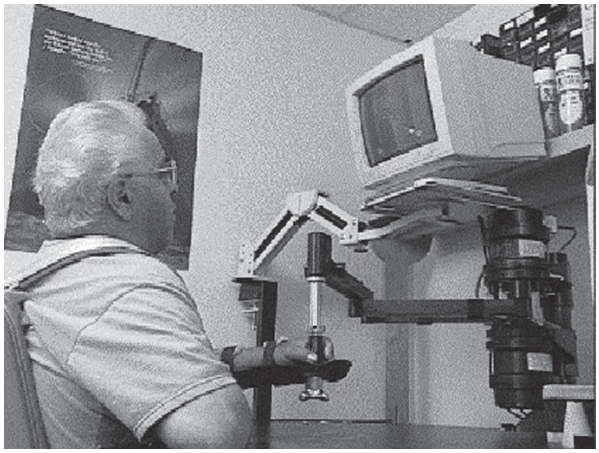

Figure 2.4 - A stroke patient in a therapy session using the MIT Manus [11]

The MIT Manus has been a very successful system for proving the efficacy of robotic rehabilitation; however, being confined to a 2 dimensional coordinate system for patient exercise is a major limitation with regards to the adaptability of the system for further investigating the effects of different exercises on the rehabilitation of the system. Also, as every person is individual, it is fair to assume that each person may have their own idiosyncrasies with regards to the path they choose to complete the set tasks of the Manus, and having the machine drive them in set trajectories may impact on the result. A more dynamic approach to the guidance of the hemiparetic hand that models itself on the patients on movements may be beneficial.

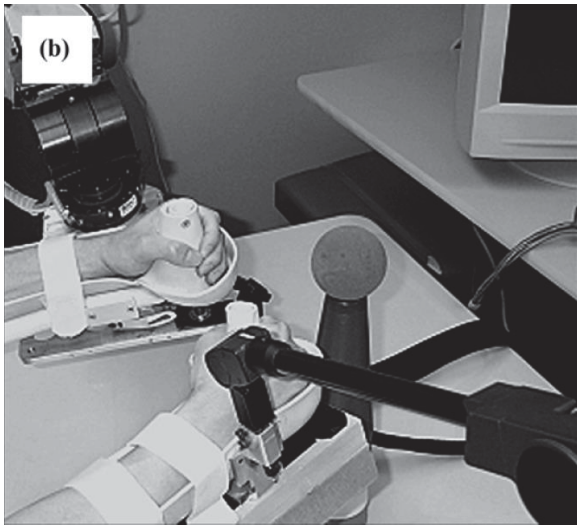

Figure 2.5 - A patient in therapy with the MIME system performing bilateral exercise [55]

The MIME project utilised an industrial robot to manipulate the patient's hemiparetic arm. First generations of the system used a Puma 260 robot, which was replaced with a more powerful Puma 560 robot in later developments of the system. The MIME has the ability to function in both unimanual and bimanual fashion with four modes of operation – passive, active assisted, active constrained and bilateral [56].

When in passive mode, the patient's affected limb is relaxed (passive) while the robot moves it in predetermined paths towards a target. For active assisted mode the patient initiates the motion and works with the robot to reach the target. Active constrained mode provides a "viscous" resistance to the motion encouraging the patient to exert maximal force to reach the target. In bilateral mode, the patient attempts to move both limbs in a mirrored bimanual fashion. The robot is controlled by the trajectories of the healthy arm, while guiding the hemiparetic arm in a mirrored motion to these trajectories. Of the four modes that the MIME operates in, the bilateral mode is of most interest to this project.

This system has also undergone clinical trials with stroke patients to prove its efficacy, and investigate the best therapy approach utilising the different operating modes

of the system. The mime trials, as with the MIT Manus trials, showed a significant improvement with the robotic therapy groups, as compared with the control group, which was exposed to a similar intensity regime of conventional therapy [55, 57] with ongoing investigations into acute therapy and the effect of the dose rate of the therapy [58].

An interesting point though, is that there did not seem to be any advantage to the bilateral mode of robotic therapy unless it was coupled with the unilateral mode during the same treatment session (combined therapy). However further studies into the effects of bilateral movement on stroke rehabilitation utilising either robot assisted and manual therapy have been completed by other groups, with results suggesting a favourable outcome for the use of bilateral exercise over unilateral exercise [59-65].

The MIME project overcomes the drawback of the Manus system in which the patient's exercises are constrained to 2 dimensions, by allowing 3 dimensional movements. However, the lack of visual stimuli for the patient is a disadvantage to this system. The fact that a reasonable number of alternative research groups had success with bilateral movement therapy suggests a deficiency in the design of the MIME system or trials. The unfavourable results for bilateral movement in the MIME project could result from a lack of focus from the patient as they try to focus on moving both arms simultaneously. Potentially this focus could be restored by adding visual stimuli to the system, focusing the concentration of the patient on the affected arm.

The previous two projects described are of great interest to this research proposal, and therefore have been discussed in length. The following are brief descriptions of some of the other works in the field, that, although of lesser importance to this research, are still of significance to the field of rehabilitation robotics.

Assisted Rehabilitation and Measurement (ARM) Guide was developed to measure and apply assistive or resistive forces to linear arm reaching movements within a large working envelope. The unit has a linear track with a hand piece attached. It is actuated by a DC servomotor. This device is counterbalanced so as to remove gravitational load from the arm. Yaw and pitch angles can be adjusted to give a range of different reaching directions [66].

In the case of the Arm Trainer the subjects sat at a table with their elbows bent 90° and put their forearms in the mid-position between pronation and supination into an arm trough. Each hand grasped a handle and was held in place by a 6cm strap with Velcro Two handle sets were available for horizontal axis for the elbow and vertical axis for the wrist movement. Online regulation of position and strength was accomplished through a position control and the retractive forces of the drive. Data collection and drive control were accomplished by a computer, with a display showing the number of performed cycles. A digital control unit helped to select the operational mode, side of hemiparesis, range, speed, and the resistance of movements. One repetition of each movement pattern included both movement directions [65].

The GENTLE/s entails the subject sitting at a workstation with a table and a computer monitor. The arm is supported in a de-weighting system which counterbalances the effects of gravity. The subject interfaces with the robot through a mechanism comprising a gimbal and a wrist orthosis incorporating a magnetic safety device which is activated should any unwanted forces be generated.

GENTLE/s software allows for individually tailored exercises, with the appropriate level of assistance or resistance being provided through three exercise modes, passive, active-assisted and active.

In all of the modes outlined, the haptic interface provides feedback on the direction of movement required. Visual feedback of the movement is presented in the virtual environments on screen. The participant in this study used the passive mode for the initial 10% of the time to introduce the concept, and the active-assisted mode thereafter [67].

NeReBot (NEuroREhabilitation roBOT) is a three degree of freedom wire based robotic system designed to provide rehabilitation for sub-acute stroke patients. This system is relatively light weight and designed to be easily transportable. The NeReBot can be used in hospital settings when the patient is unable leave their bed as the system is designed to accommodate patients that are seated or lying in bed [68].

REHAROB is a robotic rehabilitation system using 2 industrial robots that work simultaneously together. This system is intended not only to aid the patient's rehabilitation, but also to help the physiotherapist by performing the repetitive slow movements required to exercise the patient's hemiparetic limb. The system was designed using an IRB 140 robot to manipulate the upper arm, and an IRB1400H robot manipulates the patient's lower arm [69].

ARMin is a rehabilitation robot designed for the training of activities of daily life in a clinical setting. This is an exoskeleton type device with six degrees of freedom. Position and force sensors are used for feedback to the control system which utilises impedance and admittance based patient-cooperative control strategies [70].

The ACRE system comprises of a robotic arm support mounted on a wheel chair. The arm support mechanism is gravity compensated. Adjustment can be made to the robotic arm device to alter the strength, speed and accuracy of the robotic assistance provided to the patient. The robot arms position is recorded in real time by means of angle encoders.

The position is represented on a computer screen as a ball in a three dimensional space. Data records are kept of the positions, speeds and angles of the arm [71].

All of the investigations into robotic rehabilitation noted above have shown success in achieving some degree of improvement in patient's rehabilitation over that of conventional treatment alone, further building on the evidence of the validity of this approach.

Avraam et al. have developed a device based on a rotational MR-fluid brake actuator that has an exercise regime programmed into an embedded microcontroller by a physiotherapist using a laptop computer, and a PDA is supplied to the patient allowing them to use the device at home. This provides the patient with a visual feedback of the exercises and stores the measured results to then be transferred to the physiotherapist's laptop for analysis. This is currently in a prototype stage requiring clinical trials to prove its efficacy [72].

Fu et al. are developing an exoskeleton device for hand rehabilitation. This device is intended to be portable, and is also intended to study the true efficacy of continuous passive motion as a means of hand rehabilitation. From the literature available, it is unclear if this device has been completed [73].

A team at the University of Washington are developing a 7 degree of freedom exoskeleton arm. This device is intended to aid people in activities of daily life, or as a therapeutic device for patients suffering from conditions such as stoke, although it may also find applications for use by healthy individuals. The design of this exoskeleton arm is based on in-depth studies of the kinematics of the human arm [74, 75]. Real-time myoprocessor control has been employed as the control model for the system utilising the

electromyographic (EMG) signals from the muscles of the user [76], in a similar manner to the HAL exoskeleton.

The uBot series of robots, resulting in the uBot-4 [77] and finally the uBot-5 which is reported to be a small light-weight bi-manual robot developed to be mobile for easy relocation by the Laboratory for Perceptual Robotics at UMass Amherst. This is an interesting project, as it moves away from the more traditional assist and support approach to robotic rehabilitation systems. This system sits opposite the patient, and does not remain in contact with them as other systems do. The robot has 2 end effectors that are used to provide targets for the patient to reach for without assistance. The exercises start with less challenging reaching exercises, with the level of difficulty being increased as the patient becomes more able. This system has been used in 2 single subject case studies, with promising result, both observable, and when measured with standardized testing [78, 79].

The EXO-UL7 exoskeleton type upper limb robotic rehabilitation system, initially named CADEN-7 in earlier literature [80, 81], is a robotic rehabilitation system capable of providing unilateral and mirrored bilateral exercises. The system consists of 2 exoskeleton arms. This system does not fully assist the patient during exercise, being described as partial assistance, but gives the patient's arm a guiding push, without forcing the arm into precise positions. In bilateral operation, the exoskeleton arms have a master/slave control approach, utilising PID control. This system also employs visual stimulation component similar to the MIT Manus, utilising video games to engage the patient and drive the exercises. A recent trial with this system has found significant improvement in the in the motion of the shoulder joint, but not in the elbow or wrist [82].

Wear-A-Ban is a project in its infancy, with the current literature focused on the development of a wearable wireless sensor for use as control of an industrial robot [83]. The literature introducing this project alludes to a system used for assisted mirror therapy, however, there is no mention of visual feedback at this stage, and it is assumed that by mirror therapy, the author of the literature is referring to mirror image therapy utilised in bilateral robotic rehabilitation projects (such as the MIME).

Another interesting robotic rehabilitation system in its infancy is a project reported in literature by Shahbazi et al. [84]. This system uses a single slave robot to manipulate the patient's hemiparetic arm, but has 2 master controls with weighted authority. One of the controls is used by the patient, while the second is used by the therapist to supervise and guide the rehabilitation regime. This arrangement allows the patient to override the therapists control if they feel discomfort.

2.3.5 **Mirror Therapy**

Initially proposed as a potential treatment for phantom pain in amputees and stroke patients, and hemiparesis in stroke patients, mirror visual feedback was introduced in 1992 [85].

Mirror therapy is usually administered using a "mirror box". This piece of apparatus consisting of a box with the front and top removed, and a mirror placed in the central vertical plane of the box which is intended to be in line with the patient's sagittal plane. Both of the patient's limbs are placed into the box on either side of the mirror separator (the healthy limb being on the reflective side of the mirror). The patient then moves both limbs in a symmetrical bilateral manner while observing the reflection of the healthy limb, which appears to be superimposed over the hemiparetic or amputated limb.

Observation of the healthy limb's reflection gives the illusion that the affected limb is functioning as instructed.

Figure 2.6 - An example of the mirror box [86]

Studies have been conducted into the use of mirror therapy for the treatment of hemiparesis in both the upper and lower limbs of stroke patients with varying degrees of success [87-90] while two other studies [91, 92] reported significant improvements in limb function, but that the therapy showed no effect on spasticity (or muscle tone) as compared with their control groups.

Ramachandran and Altschuler [85] suggest that this variability in findings shows the effectiveness of mirror therapy may be dependent on factors such as the location of the lesion and the duration of paralysis post stroke. They continue to say that these factors require further investigation but suggest that there is no reason why mirror therapy would not be a useful adjunct to other approaches in the treatment of stroke, due to its procedural simplicity.

Being such a simple passive procedure, mirror therapy lends itself to being easily developed in a virtual environment. Projects have already been undertaken to produce virtual mirror environments with the aim being to make the exercise more engaging, thereby increasing patient participation [93-95]. To this end, virtual mirror therapy is

perfectly suited to be combined with bilateral robotic therapy to increase patient participation, giving them visual stimulus to increase motivation.

The underlying mechanism for the success of mirror therapy is still unclear although it is suggested that the visual feedback may excite mirror neurons in the brain [85]. To investigate mirror neuron activity due to mirror reflection, Matthys et al. [96] conducted a study to evaluate brain activity during observation of a mirror reflection exercise (tapping their right hand). The participants completed the exercise twice – once without mirror visual feedback, and once with mirror visual feedback. It should be noted that the participants were not asked to move their left hands during the exercise, whereas in mirror therapy the subject is instructed to try and move their affected limb. Brain activity was observed during each exercise by means of an fMRI scanner. The scans did show differences in brain activity between the mirror and no-mirror exercises, but it was inconclusive as to how much involvement the mirror neurons had. Further research in this area is suggested.

2.3.6 **Virtual Rehabilitation Systems**

Information Technology has enabled therapy to be conducted in a "virtual" world through the use of telecommunication and the Internet as vehicles for the delivery of exercise routines, and feedback and measurement of progress to remotely situated therapists. Yang, Wu and Zhao describe the management of hand rehabilitation utilising telecommunications and haptic user interfaces accessible to both patient and therapist simultaneously [97].

Other authors describe the use of virtual environments in stroke rehabilitation [98-100], the treatment of chronic pain and disability [101] and cortical reorganisation for a child with hemiparetic cerebral palsy [102]

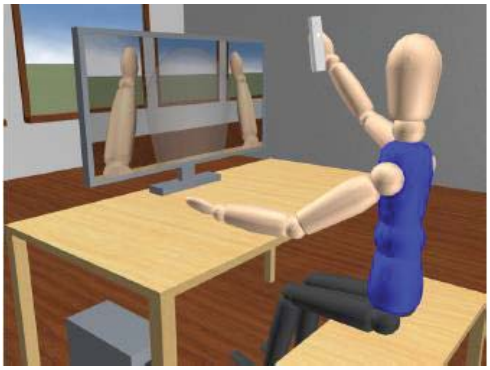

Figure 2.7 - The virtual mirror therapy system utilising the Wiimote, proposed by Palmke et al. [95]

Palmke et al describe the development of a virtual mirror therapy system utilising the Nintendo Wiimote [95]. This exemplifies utilising existing technology developed for gaming as an adjunct to virtual therapy, exploiting the Nintendo products Blue Tooth capabilities to enhance and simplify communications between the patient and the therapeutic devices.

Although virtual rehabilitation therapy is a more engaging than other forms of rehabilitation due to the immersive environment, which could encourage longer and more frequent therapy session, as well as home based therapy, conventional physiotherapy and robotic therapy prove the effectiveness of manipulating the affected arm throughout the exercise – an aspect that is missing from virtual rehabilitation.

A team from Finland in 2011 (approximately 2 years after the commencement of this project) proposed the development of a virtual reality mirror therapy system, utilising a robot to aid in the patient in exercises, similar to the approach offered in this project [103]. The proposal from the Finland team is not clear on the role of the robot in the system, and deviates from this project by the use of a fully virtual reality based approach to the mirror therapy component, rather than the diminished reality approach employed here. There is no further progress reported from the Finland team. A study was conducted

using functional Magnetic Resonance Imaging (fMRI) to investigate brain activity with respect to visual stimuli from observation of a real (biological) object, or a virtual (non-biological) object to determine which is more effective [104]. It was found that for both cases, similar brain activity was observed. If the project from the team in Finland were to be completed, it would be interesting to compare the virtual reality (non-biological) approach with the diminished reality (biological) approach to confirm the results found by the fMRI study.

2.4 **Summary**

Research into robotic assistive devices in the field of rehabilitation is an emerging, and highly active area of interest. Although there are currently many projects in this field, there are still many questions left unanswered. Mirror therapy and virtual rehabilitation are also emergent areas of research that are proving to have positive results, however in the field of mirror therapy in particular, there are many aspects still to be studied. The literature presented in this review shows that there is a logical step to be taken in devising a system that combines all three of these approaches.

3 Conceptual Design

At the core of the robotic therapy system was a small six degree of freedom industrial robot. The requirement for six degrees of freedom ensuring that the robot would be able to achieve suitable rehabilitation exercises for the patient. The main control for the robot was to be based on the motions of the patient's healthy arm. To achieve this, motion capture of the healthy forearm was to be performed by suitable system that would capture the motion of the healthy arm, in six degrees of freedom, for use as the control mechanism for the robot arm. Force feedback was also utilised to monitor the reaction forces between the robot and patient. This was to be achieved by mounting a small force sensor in the system, and was used to introduce a level of active compliance to the system, as well as added safety for the patient. Response time of the system is also an important factor, with a suggested value for this being 0.1s [105].

The virtual mirror therapy was to be provided using a web cam, with the video stream from the webcam being manipulated in real time processes. The video stream was altered to produce a mirror image of the patient, and remove the robot from the image to give the patient the illusion that they were achieving the exercises unaided. Figure 3.1 shows the initial conceptual layout of the system.

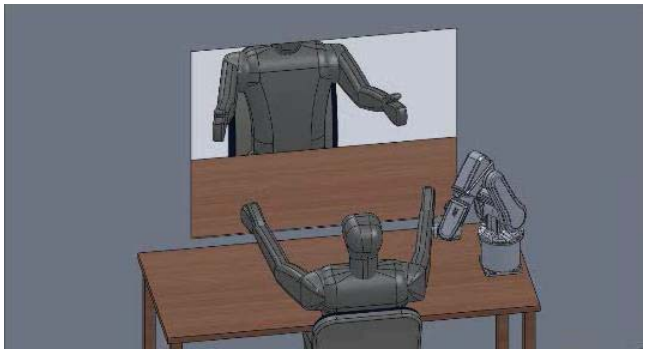

Figure 3.1 - An illustration of the proposed system

There were many considerations in the selection of the various components required for developing the prototype system. The following sections discuss these considerations in further detail, and define the required specifications for the components based on these considerations.

3.1 **Safety**

Safety was an important consideration with respect to the estimated loadings that would be appropriate for the patient. The considered injury risks for this project were bruising, or soft tissue injury, to broken bones in the worst case scenario. To prevent injury, the maximum acceptable forces exerted on the patient through the robot patient coupling would be determined to be low enough as to reduce the risk of bruising, and minimise the risk of further injury.

Appropriate forces for human bruising were investigated. Although few findings indicating forces producing bruising in humans were found due to the ethical issues inherent with testing the mechanics of impact injuries on live subjects, an interesting study [106] indicated that bruising can occur in a healthy adult with impact forces from 342N (~35kg), which was used as a starting point for estimating the acceptable maximum forces exerted on the patient.

As this system was intended for use primarily with elderly patients, who have higher risks of bruising and injury, and that it is understood [107] that the individual physiology of people will give different bruising force values, a safety factor of 10 was selected, reducing the maximum applied force on the patient to ~3.5kg, in the aid of reducing the risk of injury to the patient, while still enabling the system to exert sufficient force to be able to perform the manipulation necessary to achieve the tasks for the rehabilitation exercises.

3.2 **Robot Selection Criteria**

The selection of the robot was dependant on three aspects, firstly, the required payload capability of the robot would need to be sufficient to carry the weight of the patient's arm, while limiting the maximum applied forces from the robot to minimise the risk of injury to the patient.

As a starting point, the average weight of an adult human arm is approximately 3.2kg [108]. Assuming that the patients shoulder supports approximately half of the arm's weight, the loading needed to be in excess of 1.6kg (15.7N). To confirm this, the weights of people's forearms were measured at resting position with the average obtained taken as an estimation of the expected dead-load of the human forearm as a loading for the robot. Subjects used for the estimation of the forearm weight were healthy individuals, aged between 20 and 30 years.

The forearm weight was measured using a small digital scale, accurate to 5g. With the subject's upper arm at rest, hanging vertically from the shoulder, the scale was placed halfway along the length of the span between the elbow and wrist, slightly below the elbow, to ensure that the weight of the upper arm didn't affect the measurement, as it was assumed that the upper arm would be supported by the shoulder during exercise. This assumption is based on the concept that the initial trials of the system would be with patients who have completed the current standard rehabilitation, as was the case with the early trials of both the MIT Manus, and the MIME projects. This would mean that the patients are no longer in the acute stage of recovery, having regained some motor function, meaning they would have the ability to attempt the rehabilitation exercises, and support some of the weight of their arm.

The subject was then asked to rest their forearm on the scale, so the measurement could be taken.

Subject	Weight of Forearm at Rest (kg)
1	2.235
2	2.550
3	1.330
4	1.220
5	1.380
6	1.630
7	1.550
8	1.860
9	1.830
10	1.720
Average	1.731

Table 3.1 - Sample of human forearm weight for load estimation

As shown in Table 3.1, the average forearm weight of the subjects measured was 1.73kg, and taking into account the requirement for the added weight of the coupling mechanism that would be required for connecting the robot to the patient; an estimated payload criterion for the robot was set at 3kg. Also considering the safety requirements discussed in section 3.1, suggesting a safe maximum loading of approximately 3.5kg, the robot payload should not be more than 5kg, with provisions in place to limit loadings exerted by the robot to 3.5kg as necessary.

The second aspect of the selection criteria was the reach of the robot. The robot was required to have a large enough working envelope to allow the patient to achieve reaching exercises without hindrance from the robot.

As an estimation of the required reach of the robot, measurements were taken of healthy individuals to determine an average working area between the midpoint of their forearm and their sagittal plane, when reaching their arm out at approximately 45º to their sagittal plane. The value of 45º was deemed as a comfortable maximum outer extension of the arm for reaching exercises, while allowing the majority of reaching exercises to be

set between 45º and the sagittal plane, as most every day activities require reaching within this region.

To estimate the required reach, each subject's arm was measured from the shoulder to the mid-point between their elbow and wrist with their elbow extended, as well as the distance from their shoulder to an approximation of their sagittal plane, and then the span between the forearm mid-point and sagittal plane was calculated.

Subject	shoulder to forearm midpoint (mm)	shoulder to sagital plane (mm)	forearm to sagital span (mm)
1	410	240	455
2	400	155	365
3	405	230	443
4	410	180	395
5	360	155	344
6	405	150	363
7	425	210	433
8	390	160	365
9	415	180	398
10	375	160	357
		Average Span	392

Table 3.2 - Average arm measurements for robot required reach estimation

On review of the data obtained in Table 3.2 for estimating the required robot reach, it was determined that the reach of the robot should be no less than the average of 392mm, however, considering the range of the data obtained, a target reach for the robot was selected as a minimum of 500mm to ensure freedom of movement for patients with greater arm lengths or broader shoulders.

For patient convenience, the rehabilitation system was intended for use in local rehabilitation clinics, making it easier for patients to access the therapy in the aid of ensuring patient participation for clinical trials. This meant that the system would need to be reasonably portable as trials would potentially be run in different clinics to ensure large enough trial groups for meaningful results to evaluate the system.

Therefore, the final criterion for robot selection was the weight of the robot. This was less important than the other two criteria; however, this would be a defining factor in the selection process, with a lighter robot being preferable.

3.3 **Motion Capture Selection Criteria**

A suitable system was required to capture the motion of the healthy arm of the patient which was used for the main control of the robot. The requirements for the motion capture system were that it would be simple to setup and use, as the end system would be intended for use by clinicians who may be unfamiliar with this type of equipment, and in a clinical situation, minimal setup time is essential.

The system also needed to be non-invasive to the user, ensuring that their mobility wasn't hindered by the equipment. This suggested that if the patient needed to have the part of the system attached to their arm, it needed to be lightweight, simple to attach, comfortable, and free-moving in the three dimensional workspace that the patient's arm would be moving in.

The system selected would also need to have a good degree of accuracy, with the assumption that an accuracy of approximately ±5mm in each of the 3 axes (X, Y, Z) would be sufficient. This assumption was supported by research into proprioception of humans[109], finding in tests to determine the accuracy of human proprioception, a variance of approximately 10mm when attempting to accurately position a pointer on a known position using proprioception as the sensory input. This suggests that an accuracy of at least ±5mm would be within the accuracy of human proprioception found in literature.

The range of the sensor was also important in selecting the motion capture device. As the robot' s reach was determined as being required to be at least 500mm, the range of the motion capture system must at least equal this value, to ensure full use of the robot's range of motion. However, as the position of the motion sensing point on the healthy arm would be a mirrored position of the hemiparetic arm, which was to be mounted off the end of the robot's end effector via a coupling system, the range of the motion sensor it was necessary to include allowance for the coupling. A 300mm allowance was included in the range of the motion sensor to allow for the design of the coupling system, resulting in a range criterion for the motion sensor of at least 800mm.

3.4 **Force Sensor Selection Criteria**

The first criteria of the force sensor was that it measured 6 degrees of freedom to ensure that it was capable of giving feedback for both linear and torsional loads. These were needed as feedback for the input of the compliance control of the system. The load ratings of the sensor, both linear loadings and torques, needed to be high enough to ensure that the sensor would not be overloaded by the weight of the patients arm, and the apparatus that was to be designed to connect the patient's arm to the robot. As stated previously in section 3.2, based on the average weight of an adult human forearm, the load rating of the force sensor was required to be at least 1.73kg (17N). However, considering the loading conditions of the discussed in section 3.1, and the payload criteria for the robot selection being between 3kg & 5kg, the greater loading of 5kg (49N) was taken as the selection criteria for the force sensor, ensuring that the sensor would be suitable for monitoring the loadings exerted on the patient's arm, and would cope with the loadings applied by the robot.

As the safety of the patient is an intrinsic necessity of the system, there were several systems in place in the integrated system to ensure that there was sufficient redundancy in

the safety systems, to ensure that the patient would not be harmed due to errors or malfunction of the system. As the main component providing an input active safety system of the system, it was also important that the force sensor was capable of high sampling rates to ensure near instantaneous reaction in the case of overload, or sudden changes in force or torque.

Weight was also a consideration for the force sensor, as it was to be mounted on the end effector of the robot, reducing the allowable weight of the coupling system; therefore a lightweight solution was required to ensure that it had minimal impact on the robot's loading, ensuring that, dependant on the robot selected, it will not be overloaded when in operation.

3.5 **Summary of System Requirements**

For development of a prototype rehabilitation system, the proposed system requirements are summarised here.

Robot reach is not less than 500mm.

Robot payload between 3kg and 5kg

Robot unit weight less than 50kg for portability

Force sensor degrees of freedom = 6

Force sensor load rating > 5kg, or approximately 50N

Motion sensor Range > 800mm

Motion sensor accuracy < ±5mm

The system response time < 0.1 seconds

4 Development of the virtual mirror

There are differing forms of computer mediated reality available with current technologies. The mirror therapy aspect of this research project takes aspects of both diminished reality, and augmented reality to achieve the end goal. Diminished reality is implemented by means of an approach to remove the robot from the video image viewed by the user, while basic augmented reality is utilised to achieve the interactive game interface to engage the patient in reaching exercises. A common understanding that the term "virtual mirror" refers to a mirror interface used in sales applications, often online, to allow a customer to view themselves in clothing, for example, without physically wearing the item. However, in the context of this thesis, the term is used to refer to the mirror interface that utilises both diminished and augmented reality, for simplicity.

The virtual mirror component is required to achieve the mirror therapy aspect in the final system. The concept for this component is to produce a mirror image visual display for the patient to observe while attempting the robotic therapy exercises. To achieve a mirror therapy component that is as close to passive mirror therapy as possible, it is considered that the patient should view their actions as if they are moving their limbs without assistance. This outcome requires that the image of the robot be removed from the video stream that the patient views.

4.1 **Overview**

The removal of the robot from the video stream poses an interesting task in identifying and removing a single element from non-static foreground objects of the video stream with minimal disturbance to the final image. This task must also be achieved in a "real-time" implementation, rather than in a post processing implementation, meaning

that processor resources are also a large consideration to avoid lagging and delays in the video output.

4.2 **Chroma Key Approach**

Initially, what was viewed to be a simplistic approach was undertaken in this project to remove the robot from the image as a novel approach to the problem. As the robot was able to be painted a solid block colour, the use of Chroma key was chosen to remove the colour range of the robot from the image. Chroma key is a widely used technique for removing backgrounds from images so that the foreground can be superimposed on another background, such as a weather map or a fictional landscape. This is achieved by filming the action scene in front of a solid blue or green screen, giving an isolated colour range that can easily be removed by simple algorithms. However, this technique, although simple, is not as well suited to the removal of moving objects in which the colour range changes in the illuminated surfaces of the object due to reflection of light, or shadowing. The challenge was to develop a method to limit the effect of the Chroma key algorithm on the image in the areas away from the object being removed from the video stream. The proposed solution to this was to use edge detection algorithms to create a region of interest around the robot and then infill that region with a block colour so that the Chroma key colour range could be reduced to removing the single colour value that had been in filled.

4.2.1 **Chroma Key Implementation**

To simplify the programming of this software, the OpenCV C++ library was chosen as it already has many inbuilt algorithms such as Laplace and Canny edge detection and flood fill – an algorithm that re-colours pixels relative to the original “seed” or starting

point of the filling operation, or relative to the neighbouring pixels depending on the parameters used when calling the flood fill algorithm.

Initially the raw chroma key algorithm was implemented to experiment with the colour ranges required to remove the robot. This also demonstrated the flaw in using this type of algorithm for foreground non-stationary object removal. Figure 4.1 shows an example of the differing colour ranges as the illumination changes when the robot moved.

Figure 4.1 - Demonstration of altered colour range as object moves

With a correctly functioning implementation of chroma key achieved, the next step was to implement the edge detection algorithm which would be later used to create the region of interest for the colour infill. Laplace edge detection was selected as the initial algorithm for edge detection to create the region of interest that would restrict the chroma key algorithm. Laplace edge detection produces good definition of the object outlines, without requiring intensive processing power. Figure 4.2 shows the implementation of Laplace edge detection.

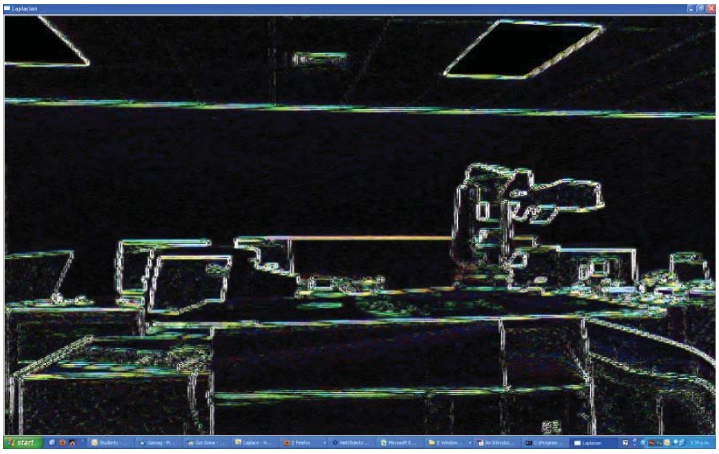

Figure 4.2 - Implementation of Laplace edge detection

To implement the Floodfill algorithm that is included in the OpenCV library, an iterative approach was adopted to search through the image to find groups of pixels within the correct colour range, and then fill the region containing this group of pixels with the pre-determined block colour for the chroma key to filter out. The Laplace output image was used as a mask for the Floodfill algorithm which was implemented such that it will not fill across non-zero pixels in the mask (i.e. the object edges), keeping the operation within the required region. A demonstration of the Floodfill algorithm implemented on an image processed with Laplace edge detection is shown in Figure 4.3.

Figure 4.3 - Implementation of Floodfill

Now that there was a set block colour within the bounded region of the robot, it was simple to use the chroma key algorithm to remove the set RGB colour (in this case 255, 0, 0 was used for the RGB block colour). Figure 4.4 shows the both the implementation of the chroma key algorithm with the use of Laplace edge detection, and without the use of edge detection for comparison.

Figure 4.4 - A demonstration of chroma key applied with edge detection implementation (left) and without edge detection implementation (right)

As shown above, the implementation of the edge detection and chroma key algorithms combined improved the outcome for removing dynamic foreground objects, however, the result shown above still needed further improvement to be suitable for use in the project.

4.2.2 Chroma Key Discussion

The major weakness of this approach has proven to be the strength of the Laplace edge detection. As the video image from the webcam was low resolution, with relatively high noise, Laplace edge detection proved to be less effective for this application due to its sensitivity to noise [110] without strong definition between the object colour and its surroundings due to the noise in the image, the outlines of the edges produced by the Laplace algorithm become weak, with small (sometimes pixel sized) breaks in the edges

allowing the Floodfill algorithm to “spill out” and fill larger areas of the screen. This was unacceptable for the operation of the virtual mirror system, and therefore the approach for removing the robot from the video stream required alteration. The Laplace edge detection algorithm was replaced Canny edge detection, which has better response to noisy images than Laplace edge detection, but is more computationally complex. The Canny edge detection improved the quality of the image output, producing more defined edges around the robot, but on visual examination of the real-time video stream, the added computational complexity had a detrimental effect on the response time of the video stream, producing a jittery video image.

The use of a controlled environment helped to improve the quality of the robot removal algorithms, by using a contrasting background to the robot, and adjusting lighting to minimise reflections/shadowing. However, the video image was still unstable, and further investigation was required.

4.3 **Contours Approach**

As the Chroma key implementation proved unsuccessful, further investigation was undertaken into potential methods to remove the robot from the video stream. The use of blob detection was then decided on as the process for identifying the robot in the video stream for removal by means on in-painting.

4.3.1 **Contours Implementation**

Blob detection is a commonly used approach to detecting items in a video stream. In the OpenCV libraries, there are different functions to available to achieve this goal. Generally, blob detection is used for applications such as motion tracking, to follow certain objects in a video stream. This is useful in applications such as robot vision, where

a video control system is used to guide a robot to achieve its task (e.g. tracking items on a conveyor belt for a part picking application) in 2D space. In this general approach to blob detection, the algorithm draws a geometric shape around the object, such as a circle or ellipse, which follows the object in the video stream. For this application, the general approach to blob detection was not suitable, as it was critical for the object detection to conform to the changing shape of the robot in the video stream as it moves through the image.

OpenCV also includes a function in its libraries for identifying and drawing the contours, or outlines, in an image. This approach is simpler than the edge detection used previously, and potentially less accurate. However, this approach is more suitable than the general blob detection, allowing a rough outline of the robot to be obtained, and used for object removal. The contours functions determine closed contours in the image, and store them in memory, ranked by levels of contours within contours. By ensuring that the colour of the robot contrasts to its surroundings and smoothing the image to reduce the number of contours in the image, it is possible to ensure that the outline of the robot is the top ranked contour.

Before the contours function could be applied, the initial video capture required some processing to identify the correct colour range to look for in the image. This was achieved by converting the image from RGB colour space to HSV colour space for further processing as many of the OpenCV functions require HSV colour space. Once converted, the image was smoothed to remove noise from the image, in aid to reduce the potential contours in the image. From the smoothed image, the robot was identified in the image by its colour values, based on a user input colour range to allow for adjustment in different lighting environments. In this initial case, the user selects the colour range by use of

sliders for each of the HSV components, by means of an upper and lower value to give a range to allow for variance due to shadowing and reflection.

The use of sliders as a primary means of selecting the required colour range for determining the robot in the video stream proved to be cumbersome, and difficult to pinpoint the correct colour range to successfully identify the robot. This process was improved by the addition of a colour picker for selecting the centre point of the colour range, with pre-set range limits that are user adjustable for fine tuning. By use of the colour picker, the supervisor of the system is able to select a point within the robot's image, thereby determining the required colour range. The slider interface, shown in Figure 4.5, was still kept for fine adjustment to the colour range limits by the system supervisor to compensate for differing lighting conditions.

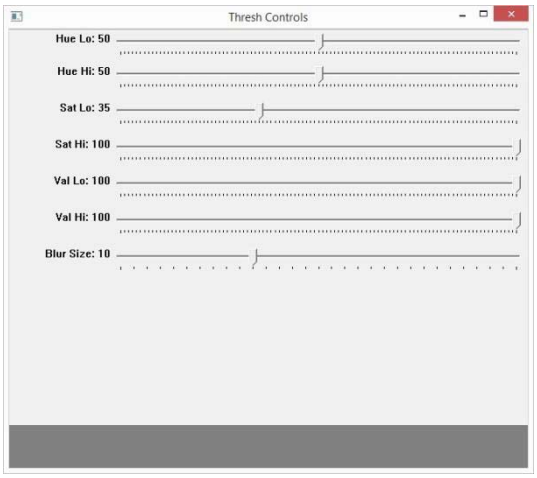

Figure 4.5 - Slider control interface

With the correct colour range selected, the region of interest containing the robot was then mapped into a black and white image for determining the contours. The top level contours were then drawn in white on blank image and the Floodfill function was used to fill the image outside the contours, taking advantage of the property of this function that

stops filling when the image when it encounters white pixels (i.e. the contour outlining the robot). This procedure then formed a masking image to isolate the robot's outline.

Figure 4.6 - Image of robot mapped to black and white image

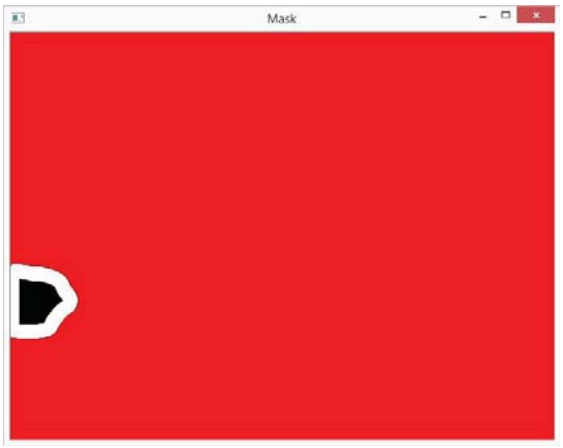

Figure 4.7 - Resulting masking image

The final step required the use of the mask image to combine the current video stream with a suitable background to fill the area of the image where the robot should be. Initially the background image used was a static image captured at the beginning of operation, that would show the area being filmed without the robot in shot, however, this was found to be an unsatisfactory background, as it would create disparity between the current video image and the background image that was very noticeable. To improve this result, the static background image was replaced by using the N-1 image result (i.e. the result of the previous iteration) of the algorithm, with the static background image used in

the first iteration as there was no previous iteration result to be used. Figure 4.8 shows a comparison of the original image captured beside the final result.

Figure 4.8 - Raw image and edited image

4.3.2 Contours Discussion

This approach proved more successful than the Chroma key approach previously developed. It has proven to be a simpler approach, requiring less intensive resources, with a more successful result, that has achieved the goal of removing the robot from the video stream in a "real time" execution, with minimal impact on the response of the video image. However, the extra processing, when compared to an unedited video stream, does still produce a slight delay, visible to the naked eye.

4.4 Game Interface

For the initial prototype, the video game interface was developed based on the gesture type interaction as developed for gaming platforms such as the Sony PlayStation2 EyeToy, and the Xbox Kinect. This style of interface uses a webcam to film the player and their image is superimposed into a virtual world. The game developed for this system took the guise of a simple bubble popping game, requiring the patient to reach for virtual bubbles, randomly falling down the screen, to pop them. This method of game play was

well suited to integrate with the virtual mirror visual feedback system as the virtual mirror therapy already required the inclusion of a webcam and video display. Adding physical reaching tasks by means of an on-screen video game was a logical step to engage the patient and direct the therapy routine.

The operation of the game has 2 small images (loaded from an external file) starting at the top of the screen placed at a randomly selected, equal distance from the screen's vertical centre line. The participant then attempts to pop each bubble with the corresponding hand.

Initial tests of the game proved the necessity to use small pointers in each hand to ensure that the bubbles were popped by the action of the hands, and not randomly moving objects in the video image. The same object identification approach as the contours approach used for the robot removal. For this, a second colour picker was also included to differentiate the pointer from the robot colour range. This stipulates that the pointers be contrasting in colour to that of the robot.

5 Robotic System Development

As set out in section 3.2, the selection of the robot arm used in the project is dependent upon set criteria to be able to achieve an appropriate payload, while not being able to exert enough force to cause injury. The robot also needs to have a suitable range of motion for effective exercises for the patient's rehabilitation. On evaluation of different robotic systems available on the current market, this would require compromise between these two criteria, as the payload of the robotics systems, although not strictly proportional, tend to increase with the size of the working envelop of the robot, as does the price, which was limited by the project budget.

As the intended use of the final system is for clinical trials to investigate the efficacy of the proposed combined robotic and mirror therapy approach to stroke rehabilitation, the power requirements of the robot were also an important consideration. Most industrial robotic arms require 3-phase power, while common-place in the industrial environments they are intended for, cannot be guaranteed to be available in the clinical environments that the clinical trials would be conducted.

The portability of the final system is also an important requirement, and therefore the weight.

The ABB Robotics IRB120 robot was selected for use in the project. Details of the selection process are included in Appendix A – Robot Selection. This robot has a 3kg payload, which is comparable to that of the Puma 560 robot successfully used in the MIME system [57]; however the 580mm reach of the ABB unit is less than that of the Puma 560, but should still be adequate. The wrist of the robot is to be attached to the middle of the hemiparetic forearm by a custom designed end effector.

ABB provide a proprietary software package with the robot, including Rapid, a programming language specifically for the ABB brand robots, and Robot Studio, used for simulating the robot units on a computer. Rapid uses data structures called robot targets or joint targets to give the given positions of for the robot during operation. Robot targets are constructed from four pieces of information, the XYZ position of the tool tip, the rotation of the tool (using quaternions), the configuration data of the joints that will cause singularity, and optionally, the positions of any auxiliary axes that may be added to the system by the user. The configuration data is specific to each robot model (in the case of the IRB120, this is joints 1, 4 and 6, as well as an auxiliary axis for the tool) determined by the joints that will cause singularity when the specified joints are in alignment. Singularity being any position where two or more of the joints are in alignment, resulting in an infinite number of solutions of the robot's joint positions to achieve the given position.

The configuration of each joint is a single integer ranging between -4 and 3, specifying the required quadrant for the given joint to move to. This data is required by the rapid program to be able to determine the correct solution for the robot when one or more of the joints are required to rotate through an angle greater than 90º to achieve the new position, and is also used in the rapid program when a set of joint angles requires calculation without instructing the robot to move.

The joint target is less complicated, as it simply specifies the absolute position for each of the joints, including auxiliary axes if required. However, when joint targets are used as opposed to robot targets, the path of the robot is not linear between points.

In the rapid programing language, it is possible to set the system to disregard the configuration data during operation, by disabling an inbuilt routine that monitors the

robot configuration of each robot target ensuring that it is correct for the given position. It was assumed that as the motion sensor was capable of sampling at 50Hz, the requirement for the robot controller to monitor the configuration would not be required, as the incremental positions being obtained would be small and require joint movements less than 90º. This assumption would mean that the calculation of the configuration data would not be required, saving processing time and resource for the system. However, during initial integration and testing of the robot and motion sensor, this assumption was proven to be incorrect, as the number of samples being taken was excessive resulting in lagged response from the robot. The small increments between positions did not prevent joint motions greater than 90º, and without the configuration being monitored, there was no provision to catch singularities. This means that it was determined that this option was not feasible, as unpredictable motion from the robot would result when one of the joints monitored by the configuration would require a movement greater than 90º (this was usually joint 4) or the system would simply crash in the case of singularity.

For the majority of the programming, robot targets were used, to ensure linear movement between points, except when the robot was close to singularity, where joint targets were used. This would usually occur when the robot was near its full reach.

In the case of pre-determined robot paths, as typical in industrial applications, where the robot path is determined before operation, it is easy to determine the robot configuration required for each robot position to achieve the points through the path, as these can be obtained by either positioning the robot via it's teach pendant, or calculated and tested prior to execution of the program. For this project however, this task is more complicated, as this information was required to be calculated "real-time" by the system, based on the information being taken from the motion or force sensors, as the program

was being executed. The calculation of the configuration data during operation was fundamental to the operation of the system, firstly for safety, to ensure that the robot wouldn't execute any excessive movements that may cause injury to the patient, and secondly, to be able to determine, and appropriately process, any positions during execution that may cause a singularity situation, which would cause the rapid program to end unexpectedly.

The first step to calculating the configuration data and determine the required robot positions, was to develop the closed form solution for the IRB120. Once determined, this was used to calculate the joint positions limiting each joints range of motion to reduce the number of possible solutions for a given end effector position, and then determine the configuration data for the robot target. The determination of singularities was executed by in-built algorithms in the rapid run-time environment, and when a singularity occurred, the robot was positioned by direct positioning of the individual joints based on the results of the calculation of the closed form solution, in place of the robot target that threw the error.

The execution of the compliant element of the system, required both for safety, and when the robot is acting in a passive state, following the patient's hemiparetic arm's motion is also dependant on the development of the closed form solution. In this state, the system would calculate the next position for the robot based on the force and torque vectors obtained by the force sensor, to minimise the reaction force between the patient and robot. The target was to minimise these forces to zero, to try and produce as little impact on the patient's motion as possible in this state. Therefore the next robot position would be calculated utilising the same algorithm based on the closed form solution, and

using a simple proportional control algorithm to aid in determining the relative offset and change in orientation to reduce the reaction force.

5.1 Closed Form Solution for IRB120

Developing the closed form solution for a given robot is a fundamental procedure in robotics, and is important to be understood for the development of robotic systems to be able to calculate the inverse kinematics for each robot. This topic is extensively covered in literature. For the development of the closed form solution for the IRB120, direction was taken from [111, 112] the latter being a useful paper which covers the closed form solution development for a wide range of robot configurations with arbitrary link lengths.

Essential to the process of determining the closed form solution for any robot is the assignment of the link frames for the robot. In the case of the IRB 120, joint 1 is offset from the base frame along the rotation axis with the rotation axis of joint 2 intersecting the rotation axis of joint 1, so for the simplification of the calculations, both joint 1 and the base frame were taken as acting at the same origin as joint 2, with the offset to the base frame of the robot in relation to joint 2 being accounted for in the Z component of the robot target. The three axes (4, 5 and 6) that form the wrist, and therefore the orientation of the end effector were also taken as being on the same origin, at the point where the three axes intersect. Figure 5.1 shows the assignment of the joint frame orientations and the relevant link dimensions, while Table 5.1 shows the Denavit–Hartenberg parameters.

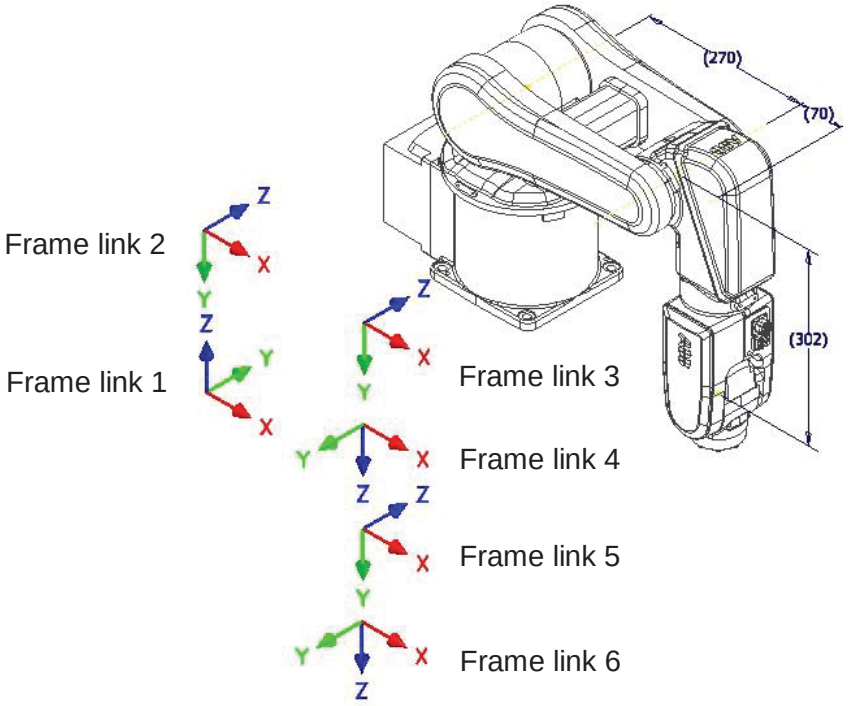

Figure 5.1 - Robot link frame assignments

Denavit–Hartenberg parameters				
Link	α_{i-1}	a_{i-1}	d_i	θ_i
1	0	0	0	θ_1
2	-90°	0	0	θ_2
3	0	0.27	0	θ_3
4	-90°	0.07	0.302	θ_4
5	90°	0	0	θ_5
6	-90°	0	0	θ_6

Table 5.1 - Denavit-Hartenberg parameters

With the assignment of the Denavit-Hartenberg parameters, 6 transformation matrices are derived, one for each link of the robot arm:

$$ {}^{0}_{1}T \begin{bmatrix} \cos\theta_1 & -\sin\theta_1 & 0 & 0 \\ \sin\theta_1 & \cos\theta_1 & 0 & 0 \\ 0 & 0 & 1 & 0 \\ 0 & 0 & 0 & 1 \end{bmatrix} $$

$$
{}^{1}_{2}T \begin{bmatrix} \cos\theta_2 & -\sin\theta_2 & 0 & 0 \\ 0 & 0 & -1 & 0 \\ \sin\theta_2 & \cos\theta_2 & 0 & 0 \\ 0 & 0 & 0 & 1 \end{bmatrix}
$$

$$
{}^{2}_{3}T \begin{bmatrix} \cos\theta_3 & -\sin\theta_3 & 0 & 0.27 \\ \sin\theta_3 & \cos\theta_3 & 0 & 0 \\ 0 & 0 & 1 & 0 \\ 0 & 0 & 0 & 1 \end{bmatrix}
$$

$$
{}^{3}_{4}T \begin{bmatrix} \cos\theta_4 & -\sin\theta_4 & 0 & 0.07 \\ 0 & 0 & -1 & 0.302 \\ \sin\theta_4 & \cos\theta_4 & 0 & 0 \\ 0 & 0 & 0 & 1 \end{bmatrix}
$$

$$
{}^{4}_{5}T \begin{bmatrix} \cos\theta_5 & -\sin\theta_5 & 0 & 0 \\ 0 & 0 & 1 & 0 \\ -\sin\theta_5 & -\cos\theta_5 & 0 & 0 \\ 0 & 0 & 0 & 1 \end{bmatrix}
$$

$$
{}^{5}_{6}T \begin{bmatrix} \cos\theta_6 & -\sin\theta_6 & 0 & 0 \\ 0 & 0 & -1 & 0 \\ \sin\theta_6 & \cos\theta_6 & 0 & 0 \\ 0 & 0 & 0 & 1 \end{bmatrix}
$$

From the 6 individual transformation matrices, the complete matrix, ${}^{1}_{6}\mathrm{T}$, was derived, and the equations for each joint were also determined, the procedures for deriving the formulas for each joint are explained in detail in literature. The resulting closed form solution for the ABB IRB120 is presented below:

$$\boldsymbol{\theta_1 = Atan2(y, x)} \quad \textbf{(1a)}$$

Or

$$\boldsymbol{\theta_1 = Atan2(-y, -x)} \quad \textbf{(1b)}$$

$$\boldsymbol{\theta_2 = Atan2(b, a) \pm Atan2(\sqrt{a^2 + b^2 - c^2}, c)} \quad \textbf{(2)}$$

Where:

$$a = 0.34 * \cos(\theta_3) - 0.302 * \sin(\theta_3)$$

$$b = -1 * (0.07 * \sin(\theta_3) + 0.302 * \cos(\theta_3))$$

$$c = x * \cos(\theta_1) + y * \sin(\theta_1)$$

$$\boldsymbol{\theta_3 = Atan2(-0.302, 0.07) \pm Atan2(\sqrt{0.096104 - l^2}, l)} \quad \textbf{(3)}$$

Where:

$$l = \frac{x^2 + y^2 + z^2 + 0.0232}{0.54}$$

$$\boldsymbol{\theta_4 = Atan2(f, g)} \quad \textbf{(4)}$$

Where:

$$f = n * \cos(\theta_1) - m * \sin(\theta_1)$$

$$g = -m * \cos(\theta_1) * \cos(\theta_{23}) - n * \sin(\theta_1) * \cos(\theta_{23}) + p * \sin(\theta_{23})$$

And given quaternion $Q = Q_W + Q_X + Q_Y + Q_Z$

Then $m = 2 * (Q_X * Q_Z + Q_W * Q_Y)$

$$n = 2 * (Q_Y * Q_Z - Q_W * Q_X)$$

$$p = {Q_W}^2 - {Q_X}^2 - {Q_Y}^2 + {Q_Z}^2$$

And $\theta_{23} = \theta_2 + \theta_3$

$$\boldsymbol{\theta_5 = Atan2(h, i)} \quad \textbf{(5)}$$

$$h = -1 * (m * (\cos(\theta_1) * \cos(\theta_{23}) * \cos(\theta_4) + \sin(\theta_1) * \sin(\theta_4)) + n * (\sin(\theta_1) * \cos(\theta_{23}) * \cos(\theta_4) - \cos(\theta_1) * \sin(\theta_4)) - p * (\sin(\theta_{23}) * \cos(\theta_4)))$$

$$i = m * (-cos(\theta_1) * sin(\theta_2 + \theta_3)) + n * (-sin(\theta_1) * sin(\theta_2 + \theta_3)) + p * (-cos(\theta_2 + \theta_3))$$

$$\boldsymbol{\theta_6 = Atan2(j, k)} \quad \textbf{(6)}$$

Where:

$$j = -s * (\cos(\theta_1) * \cos(\theta_{23}) * \sin(\theta_4) - \sin(\theta_1) * \cos(\theta_4)) - t * (\sin(\theta_1) * \cos(\theta_{23}) * \sin(\theta_4) + \cos(\theta_1) * \cos(\theta_4)) + u * (\sin(\theta_{23}) * \sin(\theta_4))$$

$$k = s * ((\cos(\theta_1) * \cos(\theta_{23}) * \cos(\theta_4) + \sin(\theta_1) * \sin(\theta_4)) * \cos(\theta_5) - \cos(\theta_1) * \sin(\theta_{23}) * \sin(\theta_5)) + t * ((\sin(\theta_1) * \cos(\theta_{23})) * \cos(\theta_5) - \sin(\theta_1) * \sin(\theta_{23}) * \sin(\theta_5)) - u * (\sin(\theta_{23}) * \cos(\theta_4) * \cos(\theta_5) + \cos(\theta_{23}) * \sin(\theta_5))$$

And

$$s = {Q_W}^2 + {Q_X}^2 - {Q_Y}^2 - {Q_Z}^2$$

$$t = 2 * (Q_Z * Q_W + Q_X * Q_Y)$$

$$u = 2 * (Q_X * Q_Z - Q_W * Q_Y)$$

To test the derived closed form solution, known positions and orientations for the robots end effector frame were used to calculate the joint positions for the robot, using the derived solution. This was achieved using an Excel spreadsheet for simplicity, allowing formulae and dependencies to be easily tracked, and simplifying the debugging process of the closed form solution. This spreadsheet was also used for later comparisons when testing and debugging during the implementation for use in the final system.

Using MATLAB and the robotics toolbox for MATLAB developed by Peter Corke [113], the IRB120 was modelled in MATLAB. Utilising the MATLAB model of the IRB120, the model was plotted using the calculated joint angles, confirming that the derived closed

form solution produced a correct set of joint angles to achieve the required end effector frame position and orientation.

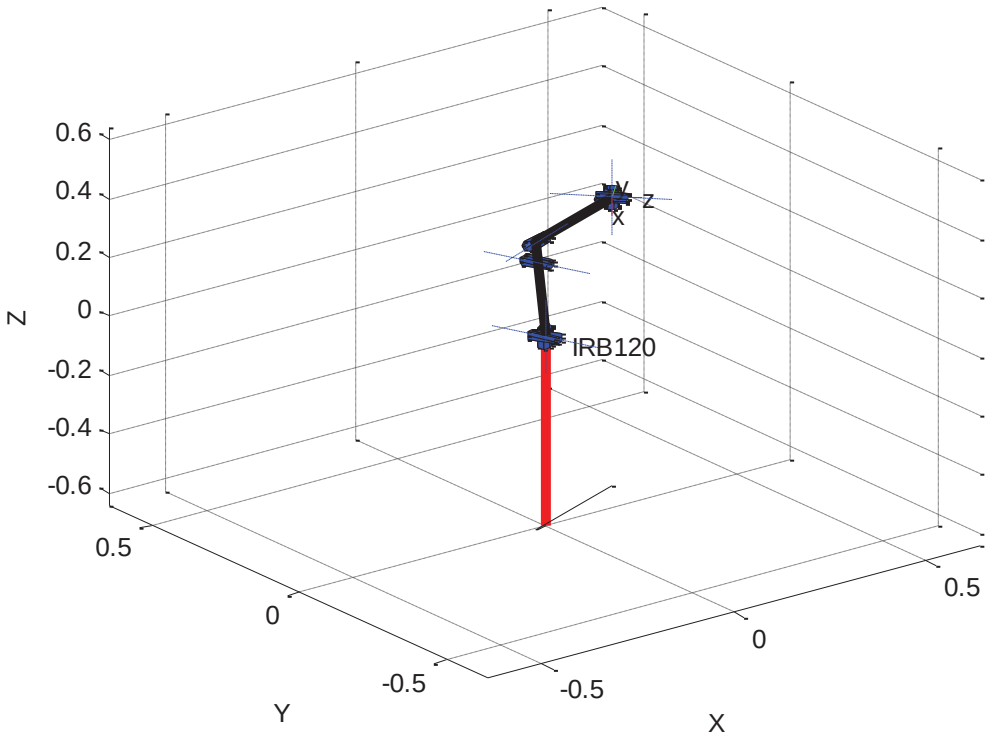

Figure 5.2 - IRB120 modelled with Robotics Toolbox

Coordinates	x=0.25	y=0.1	z=0.34	Rx = 45°	Ry = 90°	Rz=0°
Kinematic solution	θ1 = 21.80°	θ2 = -6.87°	θ3 = 6.50°	θ4 = -89.84°	θ5 = 66.80°	θ6 = 89.60°

Matlab Transform Matrix			
0.000	0.707	0.707	0.250
0.000	0.707	-0.707	0.100
-1.000	0.000	0.000	0.340
0.000	0.000	0.000	1.000

Excel Transform Matrix			
0.000	0.707	0.707	0.250
0.000	0.707	-0.707	0.100
-1.000	0.000	0.000	0.340
0.000	0.000	0.000	1.000

Table 5.2 – Example comparison of transform matrices

Taking arbitrary coordinates for testing the calculations of the excel spreadsheet; the resulting kinematic solution was used to plot the IRB120 in MATLAB. Using this model,

the transform matrix of the model was calculated in MATLAB, providing a comparison to validate the derived formulae, and the spreadsheet as a tool for calculating the inverse kinematics of the IRB120. As shown in Table 5.2, the resulting kinematic solution from the excel spreadsheet derived for this project, modelled in MATLAB, reproduce the transform matrix that the kinematic solution was based on, validating the closed form solution, and the implementation of the formulae in the spreadsheet.

5.2 **Quaternions**

A brief not on quaternion rotations is included as much of the robot control for this project was dependant on the use of quaternions for orientations.

Credited to mathematician William Rowan Hamilton who first described quaternions in 1843, quaternions are a number system extending from the complex number system, used for describing rotations in a three dimensional space. As opposed to Euler Angles, describing rotations about three axes, quaternion rotations simplify this to a single rotation about a common axis through a given angle.

The notation for a quaternion is given as:

$$\mathbf{q} = \mathbf{S}(\mathbf{q}) + \mathbf{V}(\mathbf{q}) \quad \textbf{(7)}$$

With q representing the quaternion, S represents the scalar of the quaternion and V represents the vector of the quaternion. In classical Hamiltonian quaternion notation, the vector part (V) of the quaternion can also be considered as the right part.

Quaternion rotation is commonly applied to mechanics in a three dimensional space, as well as in three dimensional computer graphics applications, and is an important concept to comprehend in robotics, as it simplifies calculations, making them more

efficient. The increased efficiency of using quaternion rotation as opposed to Euler rotations comes from the reduced number of variables required to describe the rotation, where in Euler angles there are three variables required for each rotation about the three axes, making nine variables in total, with quaternion rotation, there are only 4 variables describing the scalar and vector of the quaternion. Quaternions also provide smooth rotations as there is only one axis of rotation, whereas with Euler angles, there are three axes of rotation. These advantages of quaternions make them preferable for use in robotic applications over Euler angles, and were used as the basis of the orientation components of this project, with the orientation data from the motion sensor being formatted as quaternion orientation, and the robot controller requiring quaternion orientations for its robot control functions. Figure 5.3 shows the concept of quaternion rotation, with scalar S(q) = Qw describing the half angle of the rotation about the axis, and vector V(q) = (Qx, Qy, Qz) describing the axis of rotation.

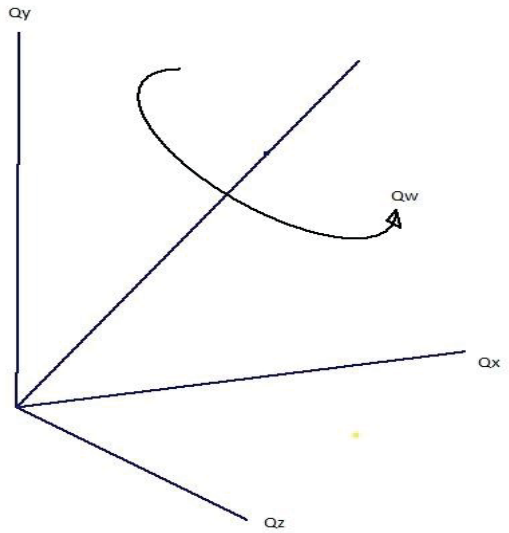

Figure 5.3 - Visualisation of quaternion rotation

5.3 **Motion Capture**

In the initial concept of this system, EMG technology was considered for use as the main control for this system, as the EMG signals from the muscles are detectable before the muscle causes motion [114, 115], which would allow the system to process these signals and predict the motion before and during its occurrence, aiding in the "real time" operation of the system. Another potential advantage of the use of EMG signals is the ability to record the signals from both arms for comparison and further analysis of both the function of the system, and the efficacy of the rehabilitation. Unfortunately EMG technology, at the time of development of this system, was currently in development, and no commercially viable equipment was available that was suitable as a control system. Therefore an alternative means for capturing the motion of the healthy arm was investigated.

The criteria for the selection of the motion capture system intended for use in this system are laid out in section 3.3. Three technologies were considered for this application; optical motion capture, magnetic motion capture & 3D digitizers.

Optical systems track markers attached to the subject using multiple cameras to triangulate the position of each marker. The markers are tracked in 3 degrees of freedom (X, Y, and Z), and the rotations of the object being tracked, in this case the patients healthy arm, are inferred by the position of 2 or more markers.

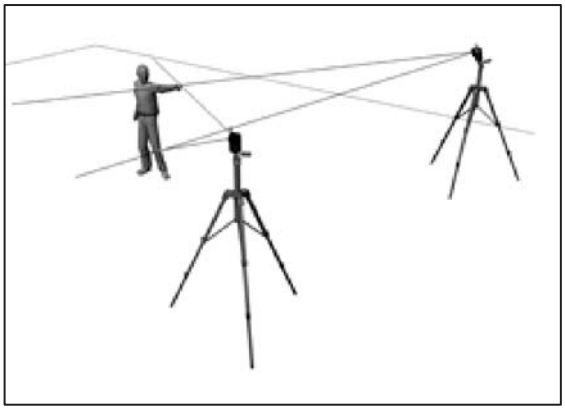

Figure 5.4 - Typical concept of optical motion capture

Optical systems have a large working envelope, but require line-of-site between the cameras and markers to be able to track the motion of the object being tracked. These systems are also complicated to setup with the accuracy of the system dependant on the accuracy of the positioning of the cameras.

Magnetic systems utilise free moving sensors that measure up to 6 degrees of freedom (X, Y and Z Cartesian coordinates and rotations relative to these three axes) relative to a base station that describes the base frame of the motion.

The position and orientation are calculated by the relative magnetic flux from coils in the sensor and base station. The main draw backs of these systems are that they have a much smaller working envelope than optical systems; however, they still provide a suitable working area for this system. Magnetic motion capture systems are also susceptible to interference due to surrounding magnetic interference (metal objects, wiring etc...).

System setup is simple as it only requires a transmitter in a set location, with sensors attached to the patients arm

3D digitizers are manually controlled articulated arm devices which are generally used for workshop measurements and reverse engineering products to produce 3D models from physical objects. The stylus of the digitizer needs to be in physical contact with the surface, or in the case of this project, the patient's arm, to be able to make the three dimensional measurements.

Figure 5.5 - Example of a 3D digitizer (Microscribe G2X)

For use as a means of measuring human arm movements, this would possibly interfere with the patient's mobility. The mechanical inertia of the system would also hinder the patient's arm mobility. 3D digitizers are commercially available with a range of workspaces, with the units reviewed for this project having working reaches up to 5m, with accuracies of less than ±0.1mm, which was in excess of the selection criteria discussed in section 3.3. However, the cumbersome nature of the mechanics of these devices means that they were deemed unsuitable when compared to the other systems investigated.

When considering the potential complication of the setup and calibration of optical systems, magnetic motion capture was deemed the preferred motion capture apparatus for this project

Magnetic motion capture systems were selected as the preferred option for motion capture due to their ease of use, and simplicity to setup. The range and accuracy of these devices met the criteria for this project as discussed in section 3.3. These devices are also lightweight, and unobtrusive, so would not affect the patient's arm mobility.

Polhemus manufacture a range of magnetic motion capture devices, which were suitable for use in this project. Table 5.3 shows the range of Polhemus units that were available for this project, listing the specifications for each of the units.

Model	Range	Accuracy	Max No Sensors	No Sensors included
	0.78m	1.4mm RMS/0.5º RMS	4	1
trakSTAR (mid range Tx)	0.78m	1.4mm RMS/0.5º RMS	4	2
	0.78m	1.4mm RMS/0.5º RMS	4	3
	2.1m	3.8mm RMS/0.5º RMS	16 (4 per unit)	1
trakSTAR (wide range Tx)	2.1m	3.8mm RMS/0.5º RMS	16 (4 per unit)	2
	2.1m	3.8mm RMS/0.5º RMS	16 (4 per unit)	3
Patriot	Up to 1.52m	@36" = 0.0113"/0.0407º	2	1
Patriot Class B (FCC and CE)	Up to 1.52m	@36" = 0.0113"/0.0407º	2	1
Patriot Wireless	Up to 3.05m	@48" = 0.109"/0.296º	4	0
Liberty	Up to 3.05m	@36" = 0.001"/0.0048º	16	1
Liberty Latus (wireless)	Up to 4.27m	@48" = 0.015"/0.046º	12	0
FASTRAK	1.22m	@36" = 0.019"/0.0558º	4	1
FASTRAK short range			4	0

Table 5.3 - Polhemus motion capture system comparisons

The system chosen for this project was the Polhemus Patriot. This is a low cost entry level unit, but it was more than adequate to meet the requirements of the project. The patriot system is capable of tracking up to 2 sensors simultaneously, giving room for future expansion.

The Polhemus Patriot uses a small magnetic transmitter mounted in a set position as the base frame, and a lightweight sensor that tracks its position and orientation relative to the base frame in six degrees of freedom. A magnetic tracking system has been selected in favour of other alternatives such as optical tracking systems, due to the compact nature

of the system and the simplicity of use (no need for calibration etc...). Also this device is unobtrusive to the patient and will have little impact on the range of motion of the healthy arm. The sensor was to be mounted on the healthy forearm of the patient, in the same relative position as the robot was connected to the hemiparetic forearm, so that the coordinates of the sensor could be translated to provide the mirrored position of the robot end effector and therefore manipulate the position of the hemiparetic arm.

Figure 5.6 - Polhemus Patriot system

Polhemus motion tracking devices are supplied with a C++ Software Development Kit (SDK) for developing custom applications for the equipment. For this project a base C++ class was developed for the Patriot system to capture the position and orientation of the sensor in the 3D work space, as required for control, with the coordinates and orientation being the output of the class. Cartesian coordinates were used for the linear transform, and quaternions for the rotation of the sensor.

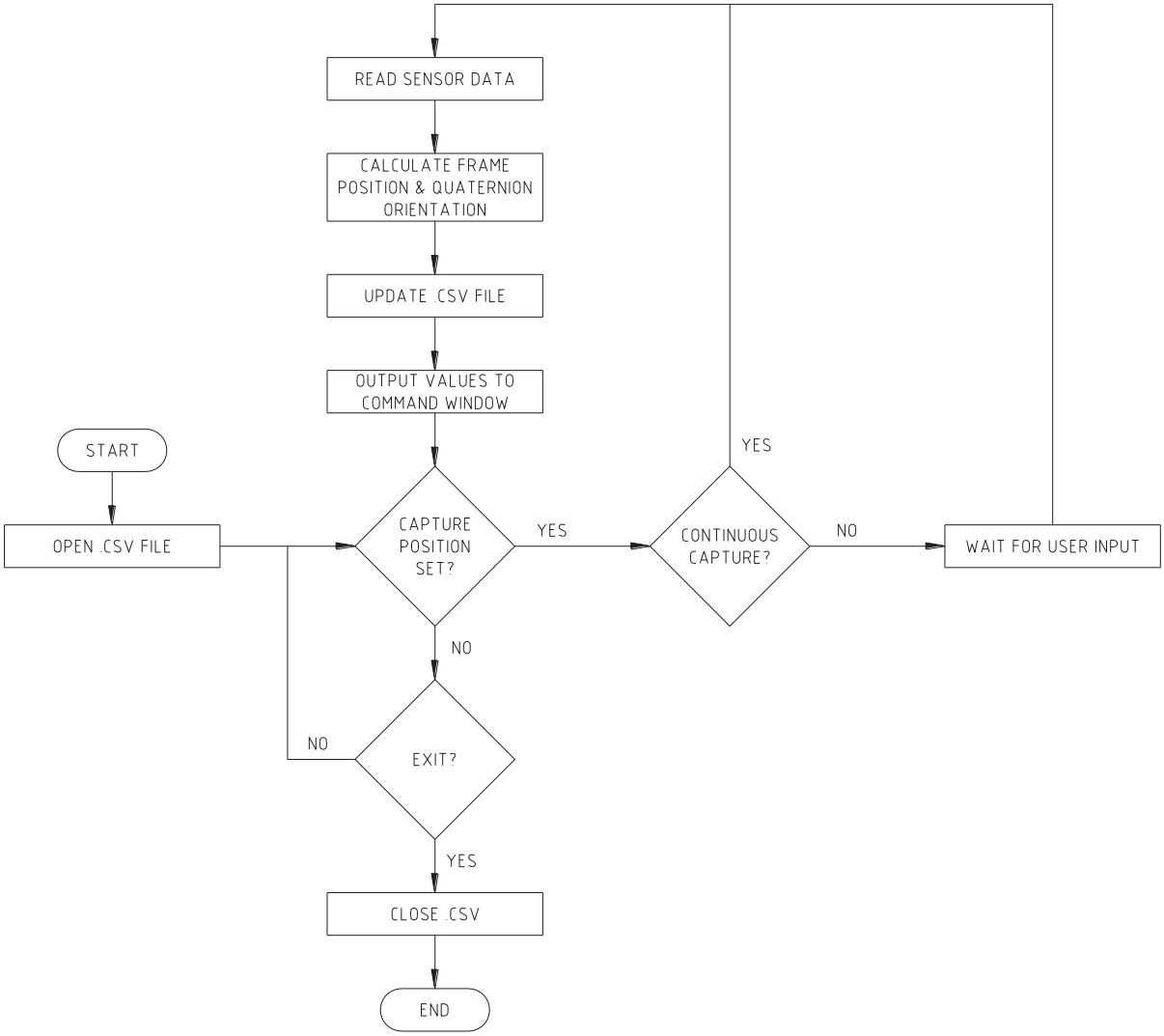

Figure 5.7 - Flow diagram for motion capture

```
VOID Tracker::DisplaySingle( float crds[3], double qrts[4] )
{
    BOOL bExit = FALSE;

    PBYTE pBuf;
    DWORD dwSize;

    cout << endl;

    if (!(g_pdiDev.ReadSinglePnoBuf(pBuf, dwSize)))
    {
           AddResultMsg("ReadSinglePno");
           bExit = TRUE;
    }
    else if ((pBuf == 0) || (dwSize == 0))
    {
    }
    else
    {
           DisplayFrame( pBuf, dwSize, crds, qrts );
    }
}

VOID Tracker::DisplayFrame( PBYTE pBuf, DWORD dwSize, float crds[3], double qrts[4])
{
    CHAR   quart[100];
    DWORD  i = 0;

    while ( i<dwSize)
    {
           int s;

           BYTE ucSensor = pBuf[i+2];
           SHORT shSize = pBuf[i+6];

           i += 8;

           PDWORD pFC  = (PDWORD)(&pBuf[i]);
           PFLOAT pPno = (PFLOAT)(&pBuf[i+4]);
           for (s = 0; s < 3; s++)
           {
                     crds[s] = pPno[s]/100;
           }

           for (s = 3; s < 7; s++)
           {
                     qrts[s-3] = pPno[s];
           }

           sprintf_s(quart, "[%+011.6f,%+011.6f,%+011.6f,%+011.6f]", -pPno[3], pPno[4], -pPno[5], pPno[6]);

           std::cout << "\n Tool Quat = " << quart << "\n";

           countout ++;

           AddMsg( string( szFrame ) );
           i += shSize;
     }
}
```

Code 5.1 - Function for frame capture from motion sensor

Prior to integrating the Polhemus patriot into the system as the main control, providing the target information for the robot, it was evaluated to ensure the correct operation of the Patriot and C++ base class. In evaluating its operation, the Patriot was tested to confirm that the accuracy of measurement of the device integrated with the C++ base class would meet the requirements set out in section 3.3.

The testing was undertaken in 2 stages. Firstly, a simple testing procedure was developed the Cartesian output of the system. The first task was to confirm the position of the systems base point with in the 75mm cubic base station.

To confirm the base point of the system, the sensor was mounted on a flat bracket which was marked to provide reference to the centre point of the sensor as given in the manual provided with the equipment. The mounted sensor was then placed on three sets of opposing surfaces of the base station that correspond to a parallel plane for each of the major axes, and the base position was . From these results, the position of the base frame was recorded for use as the base point for the continued testing.

The base station of the Patriot was mounted on a 1.2m long plastic board to provide a known and easy to measure base point for the testing. Due to the operation principle of the system, utilising magnetic fields, it was important to ensure that the base board was of a suitable material to ensure that it would not affect the magnetic field of the system, and therefore hinder its operation. This meant that the base board for testing must be free from metal elements which would distort the magnetic field.

The base board was marked out to provide a reference axis starting from the known base point of the system, measured previously. The marked out axis was then divided into equal increments of 50mm, up to 800mm. As the reach of the IRB120 robot is 580mm, 800mm was deemed to be a suitable range for the motion capture of the Patriot system, allowing full reach of the robot with an extra 200mm for the design of the robot patient coupling system.

The sensor, still mounted on its bracket to utilise the marked reference points for ease and accuracy of placement, was then placed along the marked axis at each of the 50mm

increments, with the measurements recorded by the computer in a comma separated values (.csv) file for analysis.

This procedure was used for testing the axes that would be used in the system, with the reaching exercises intended to be used in the final system being in the positive X direction as considered as perpendicular to the patient's sagittal plane, the positive and negative Y directions, considered to be parallel to the patients sagittal plane, and the positive Z direction, being considered as the vertical axis upwards, as taken relative to the robot's base frame. The Patriot base frame however is oriented so that the Z axis is vertical downwards, so the Z axis of the Patriot was evaluated through its negative X axis.

Initially the test was executed on the floor, taken as a large flat surface to aid the setup of the test rig; however the results of this initial test, as shown in Figure 5.8, produced unexpected readings.

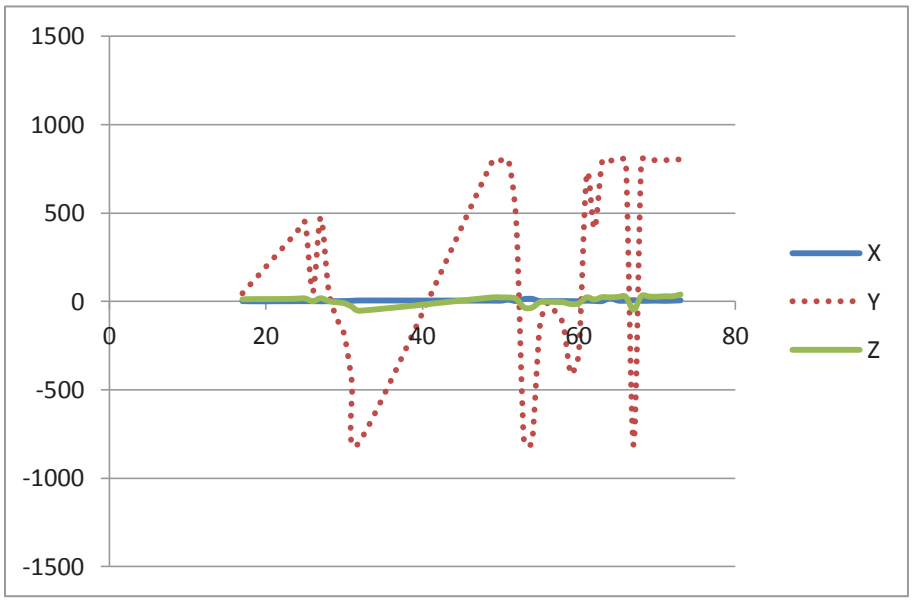

Figure 5.8 - Test Results - Faulty Polhemus Patriot results due to metallic interference

The reason for these results was investigated, and it was discovered that being a concrete floor, the metal reinforcement in the concrete was deforming the magnetic field, causing the faulty readings. The testing apparatus was moved onto a wooden desktop. However, errors continued to occurred, with the cause of the errors this time being determined as the metal runners of the desk drawers. After the runners were removed, the testing continued, with Figure 5.9 - Figure 5.11 showing the results collected.

These results illustrate the susceptibility of the system to metallic objects in the work space.

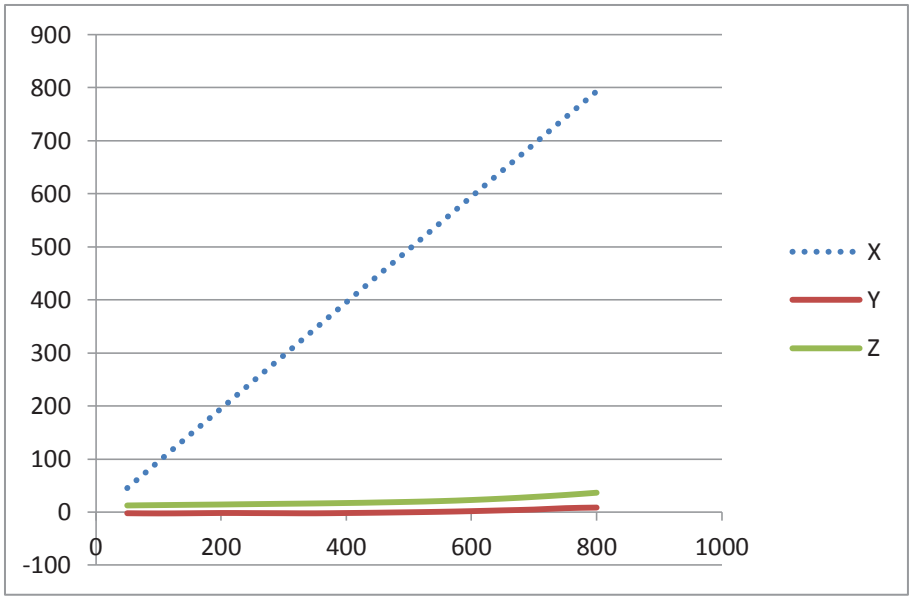

Figure 5.9 - Test Results - Measurements along X axis

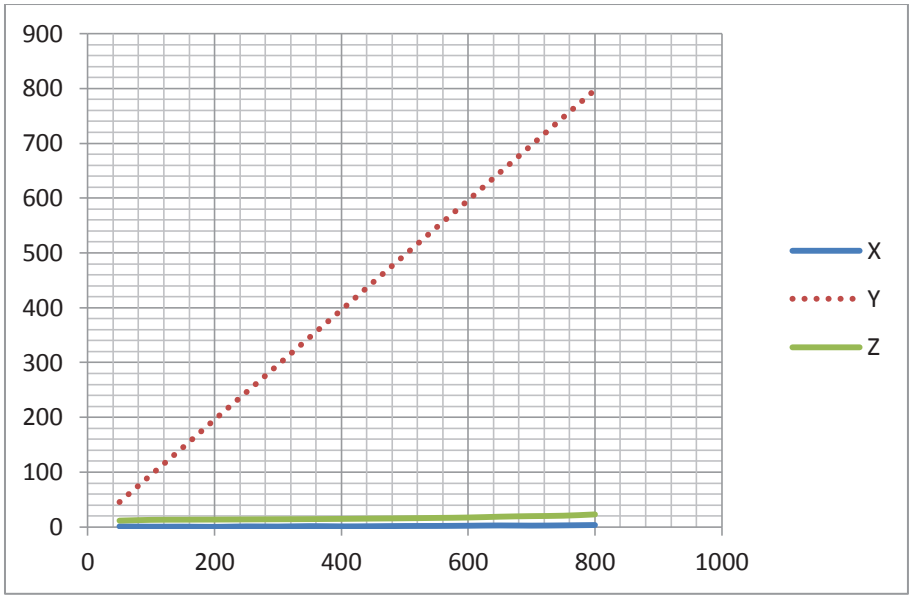

Figure 5.10 - Test Results - Measurements along Y axis

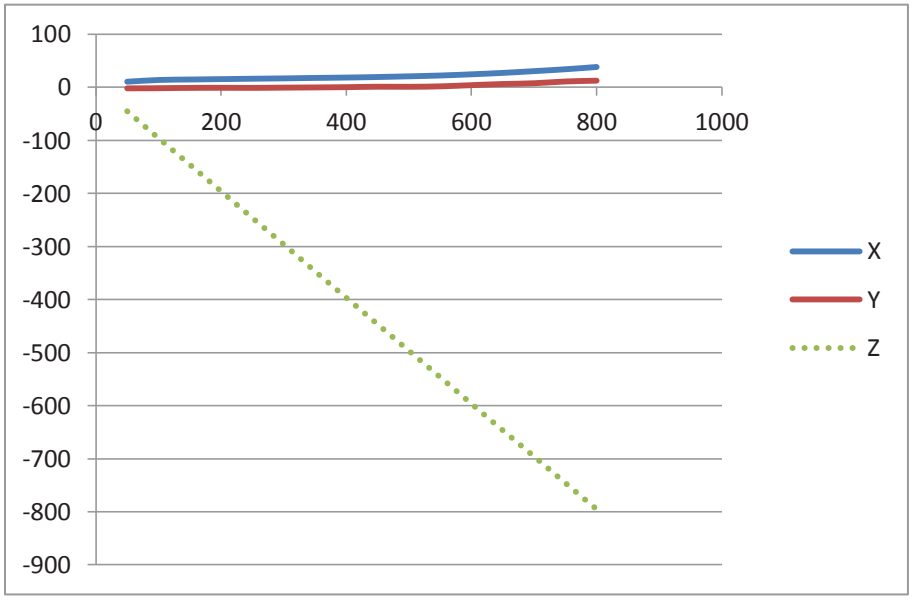

Figure 5.11 - Test Results - Measurements along Z axis

The angular measurement of the sensor was also tested. This was achieved by placing the sensor in a convenient location within the range of the system, and using the

spirit level and protractor, the sensor was set to a known angular orientation. The frame was captured via the software developed, and then compared to the orientation that the sensor was set at. As expected, the orientations captured by the sensor were equal to the set orientations.

The results above for both linear and orientation measurements of the system were positive, and validated the suitability of the Polhemus Patriot for use in this project.

5.4 **Compliant Control Utilising Force Feed-Back**

A key aspect to the implementation of this system was the use of active compliance to prevent the system from obstructing the abilities of the patient when approximately achieving the goals of the exercises. To achieve active compliance, a force sensor was employed to monitor reaction forces and torques between the robot end effector and patient. The intention was to use the readings from this sensor as feedback in the system to implement the active compliance.

This compliance was software controlled, providing control signals for the robot when in passive mode (following the patient's hemiparetic arm motion) or as a safety system, stopping the robot in case of force overload between the patient and robot. Software controlled active compliance has been used in a number of robotic applications [22, 116, 117].

As laid out previously in section 3.9, there were many requirements governing the selection of the force sensor. There were a selection of force sensors available on the market; however, the necessity for 6 degrees of freedom force and torque measurement

reduced the available options. ATI Industrial Automation manufacture a selection of force/torque sensors designed for use in robotic applications.

Based on the load requirements for the force sensor, the ATI Mini 45 force sensor was selected for this application, ensuring the capability to handle force or torque overloads without failing.

Figure 5.12 - ATI Mini 45 force/torque sensor

The Mini45 is a compact light weight force/torque sensor which measures force in the X, Y, and Z directions, and the torque about each of these three axes. It has a compact design, with a diameter of 45mm, and thickness of 15.7mm. The weight of the unit is 92gm, meaning that it would have little effect on the payload of the robot, but was still taken into consideration for the design of the mechanical robot patient coupling. Table 5.4 - Mini45 force/torque sensor parameters lists the force/torque sensor parameters.

Axes	Sensing Range (±)	Resolution	Overload
Fx, Fy	580N	1/4N	±5100N
Fz	1160N	1/4N	±10000N
Tx, Ty	20Nm	1/188Nm	±110N
Tz	20Nm	1/376Nm	±140N

Table 5.4 - Mini45 force/torque sensor parameters

The force sensor was interfaced with the main computer of the system via a factory supplied control box housing the required signal conditioning circuitry, and power supply, and a Data Acquisition (DAQ) Card. A National Instruments DAQ card, model PCI-6220, was selected for this purpose. Figure 5.13 shows the general hardware setup for the ATI Mini45 force/torque sensor.

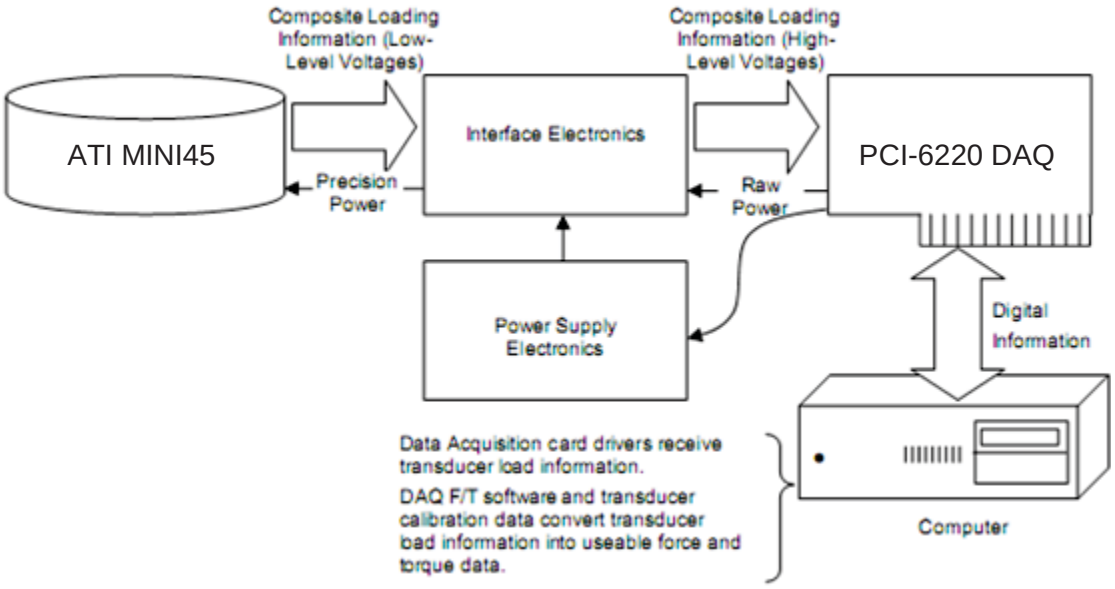

Figure 5.13 - Force sensor hardware setup

Operation of the force sensor and DAQ card was implemented using the NIDAQmx C++ SDK provided for use with the ATI force sensors.

The Mini45 force sensor was factory calibrated, with a calibration report supplied for future reference, and a calibration file supplied for use with the software and SDK supplied.

Prior to integrating the force sensor with the main system utilising the SDK, it was tested to verify that both the force sensor and SDK program employed in unison, would be suitable for the application. It was essential to verify the operation of this equipment in the C++ environment rather than using analysis software such as MATLAB with

Simulink or LabView, as the control for the final system was implemented in the C++ environment, meaning that analysis in other software, although potentially useful, would be irrelevant for the verification of the operation of the final system, or any of its individual components.

To test the force sensor, initially a basic C++ program was developed utilising the C++ library components of the supplied SDK. This program was to be the basis class for the active compliance component of the main system. The SDK provided methods for sampling the voltage readings of the force sensor from the DAQ card, making the program development relatively simple. Once the sample data was taken, it was output to a .csv file for later analysis. Figure 5.14 shows the flow diagram for the force sensor algorithm that the main function of the C++ program, Code 5.2, was based on, used for testing the force sensor.

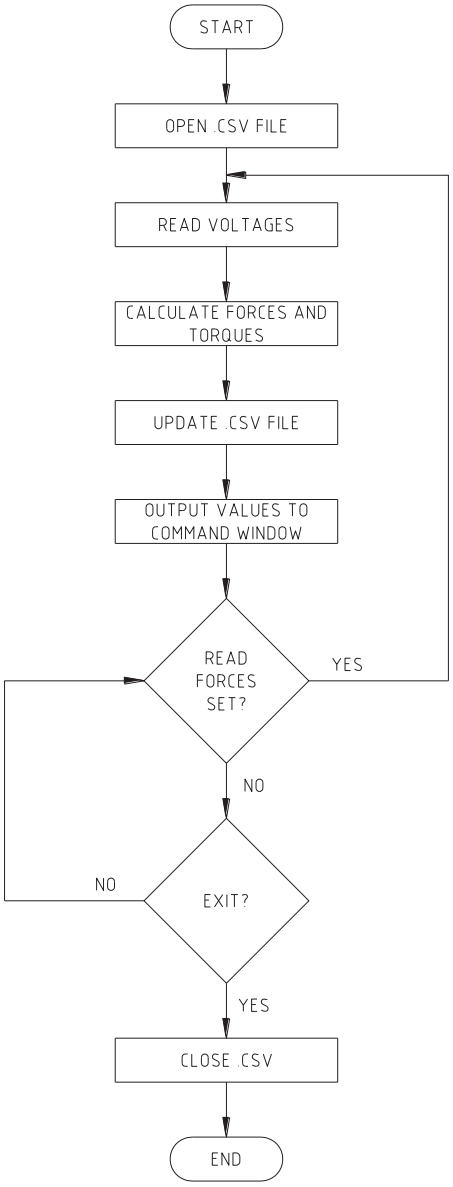

Figure 5.14 - Flow diagram for basic force sensor algorithm

A bracket was designed for testing the force sensor, allowing loads to be applied to the force sensor along the individual axes, as well as torques purely about these axes. With the force sensor mounted on the end effector of the IRB120 robot, to ensure the accuracy of the position and alignment of the force sensor, this bracket was mounted on the tool side of the force sensor.

```
void CDAQTest3Dlg::OnBnClickedupdaterdgs()
{
	static bool alreadyScanning = false;

	try
	{
		double readings[7];
		int mDAQstatus;

		mDAQstatus = mFTWrapper.GetForcesAndTorques(readings);

		for (int ind=0; ind<7; ind++)
		{
			loads[ind] = readings[ind];
		}
		UpdateGauges(readings);
	}
	catch(CException& e)
			{
				const int N = 80;
				char errmsg[N];;
				e.GetErrorMessage(errmsg,N,NULL);
				alreadyScanning = false;
			catch (DAQException* e)
			{
				e->GetErrMsg();
				alreadyScanning = false;
			}
			catch(...)
			{
				alreadyScanning = false;
			}
			frcread = true;
}

void CDAQTest3Dlg::UpdateGauges(double readings[6])
{
	CString str;
	str.Format("%4.4f",readings[0]);
	m_wndFx.SetWindowText(str);
	str.Format("%4.4f",readings[1]);
	m_wndFy.SetWindowText(str);
	str.Format("%4.4f",readings[2]);
	m_wndFz.SetWindowText(str);
	str.Format("%4.4f",readings[3]);
	m_wndTx.SetWindowText(str);
	str.Format("%4.4f",readings[4]);
	m_wndTy.SetWindowText(str);
	str.Format("%4.4f",readings[5]);
	m_wndTz.SetWindowText(str);

	UpdateQuart(readings);

}

void CDAQTest3Dlg::UpdateQuart(double readings[6])
{
	double quat[4];
	CString cstr;

	readings[2] = sqrt(readings[3]*readings[3]+readings[4]*readings[4]+readings[5]*readings[5]);

	double magq =
sqrt(readings[2]*readings[2]+readings[3]*readings[3]+readings[4]*readings[4]+readings[5]*readings[5]);

	for (int j=2; j<6; j++)
	{
		quat[j-2] = readings[j]/magq;
	}

	cstr.Format("%4.4f",quat[0]);
	m_wndQ0.SetWindowText(cstr);
	cstr.Format("%4.4f",quat[1]);
	m_wndQ1.SetWindowText(cstr);
	cstr.Format("%4.4f",quat[2]);
	m_wndQ2.SetWindowText(cstr);
	cstr.Format("%4.4f",quat[3]);
	m_wndQ3.SetWindowText(cstr);
}
```

Code 5.2 - Function used for reading force sensor

To measure the forces in each of the X, Y, and Z axes, the robot was manoeuvred manually via its flex-pendant to position these axes vertically in turn, and while in position each axis was loaded between 0 and 3kg in 50gm increments, with the readings

recorded in the .csv output file. Figure 5.15 – Figure 5.17 shows the plotted results of the forces in the 3 axes.

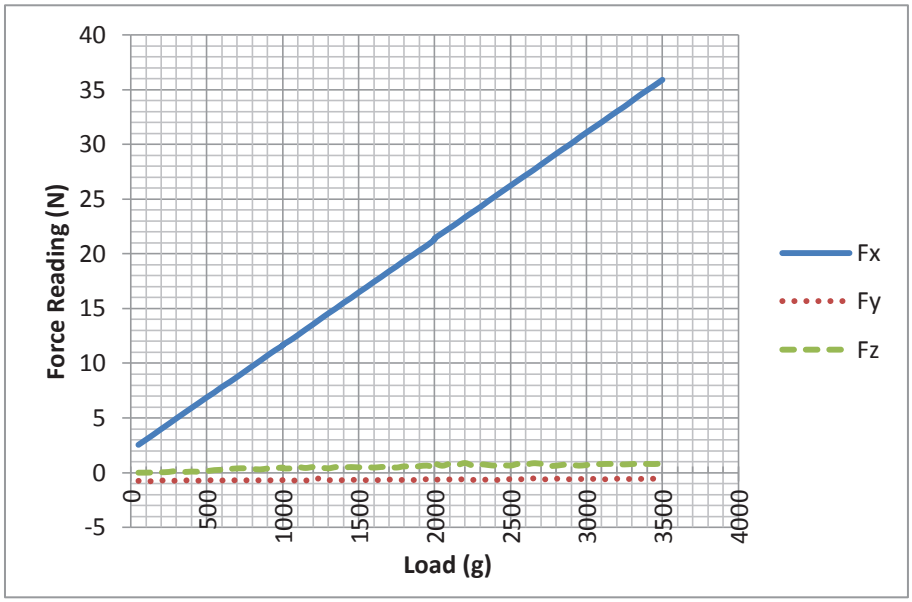

Figure 5.15 - Test Results - X Axis forces

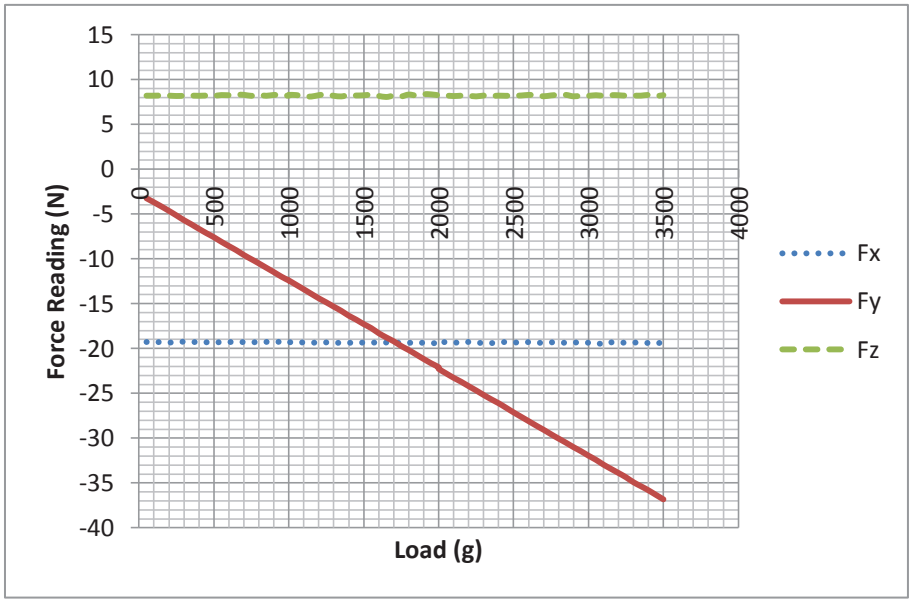

Figure 5.16 - Test Results - Y Axis Forces

Figure 5.17 - Test Results - Z Axis Forces

The torque output of the sensor was evaluated in a similar manner, using the same bracket. However, in this case the force sensor was positioned with each of the three main axes positioned horizontally with the loading offset horizontally from the axis being tested by 50mm, perpendicular to the main axis of the force sensor, 0 point of the axis. Figure 5.18 – Figure 5.20 show the plotted torques of the force sensor about the three axes.

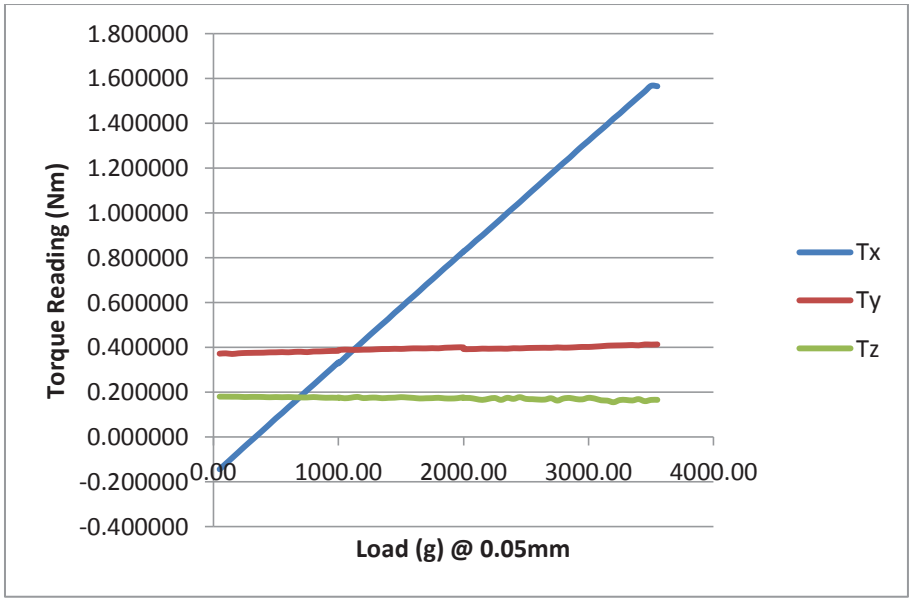

Figure 5.18 - Test Results - Torque about X Axis

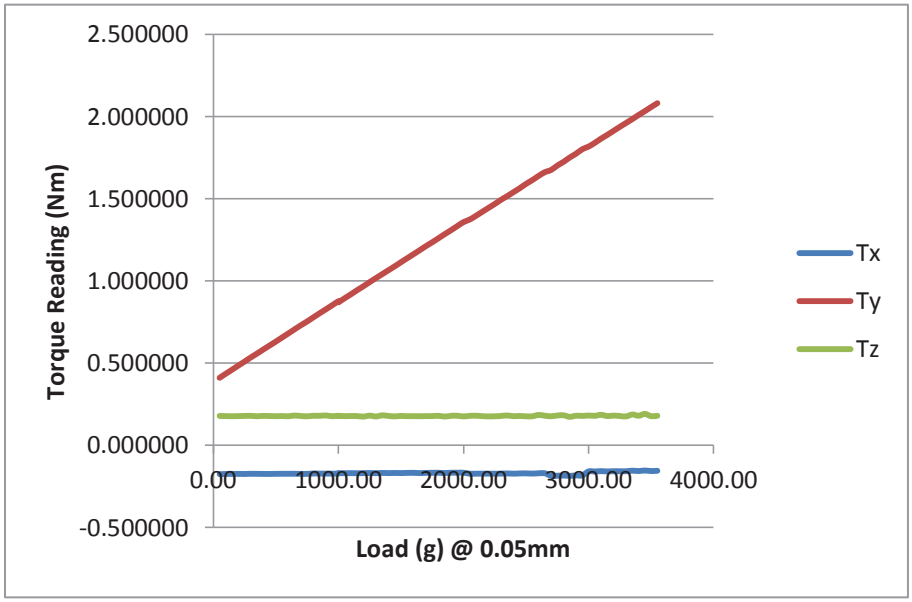

Figure 5.19 - Test Results - Torque about Y Axis

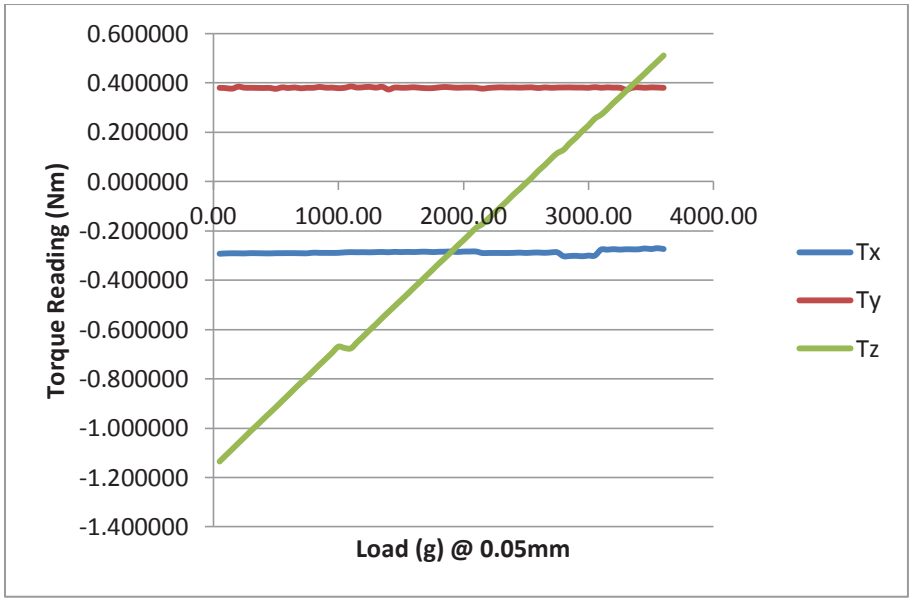

Figure 5.20 - Test Results - Torque about Z Axis

As Figure 5.15 - Figure 5.20 shows, the force sensor has good linear operation over the range tested, with each axis having an offset at zero loading. This offset is to be expected, and provision is supplied in the SDK by way of a bias function for re-zeroing the sensor readings. This offset shown in the graphs, maybe due to a number of aspects including thermal expansion in the mechanical structure of the sensor or the weight of the bracket used during the verification procedure. This offset however needed to be accounted for in the final system, to ensure a zero reading which was to be used as the target force in the compliance control algorithm. The bias function was integrated into the force sensor class to be used in the final system, as shown in Figure 5.21. An advantage of the capability of biasing the sensor would mean that the system would be capable of being zeroed with the patients arm in situ, giving a true zero point for the system, regardless of the variation of arm weight of individual patients.

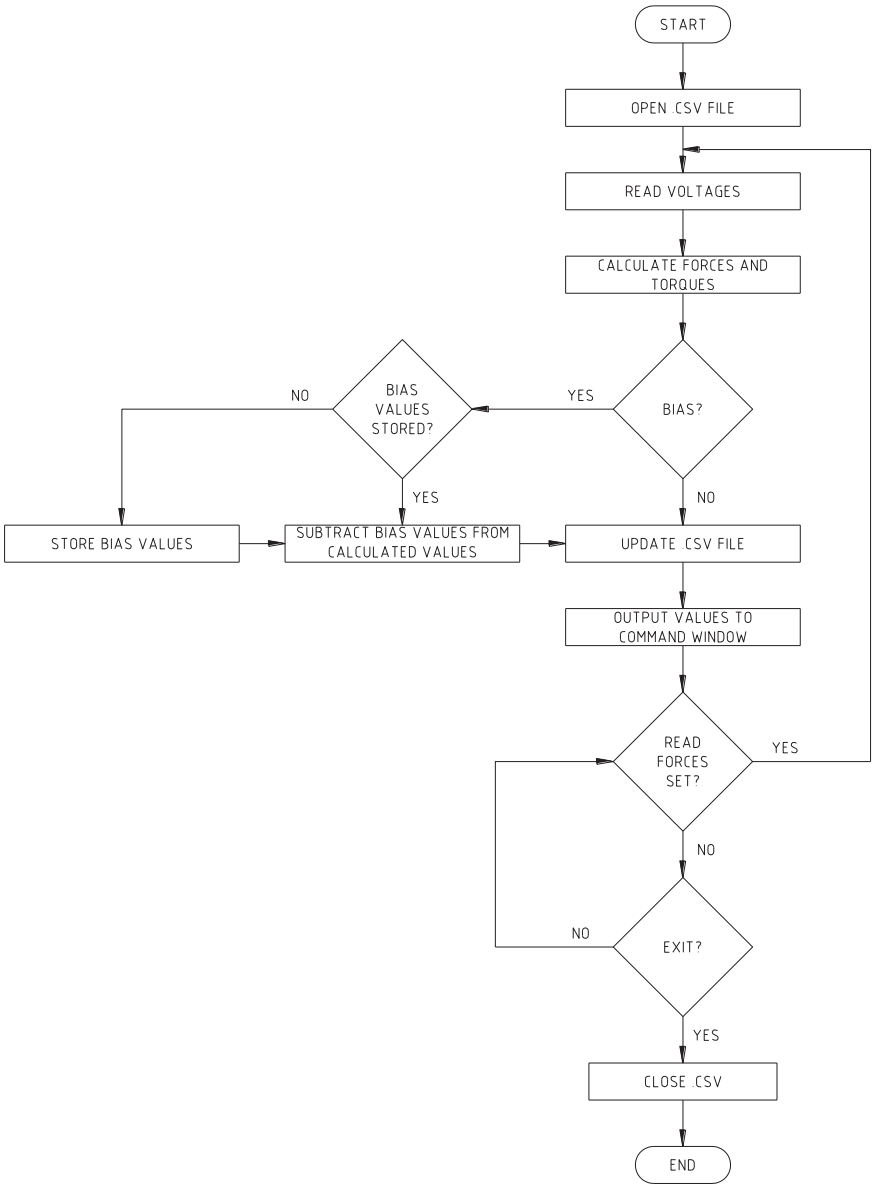

Figure 5.21 - Force sensor algorithm updated with bias function

```
void CDAQTest3Dlg::OnBnClickedBias()
{
	if (Biasval)
	{
		Biasval = false;
	}else
	{
		Biasval = true;
	}

	if (Biasval)
	{
		mFTWrapper.Bias(true);
	}else
	{
		mFTWrapper.Bias(false);
	}
}
```

Code 5.3 - Function for controlling bias state

5.5 **Mechanical Robot-Patient Coupling system**

For the final system to operate as a rehabilitation system for stroke, it is essential to devise a method of connecting the robot to the patient to be able to manipulate their limbs during exercises. As industrial robots such as the IRB120 are not usually used for this type of application, and robot manufacturers don't recommend the use of their robots for this purpose, there are no mechanisms on the market that could be obtained for this project. Therefore a mechanical robot patient coupling was designed for this project. This device was to be a rigid connection between the robot and the patient to ensuring that the manipulation forces of the robot would be transferred to the patients arm when needed. The ATI Mini45 force/torque sensor would also be part of this mechanism.

5.5.1 **Considerations**

The first consideration of this device was safety. As this is the connection between the robot and patient, it is essential to consider the safety of the patient at this point. To prevent the patient from being injured by the robot, it was decided that, in the case of force overload from the robot, the robot should be instantly decoupled mechanically from the patients arm.

As discussed in section 3.1, the considered injury risks for this project were bruising, or soft tissue injury, to broken bones in the worst case scenario. To prevent injury, the maximum forces exerted on the patient through the coupling were limited to ~3.5kg, with the coupling intended to disconnect at this loading.

Although it was intended that this mechanism would be able to decouple the robot from the patient in the case of overload, it was also important that the coupling be rigid. This was necessary to ensure that the robot will move the patients arm to the correct

positions where necessary, without flexure that would cause incorrect positioning, which could also affect the accuracy of the Mini45 readings.

5.5.2 **Design**

There were a number of physical attributes that needed to be considered in the design of robot-patient coupling system. The obvious requirements being that the coupling assembly needed to be able to be mounted on the end effector of the IRB120, the Mini45 force/torque sensor needed to be an integral part of the assembly, and the patients arm needed to be comfortably supported at the opposite side of the coupling to the robot. However, the assembly also needed to be as lightweight as possible, and the length needed to be kept to a minimum to reduce the moment induced on the robots end effector.

Taking inspiration from the MIME project, an orthopaedic wrist brace was selected to hold the patients arm. This was a lightweight, rigid, padded wrist brace that supported the forearm, wrist, hand and fingers, allowing the hand and fingers to rest in a neutral position, with the forearm slightly supinated (rotated about the axis of the forearm), allowing the patients arm to sit in a comfortable relaxed position. Figure 5.22 - Wrist brace selected to support the patients arm shows the wrist brace selected.

Figure 5.22 - Wrist brace selected to support the patients arm

Both left and right handed wrist braces were employed in this project, with one side used for mounting on the robot-patient coupling, and the other used for mounting the sensor of the Polhemus Patriot motion sensor via a flat plastic bracket. As strokes can effect either side of the human body, depending on where they occur in the brain, the wrist braces were mounted in a manner that would allow them to be mounted with either the robot-patient coupling, or the motion sensor bracket, meaning that the system would be capable of rehabilitation exercises with patients effected by stroke on either side of the body.

A lightweight material was required for the main assembly of the robot-patient coupling. Composite materials were considered for this purpose, but aluminium was selected instead for ease of manufacture, ensuring the rigidity and simplicity of the assembly.

As stated previously, the safety of the patient was a key aspect to be integrated into the design of this mechanism. Although this was considered to be a redundant safety feature, as there were to be other safety systems in the control software, and cut out switches to stop the robot, it was possibly the most important safety feature to ensure that robot would be mechanically disconnected in a fault situation, which would potentially cause excessive forces being transferred from the robot to the patient.

Shear pins and torque limiters are commonplace in engineering to preform similar tasks in mechanisms to protect equipment from overloads. Shear pins are sacrificial elements designed to fail at pre-determined loading conditions, and can be used for both torque and lineal force loadings. Once failure occurs, shear pins are no longer functional, and must be replaced. Alternatively, Torque limiters perform a similar function, limiting torque transmitted through shafts. Grouped in to two main categories, this first limits the

transmission of torque by employing a clutch mechanism that slips when the torque limit is reached, allowing a safe level of torque transmission to be maintained, utilising friction plates or magnetic means to achieve this. The second category utilise mechanical methods such as pawl and spring or ball detent mechanisms to disconnect the drive shaft from the driven shaft, preventing torque transmission in overload situations. Shear pins used in torque applications can be considered to be included in this category.

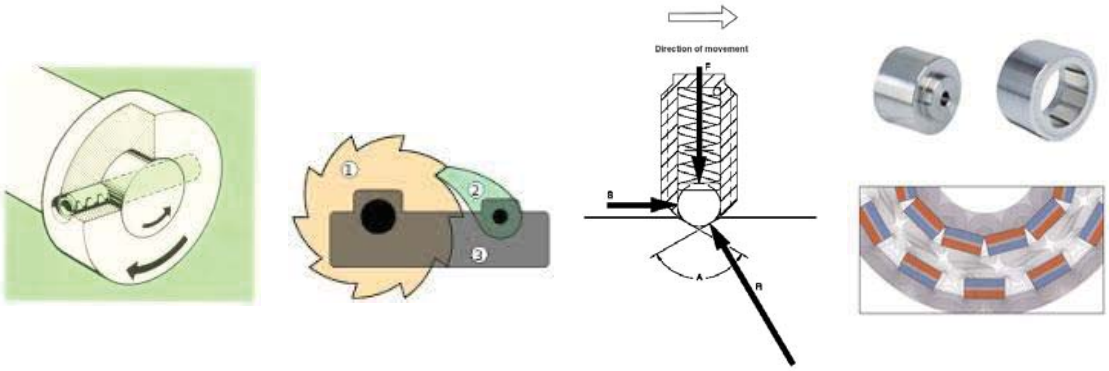

Figure 5.23 - Examples of torque limiter types.

From left to right - shear pin, pawl and spring, ball detent, synchronous magnetic coupling

For this project, the coupling required the ability to break the mechanical connection between the robot and patient in about three axes, as the motion of the robot is in three dimensions. This meant that torque limiters available on the market were unsuitable for use in this project as they are designed for use in a single axis, along the shaft. To this end, a torque limiting coupling was devised, allowing the coupling to disconnect due to excess loading about any axis.

On evaluation of the methods employed for decoupling shafts, the use of clutch mechanisms, and pawl and spring mechanisms were deemed unsuitable, as the operating principle of the mechanisms tend to limit torque by operating in a plane perpendicular to

the axis of the shaft, and generally do not disconnect the shafts. This deemed these mechanism designs unsuitable for this application.

Magnetic solutions were also unsuitable due to the risk of interference with the Polhemus Patriot motion sensor.

To develop a coupling that was capable of disconnecting the patient from the robot due to force overload in any direction, shear pins, or a ball detent mechanism would be the most suitable options. When considering the requirement for testing and evaluation of the coupling, and that the system was intended for use in clinical environments where tools may not be readily available for repair should the coupling break, it was decided that shear pins would not be suitable as they would need replacement should failure occur. This would mean a necessity for spare parts, and down time of the system which could be problematic in a clinical environment.

Therefore, a coupling was developed utilising a ball detent mechanism to decouple the patient from the robot. This would result in a mechanical coupling that would disconnect the patient from the robot from any force overload, but would be able to be put back in place easily without the requirement for tools or spare parts.

The mechanical design of this coupling system was performed using SolidWorks 3D CAD software. It was designed to be compact, and lightweight, as mentioned previously. The final design of the coupling robot-patient coupling system is shown in Figure 5.24 with Figure 5.25 showing its exploded view.

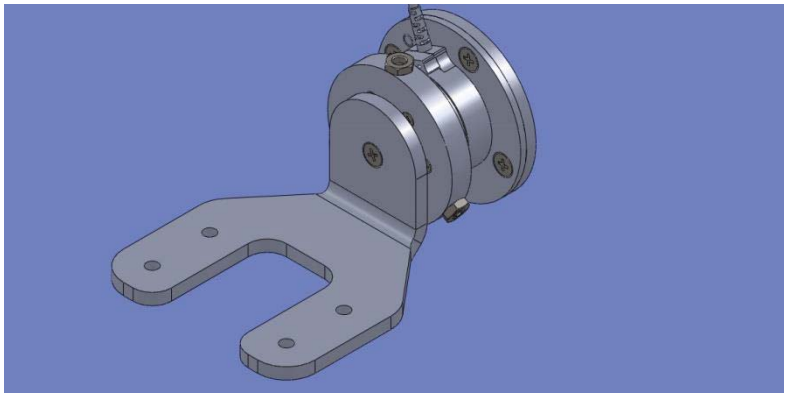

Figure 5.24 - Robot-Patient Coupling final design

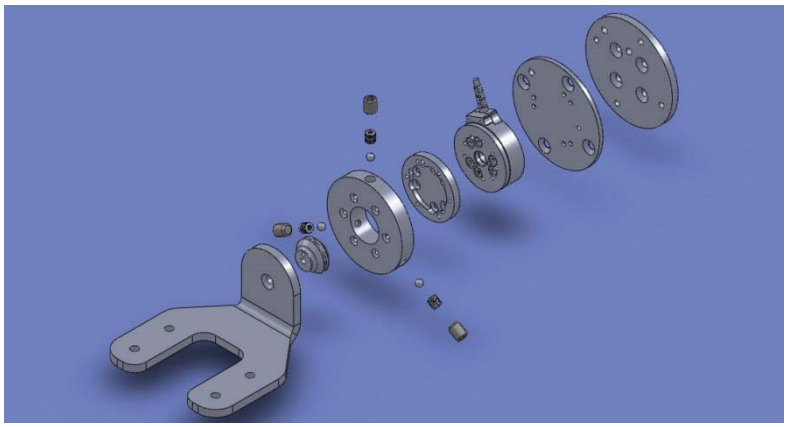

Figure 5.25 - Robot-Patient Coupling exploded view (fasteners omitted)

The size of the mechanism was based around the diameter of the robot end effector, and the Mini45 force/torque sensor, with a minimised length to reduce the moment induced about the robot wrist by the weight of the patients arm.

When designing the coupling mechanism, it was considered as a section through a cantilever beam. Regarding the loading in this manner, any forces applied by either the robot or patient would induce a moment about this point of the coupling. This means that the coupling was designed around the bending moments at this point. The detachable coupling was conceptualised as a cup and ball type arrangement (considered in kinematics as a spherical joint), which when overloaded, would allow moments about any

axis to cause the coupling to disconnect. Figure 5.26 shows the concept of the cup and ball connection.

Figure 5.26 - Cup and ball connection concept

Spherical joints tend to be free moving, allowing for misalignment of the components being coupled together. A flexible coupling was not suitable for this project, so ball detent mechanisms were employed to lock the motion of the coupling resulting in a rigid assembly that would disconnect at a set loading. The ball detent mechanisms were placed equally about the main axis of the coupling on a plane perpendicular to this axis as shown in Figure 5.27 - Illustration of ball detent mechanism placement.

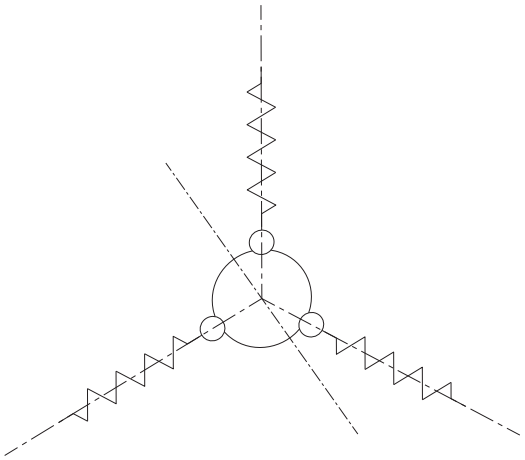

Figure 5.27 - Illustration of ball detent mechanism placement

With this configuration, two loading modes were assumed to cause the mechanism to disconnect. The moments that would result in disconnection of the coupling can be taken

as acting either about the main axis of the coupling (mode 1), or about an arbitrary axis lying on the plane of the spring detent mechanisms (mode 2). Taking a mode 2 loading condition as the starting point for the design calculations to determine the required spring force for the mechanism, based on a ball detent size deemed suitable for the size of the mechanism.

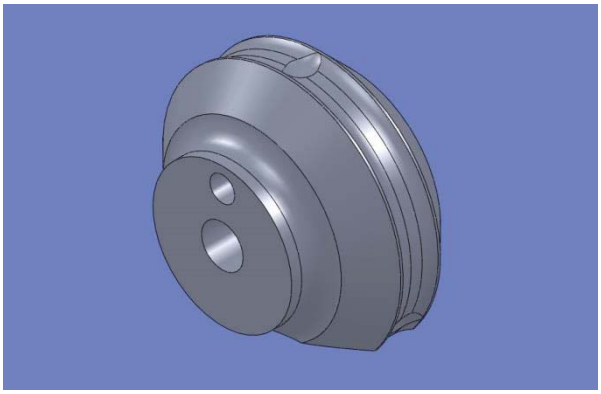

Figure 5.28 - Coupling centre showing ball detents

Figure 5.28 shows the centre of the coupling mechanism with the ball detents. Considering the two modes of decoupling loading conditions mentioned above, the mode 2 loading conditions were taken as acting about the axis running through two of the three ball detent centre points, with the third ball detent centre providing the reaction moment for the loading. This loading condition assumes, for simplification, that the decoupling will occur due to overloading of one ball detent mechanism. The mode 1 loading condition is taken as a torsional loading through the main axis of the coupling, with all three ball detent mechanisms providing the reaction moment. This meant that in this mode, decoupling would result from overloading all three ball detent mechanisms, meaning a lower loading force per mechanism than the mode 2 loading.

Therefore the approach taken to designing the mechanism was to determine the required spring loading for decoupling in mode 2, then using this spring force, determine

a suitable incidence angle for the ball detent mechanisms in mode 1 loading. The differing ball detent depths were achieved via a groove machined around the circumference of the centre piece as shown in Figure 5.28. The following shows the design process for the ball detent mechanisms.

Firstly determining the loading of the detent mechanism in mode 2

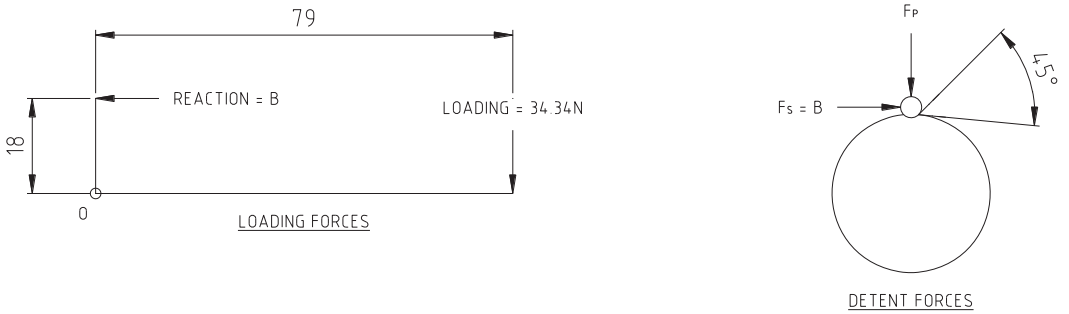

$$\sum \boldsymbol{M_O \rightarrow 0.018 * B = 0.079 * 34.34} \quad \textbf{(8)}$$

$$\therefore B = 150.69N$$

For ball detent mechanism:

$$\boldsymbol{F_S = F_P \tan \theta} \quad \textbf{(9)}$$

Where:

F_S is the side loading or breaking force

F_P is the spring loading force

θ is the angle of incidence

Given F_S = B, and θ=45º

$$\therefore \tan \theta = 1$$

$$\therefore F_P = F_S = 150.69N$$

Determining the required angle of incidence for the mode 2 loadings,

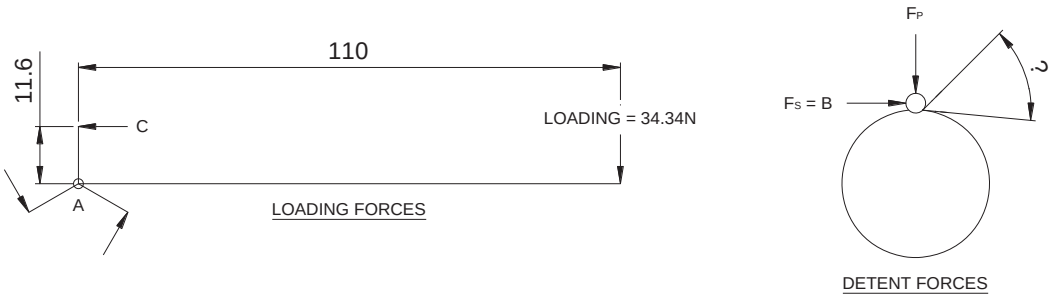

$$\sum \mathbf{M_A} \rightarrow \mathbf{0.110 * 34.34 = 3 * 0.0116 * C} \quad \textbf{(10)}$$

$$\therefore C = \frac{0.11 * 34.34}{3 * 0.0116}$$

$$= 108.55N$$

Taking (9) and rearranging

$$\mathbf{\tan(\theta) = \frac{F_S}{F_P}} \quad \textbf{(11)}$$

$$\therefore \theta = \tan^{-1}\left(\frac{F_S}{F_P}\right)$$

$$= \tan^{-1}\left(\frac{108.55}{150.69}\right)$$

$$= 36°$$

These calculations provided the target angle for the design of the detent mechanisms, and a suitable estimation for the required spring force for the selection of the springs for the ball detent mechanisms; however, this was a starting point, and a spring with a suitable spring constant was selected to provide the calculated force at approximately half compression, and the ball detent mechanisms were designed to be adjustable to provide

the correct force loadings required to hold the centre piece of the coupling. The completed mechanism was then tested to confirm the operation of the coupling, confirming the theoretical spring force calculated, and evaluating the validity of the estimated loadings stated previously.

5.5.3 **Evaluation**

The coupling centre was initially manufactured from aluminium to reduce the weight of the assembly, however, due to the loading required from the springs to ensure the rigidity, aluminium was a poor choice, as it was too soft, and experienced plastic deformation under load. This issue was rectified by replacing the original aluminium centre piece with a case hardened steel centre piece that didn't deform, but added additional weight to the assembly, with the aluminium centre piece weighing 9g and the hardened steel centre piece weighing 29g. However, this weight difference would have little effect on the overall system, when taking into consideration the variance in arm weight of 1.33kg found in Table 3.1.

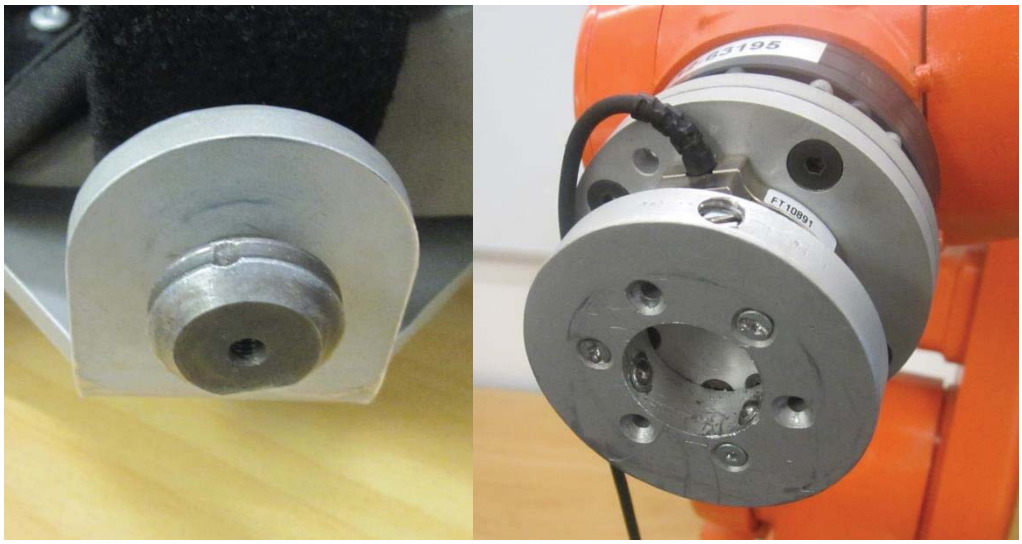

Figure 5.29 - Break joint centre piece and ball detent

Figure 5.30 - Break joint assembled with robot

The coupling, shown in Figure 5.29 & Figure 5.30, was tested for suitability of application by experimental means. Initially, the coupling was tested using a spring balance to apply and measure the load. With the coupling mounted on the robot for convenience, the coupling was positioned with its central axis horizontally aligned with one of the three spring detent mechanisms aligned vertically. The spring balance was suspended above the couplings central axis, 80mm from the central axis of the spring detent mechanism, as this was selected arbitrarily as the location for the central axis of the patients arm during the design process.

The spring balance was connected to the coupling via a turn buckle arrangement for fine adjustment. As previously discussed in section 3.1, and used as the maximum loading in the design calculations, the loading at which the coupling should disconnect was determined to be 34N to minimise risk of injury to the patient while still being capable of completing rehabilitation exercises.

The robot was used to apply a loading of approximately 30N, with the final loading via adjustment of the turnbuckle to achieve a loading of 34N. The spring tension of the

detent mechanism was adjusted to the point where the mechanism would release the coupling, thereby setting the break load.

Using a spring balance was proven to not be the best apparatus for setting the break loading, as it was discovered during testing that as the mechanism began to release, the splint end of the coupling to move in the direction of the loading force, thereby reducing this force. As the force released, the coupling remained engaged in a semi flexible state. This meant that the coupling mechanism displays a degree of passive compliance that was not expected. This is advantageous to the operation of the system, allowing the system to remain engaged while still reducing the load in the case of marginal overload conditions which may otherwise disconnect the coupling and stop the rehabilitation exercises. This behaviour would be dependent upon the depth and contact angle of the ball detent mechanism. However this will require further investigation in future developments of the system.

Due to the unexpected results of testing the coupling with the spring balance, the procedure was repeated using weights for the loading force to ensure a constant force throughout the disconnect event of the coupling to ensure the correct break loading is set. With weights used in place of the spring balance, the coupling operated as expected, disconnecting cleanly at the set loading of 34N.

To test the operation of the coupling with regard to rotation about the central axis, a bar was bolted to the centre piece in place of the splint mount, using a cap screw. The head of the cap screw was supported to remove any cantilever loading on the coupling, ensuring a pure torque loading about the axis. Considering the splint selected for use in this project (Figure 5.22), it was considered that the risk of injury would come from the arm end of the splint, where it is likely to press against the flesh of the forearm of the patient, as

opposed to the wrist and hand that were fully supported, and held firm by the splint, with minimal risk of injury. The distance from the end point of the splint to the central axis of the coupling was approximately 110mm. Therefore, the 34N loading was suspended from the bar attached to the coupling at 110mm form the central axis to simulate the loading conditions with the splint in place. With the coupling previously set to break at 34N, it was found that in a pure torque loading, the centre piece of the coupling rotated easily, and with further investigation, reducing the loading to 29N, and gradually increasing the loading by increments of 0.5N, the break loading was 33N, or 3.63Nm, which is less than the calculated value, but still acceptable for the operation of the coupling.

The difference in calculated torque loading to the actual loading measured is likely due to the accuracy of the machining of the dimple and groove of the coupling centre piece. Although the centre piece was machined to the tight tolerances (-0.02mm) of the design drawings this still allowed for an angular variance of 1.3º which would equate to a loading variance of approximately 1N as observed during testing.

6 System Control Implementation

The control system for this project was implemented in two parts, the first being developed in the C++ environment to run on a host computer, utilising the individual classes developed for the separate components of the system. These classes were integrated to develop a program that would retrieve information from both the motion sensor and the force/torque sensor, transform the target given by the motion capture system to a position mirrored through the patient's sagittal plane, calculate the joint targets for the robot and confirm that the position was within reach of the robot. If the target was within the robot's reach, this data was then transmitted to the robot controller by a socket server class via TCP/IP protocols over an Ethernet connection, otherwise, the data was disregarded, and new data would be retrieved from the sensors.

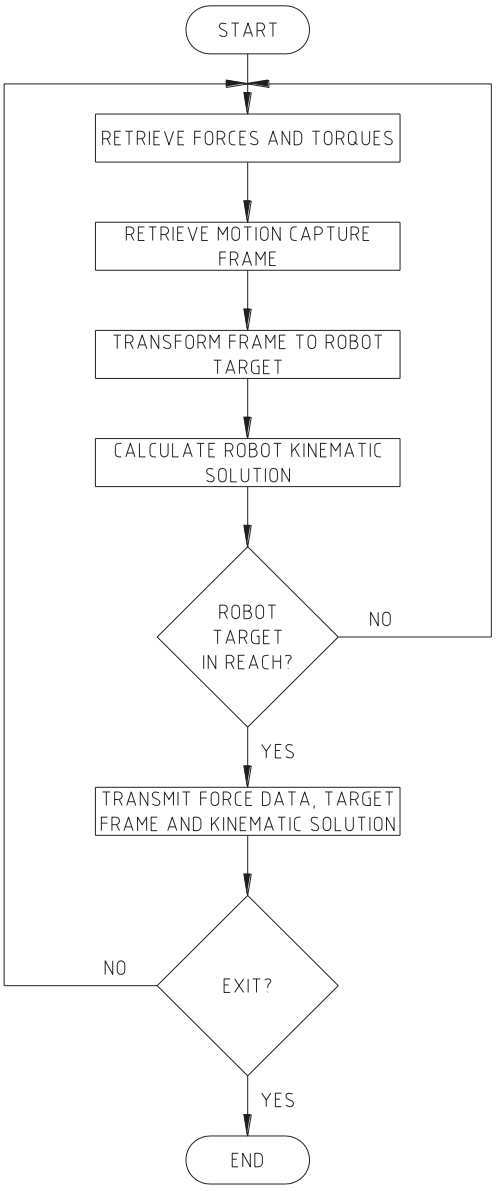

Figure 6.1 - General flow diagram for host computer control algorithm

The second part of the main control was developed in the proprietary ABB Rapid environment to run on the ABB IRC5 robot controller attached to the IRB120 robot arm. This program was used to connect to the socket server class on the host computer and retrieve the sensor and joint information for control of the robot. The target was used for comparison with the current robot position to determine whether the patient's hemiparetic arm was mirroring the motion of the healthy arm, within an allowable margin of error. If

the patient's arm was within the margin of error, the program would take a passive role in the exercise, being led by the patient. This was achieved using a simple proportional control algorithm that took the force information as an input to determine a new robot target that would move the robot to a position that would result in reducing the torques and forces, read by the force sensor, toward zero.

If the difference between the position of the robot end effector and the target position from the Polhemus Patriot was outside the margin of error, then the program would use the Polhemus Patriot target for control, thereby actively taking control of the patient's hemiparetic arm, aiding the patient in achieving the exercise.

In the case of the Rapid program throwing an error if the given robot target created a singularity condition, an error handler was developed, using the joint targets calculated by the host computer to control the robot instead of the robot target that threw the error.

For the possibility of a singularity error occurring from the robot target calculated from the force/torque readings, an error handler was developed that would disregard this target, and the program would retrieve new readings from the host computer to calculate a new target.

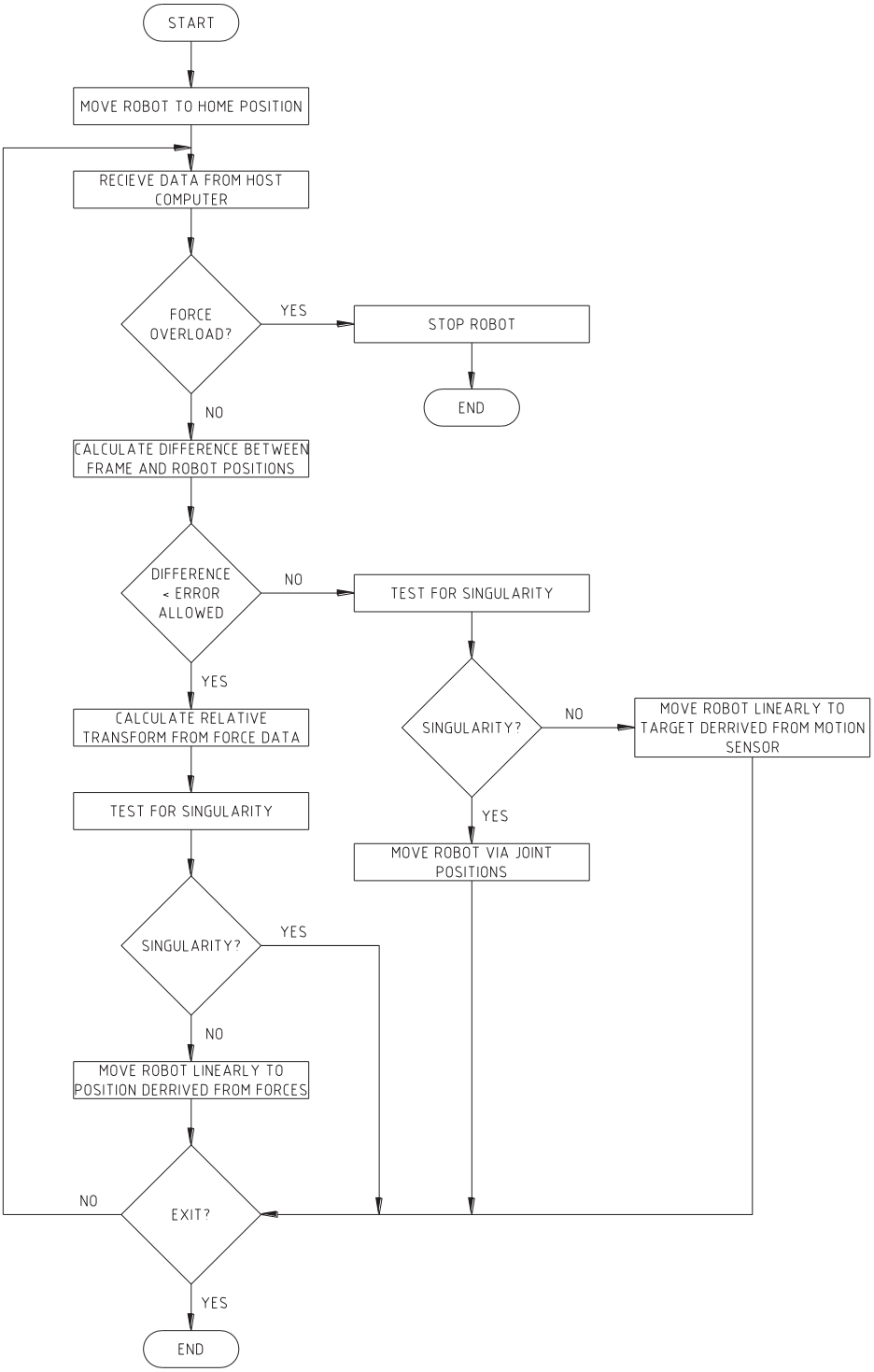

Figure 6.2 - General flow diagram for robot controller algorithm

The control for the system was divided between the two systems to aid the operation of the system, in an attempt to achieve “real time” operation of the system. The

Allocation of the data retrieval from the sensors to the host computer, while allocating the robot control algorithms to the robot controller allowed the separate processes to be executed simultaneously. However, this was also necessary due to the different programming environments required for the equipment.

6.1 Implementation of Robot Control Utilising Closed Form Solution

The first step in implementing the control algorithms for the system was to develop a C++ class to calculate and store the required joint positions of the robot for a given robot target. These joint positions were used to ensure that a given robot target was within the reach of the robot, and, in the case of the Rapid program throwing an error due to a singularity situation, to provide an alternative solution for the robot target.

The calculated joint positions were also required for determining the robot configuration data needed for the Rapid functions. The configuration data is used in the Rapid programming functions to determine the direction of rotation for the robot joint, and the desired quadrant for the joint to be moved to, thereby defining the goal for the desired kinematic solution of the Rapid program. Due to the nature of the system that was developed, which, unlike typical industrial robot applications that use predefined frames for the robot programing, used frames determined during run-time. This meant that it was also essential to develop an algorithm to calculate the robot configuration data during run-time.

As the IRB120 was a 6 DOF robot arm, there were multiple solutions for the joint angles to achieve the required end effector position. However, the number of theoretical solutions was reduced by the physical restrictions of the robot's joints shown in Table 6.1. The algorithm for the joint class systematically calculated the required angle for each joint in turn, utilising the formulae derived for the closed form solution.

Axis	Working Range
1	+165° to -165°
2	+110° to -110°
3	+70° to -110°
4	+160° to -160°
5	+120° to -120°
6	+400° to -400°

Table 6.1 - Joint ranges for ABB IRB 120

On examination of equations 1-3, it is apparent that these joints have multiple theoretical solutions; however, not all of the solutions for any given joint will be correct to provide a solution for the set of joint angles required for the robot to reach the target position. Therefore, it was necessary to determine the appropriate joint solutions to produce a correct set of joint angles to achieve the goal.

As each joint angle was calculated, tests were put in place through the algorithm to determine whether the angle calculated was suitable to achieve the kinematic solution for the robot. For all joints, the calculated angle was tested to confirm that it was within the joints range of motion. If the calculated angle was outside of the range of motion for the given joint, the next solution was calculated and tested. If no solution was available for a given joint, the algorithm would return raising a flag to indicate that the given target was out of reach for the robot. Due to the configuration of the IRB120, the Z position of the end effector was governed by the combination of the joint angles of joints 2 and 3. Because of this, it was also necessary to determine that the combination of these two calculated joint angles would produce the correct Z coordinate for the robot target, if not, the alternative solutions would be tested, and if no valid solution was found, the algorithm would also return, raising the flag to indicate that the given target was out of reach. The use of each joint's range of motion as a restriction on the theoretical solutions for the

robot also aided in simplifying the selection of the set of joint angles for the kinematic solution, reducing the possible solutions.

In the case of singularity where any pair of joints 1, 4 or 6 axes aligns so that they are collinear, producing an infinite set of solutions, it was necessary to develop a method to overcome this situation if it arises, and devise a solution that could be used if the Rapid program threw an error due to this situation. Considering the configuration of the IRB120, singularities can occur when joints 1 and 6 are aligned, or when joints 4 and 6 are aligned; however, due to the offset of link 4 (a_3 of the Denavit-Hartenberg parameters) joints 1 and 4 cannot align to produce a singularity condition, as when they are parallel, they will always be offset by 70mm.

For the case of joints 1 and 6 aligning, this could only happen when the wrist was positioned directly above the base frame with the axis of joint 6 aligned vertically, thereby lying on the rotational axis of joint 1. Taking the origin of the end effector frame at the intersection of the three wrist axes meant that this condition could be determined independently of the orientation of the end effector, simplifying the test for this singularity condition. This meant that the test for this condition was simply a case of checking the X and Y coordinates of the robot target, and if both of these coordinates were equal to zero, the angle of joint 1 would be arbitrary, and therefore set to zero. The angle of joint 6 would then be calculated accordingly to achieve the required orientation for the robot's end effector. However, this singularity condition was unlikely to occur as the positions required by the patient's movements to raise this situation would be outside the likely reach of the patient's arm.

Singularities caused by the alignment of joints 4 and 6 were dependant on the calculated angle of joint 5, as they could only be in alignment if the angular position of

joint 5 was 0º. Therefore, if joint 5 was calculated to be 0º, then joint 4 would be set to 0º, and again, joint 6 would be calculated accordingly to achieve the required goal. Figure illustrates the flow of this algorithm.

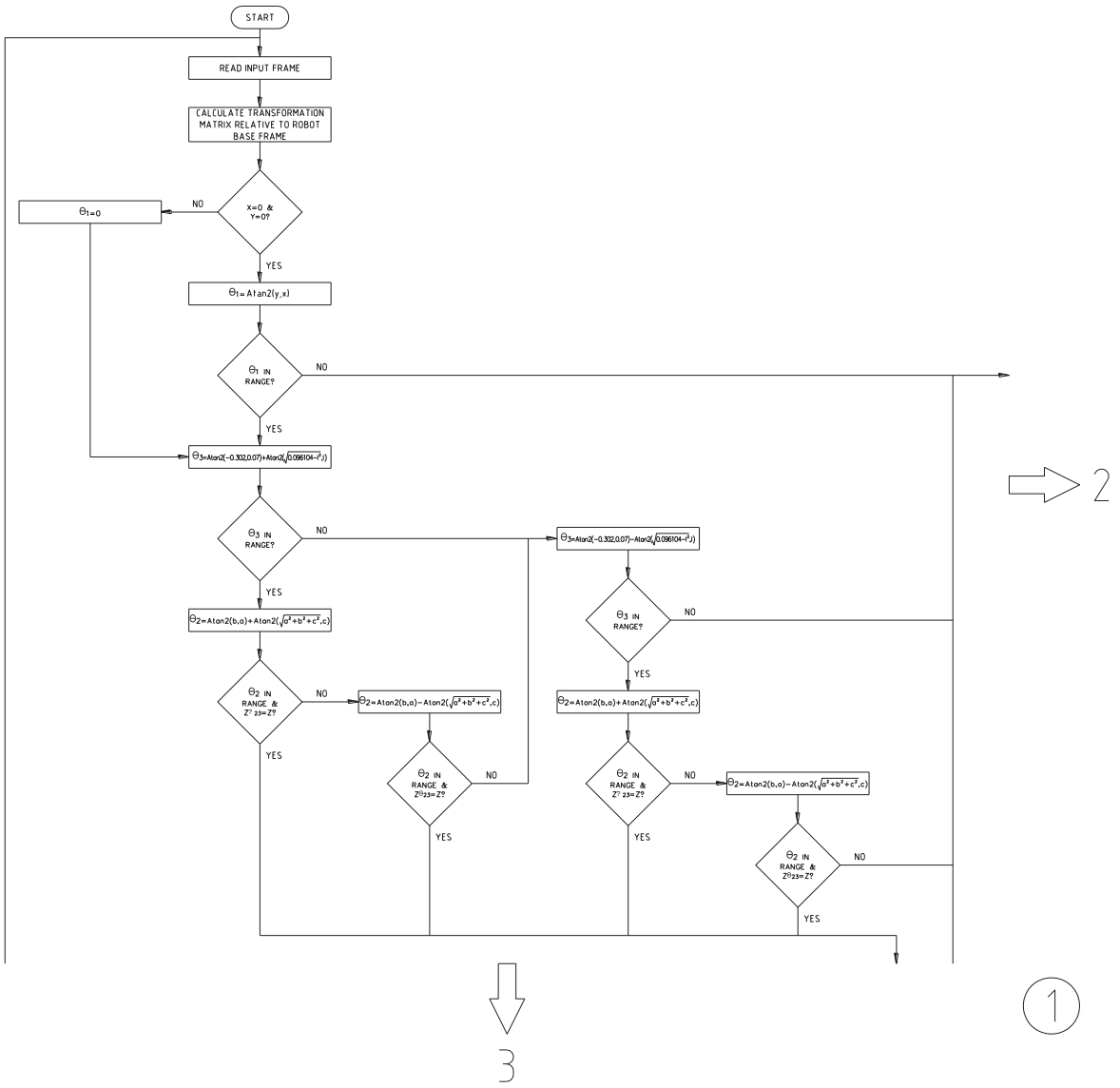

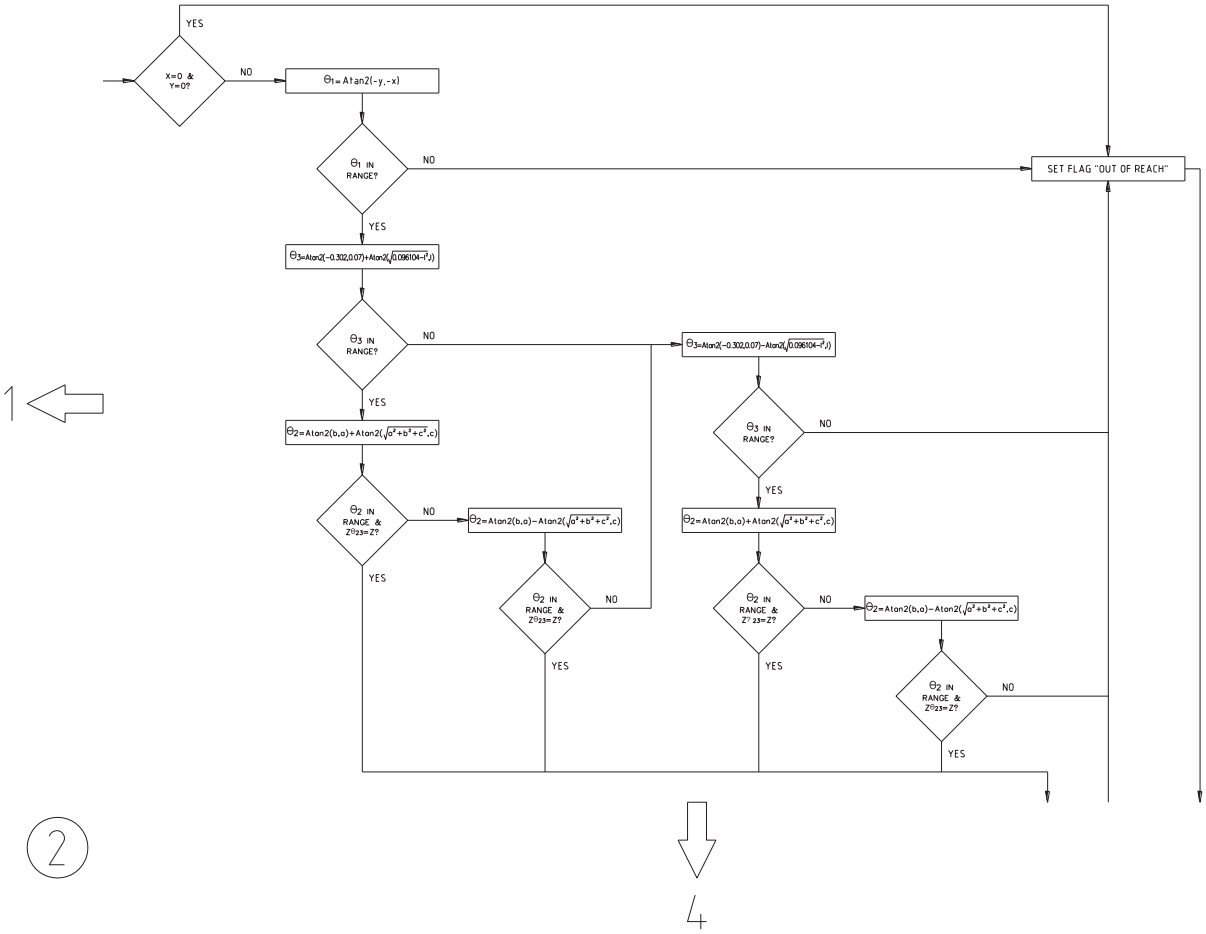
YES
X=0 & Y=0?
NO
Θ_1= Atan2(-y,-x)
Θ_1 IN RANGE?
NO
SET FLAG "OUT OF REACH"
YES
Θ_3=Atan2(-0.302,0.07)+Atan2(√0.096104-r²,r)
Θ_3 IN RANGE?
NO
Θ_3=Atan2(-0.302,0.07)-Atan2(√0.096104-r²,r)
YES
Θ_2=Atan2(b,a)+Atan2(√a²+b²+c²,c)
Θ_3 IN RANGE?
NO
YES
Θ_2 IN RANGE & Z°23= Z?
NO
Θ_2=Atan2(b,a)-Atan2(√a²+b²+c²,c)
Θ_2=Atan2(b,a)+Atan2(√a²+b²+c²,c)
YES
Θ_2 IN RANGE & Z°23= Z?
NO
YES
Θ_2 IN RANGE & Z°23= Z?
NO
Θ_2=Atan2(b,a)-Atan2(√a²+b²+c²,c)
YES
Θ_2 IN RANGE & Z°23= Z?
NO
YES
1
2
4

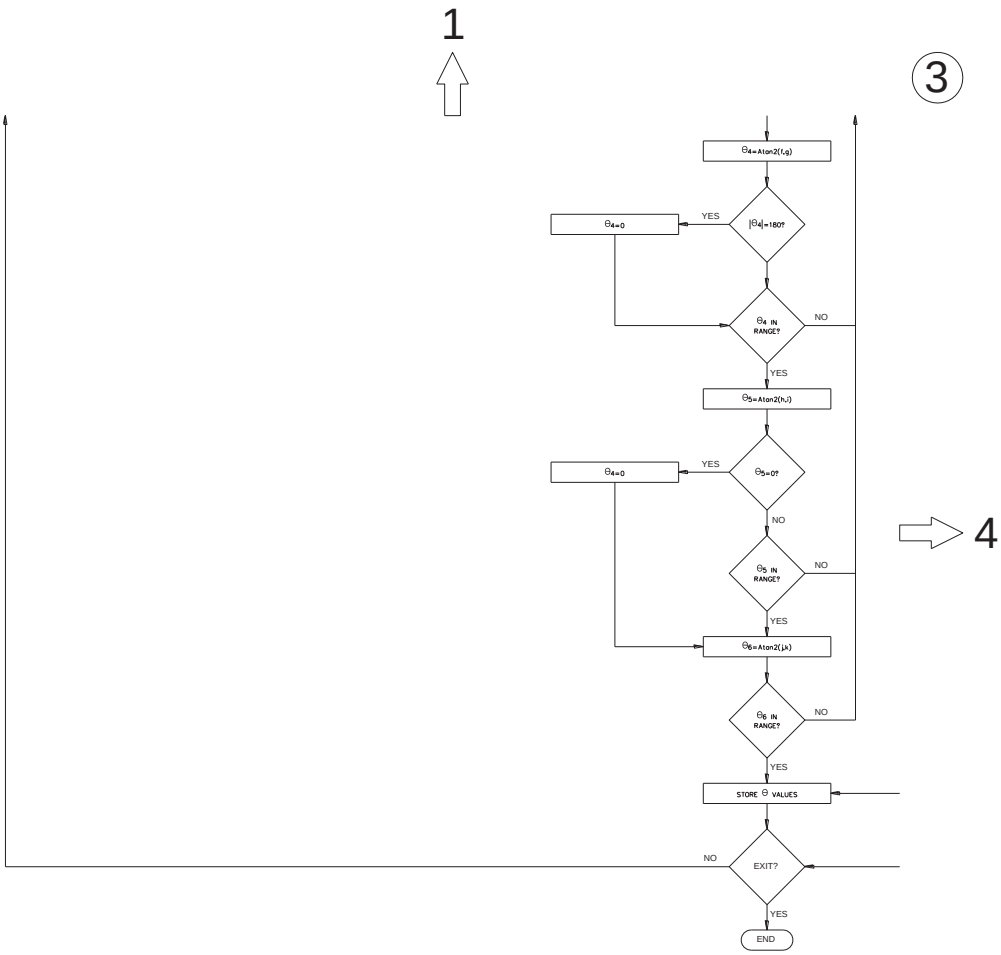
1
3
4
θ4=Aton2(f,g)
|θ4|=180?
YES
θ4=0
θ4 IN RANGE?
NO
YES
θ5=Aton2(h,i)
θ5=0?
YES
θ4=0
NO
θ5 IN RANGE?
NO
YES
θ6=Aton2(j,k)
θ6 IN RANGE?
NO
YES
STORE θ VALUES
EXIT?
NO
YES
END

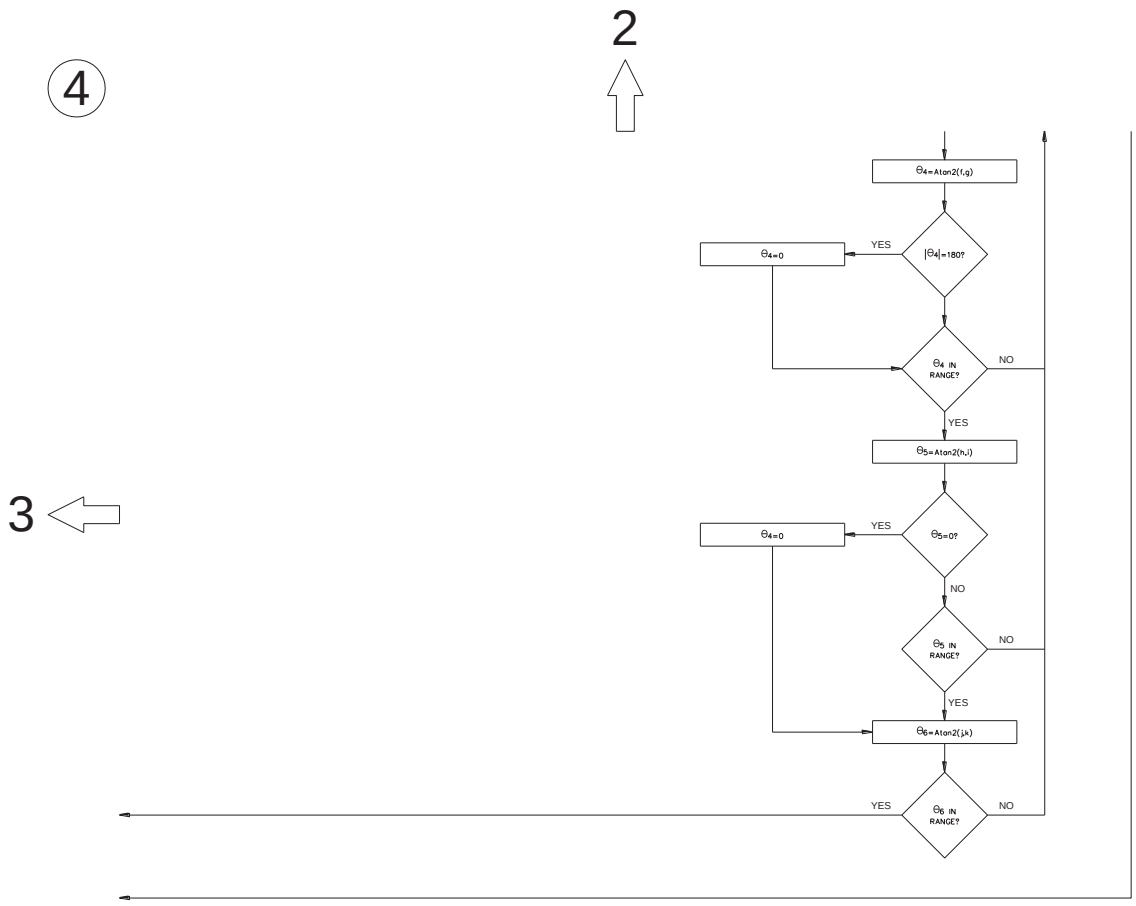

Figure 6.3 - Flow diagram of the joint calculation algorithm

```
//Robot link parameters
          a2=0.27;
          a3=0.07;
          d3=0;
          d4=0.302;

void Joints::settheta(double quarts[4], double x, double y, double z)
{
                    cout << endl << "Joints" << endl << endl;
                    cout << "quarts = " << quarts[0] << ", " << quarts[1] << ", " << quarts[2] << ", " << quarts[3] <<
endl;
                    cout << "x = " << x << ", y = " << y << ", z = " << z << endl;

                    double Wx, Wy, Wz;

                    settrans(quarts, x, y, z);
                    inrange = true;
                    theta1flip = false;

                    Wx = rot[1][4];
                    Wy = rot[2][4];
                    Wz = rot[3][4];

                    if((abs(theta[1] = atan2(Wy,Wx)*_R2D)) >= 165)
                    {
                              if((abs(theta[1] = atan2(-Wy,-Wx)*_R2D)) >= 165)
                              {
                                        theta[1] = 666;
                                        inrange = false;
                              }
                              else
                              {
                                        theta1flip = true;
                              }
                    }

                    k=(((Wx*Wx)+(Wy*Wy)+(Wz*Wz)-(a2*a2)-(a3*a3)-(d3*d3)-(d4*d4))/(2*a2));

                    if(!(-90 <= (theta[3] = ((atan2(-d4, a3)+atan2(sqrt((a3*a3)+(d4*d4)-(k*k)),k))*_R2D)) && (theta[3] <=
70)))
                    {
                              if(!(-90 <= (theta[3] = ((atan2(-d4, a3)-atan2(sqrt((a3*a3)+(d4*d4)-(k*k)),k))*_R2D)) &&
(theta[3] <= 70)))
                              {
                                        inrange = false;
                              }
                    }
                    double    theta2a = a2+a3*cos(theta[3]/_R2D)-d4*sin(theta[3]/_R2D),
                              theta2b = -1*(a3*sin(theta[3]/_R2D)+d4*cos(theta[3]/_R2D)),
                              theta2c = Wx*cos(theta[1]/_R2D)+Wy*sin(theta[1]/_R2D),
                              theta2tmp = 0,
                              Wzcheck = 0;

                    if((abs((theta2tmp=((atan2(theta2b, theta2a)+atan2(sqrt(theta2a*theta2a+theta2b*theta2b-
                    theta2c*theta2c),theta2c))*_R2D))+90)<=110) && (Wz-_10n6 <= (Wzcheck = (0.27*sin(-
                    theta2tmp/_R2D)+sqrt(a3*a3+d4*d4)*sin(((-90-theta2tmp-theta[3])/_R2D)+atan2(a3, d4))))) && (Wzcheck <=
                    Wz+_10n6))
                    {
                              theta[2] = theta2tmp + 90;
                    }else
                    {
                              if((abs((theta2tmp=((atan2(theta2b, theta2a)-atan2(sqrt(theta2a*theta2a+theta2b*theta2b-
                              theta2c*theta2c),theta2c))*_R2D))+90)<=110) && (Wz-_10n6 <= (Wzcheck = (0.27*sin(-
                              theta2tmp/_R2D)+sqrt(a3*a3+d4*d4)*sin(((-90-theta2tmp-theta[3])/_R2D)+atan2(a3, d4))))) &&
                              (Wzcheck <= Wz+_10n6))
                              {
                                        theta[2] = theta2tmp + 90;
                              }else
                              {
                                        theta[2] = 666;
                                        inrange = false;
                              }
                    }

                    theta23=(theta2tmp + theta[3]);

                    double    s4 = -rot[1][3]*sin(theta[1]/_R2D)+rot[2][3]*cos(theta[1]/_R2D),
                              c4 = -rot[1][3]*cos(theta[1]/_R2D)*cos(theta23/_R2D)-
                              rot[2][3]*sin(theta[1]/_R2D)*cos(theta23/_R2D)+rot[3][3]*sin(theta23/_R2D);
                    int adj=0;
```

```
                    if(((0-_10n2 <= s4) && (s4 <= 0+_10n2)) && ((0-_10n2 <= c4) && (c4 <= 0+_10n2)))
                    {
                              theta[4] = 0;
                    }else
                    {
                              if((theta[4] = (atan2(s4,  c4)*_R2D)) < -90)
                              {
                                        theta[4] = theta[4]+180;
                                        adj = 1;
                              }else
                              {
                                        if(theta[4] > 90)
                                        {
                                                  theta[4] = theta[4]-180;
                                                  adj = 1;
                                        }
                              }
                    }

                    double     s5 = -
                              1*(rot[1][3]*(cos(theta[1]/_R2D)*cos(theta23/_R2D)*cos(theta[4]/_R2D)+sin(theta[1]/_R2D)*sin(
                              theta[4]/_R2D)) +rot[2][3]*(sin(theta[1]/_R2D)*cos(theta23/_R2D)*cos(theta[4]/_R2D)-
                              cos(theta[1]/_R2D)*sin(theta[4]/_R2D))-rot[3][3]*(sin(theta23/_R2D)*cos(theta[4]/_R2D))),
                              c5 = rot[1][3]*(-cos(theta[1]/_R2D)*sin(theta23/_R2D))+rot[2][3]*(-
                              sin(theta[1]/_R2D)*sin(theta23/_R2D))+rot[3][3]*(-cos(theta23/_R2D));

                    if(!((theta[5] = (atan2(s5, c5)*_R2D)) <= 120 && theta[5] >= -120))
                    {
                              theta[5] = 666;
                              inrange = false;
                    }

                    double     s6 = -rot[1][1]*(cos(theta[1]/_R2D)*cos(theta23/_R2D)*sin(theta[4]/_R2D)-
                              sin(theta[1]/_R2D)*cos(theta[4]/_R2D))-
                              rot[2][1]*(sin(theta[1]/_R2D)*cos(theta23/_R2D)*sin(theta[4]/_R2D)+cos(theta[1]/_R2D)*cos(the
                              ta[4]/_R2D))+rot[3][1]*(sin(theta23/_R2D)*sin(theta[4]/_R2D)),
                              c6 =
                              rot[1][1]*((cos(theta[1]/_R2D)*cos(theta23/_R2D)*cos(theta[4]/_R2D)+sin(theta[1]/_R2D)*sin(th
                              eta[4]/_R2D))*cos(theta[5]/_R2D)-
                              cos(theta[1]/_R2D)*sin(theta23/_R2D)*sin(theta[5]/_R2D))+rot[2][1]*((sin(theta[1]/_R2D)*cos(t
                              heta23/_R2D))*cos(theta[5]/_R2D)-sin(theta[1]/_R2D)*sin(theta23/_R2D)*sin(theta[5]/_R2D))-
                              rot[3][1]*(sin(theta23/_R2D)*cos(theta[4]/_R2D)*cos(theta[5]/_R2D)+cos(theta23/_R2D)*sin(thet
                              a[5]/_R2D));

                    double thetatmp = (atan2(s6, c6))*_R2D;
//=IF('IRB 120 Quaternion'!S7 > 0, 'IRB 120 Quaternion'!S7-180, 180+'IRB 120 Quaternion'!S7)
                    if (thetatmp > 0)
                    {
                              theta[6] = thetatmp-180;
                    } else
                    {
                              theta[6] = thetatmp+180;
                    }
}
```

For testing purposes, the joint angles were output to the command window, as well as saved to a .csv file. The resulting joint angle sets calculated through the algorithm were verified by comparison with the calculated results from the Excel spreadsheet previously developed and verified during the testing process of the derivation of the closed form solution. As Table 6.2 illustrates, the same kinematic solutions were achieved in both the excel spreadsheet, and the C++ function, validating the C++ implementation of the closed form solution.

Frame Data

x = 0.25 y = 0.1 z = 0.2 Q0 = 0.650 Q2 = 0.271 Q2 = 0.653 Q3 = -0.271

Kinematic Solutions		
Joint	Excel	C++
θ_1	21.801°	21.801°
θ_2	-7.065°	-7.065°
θ_3	32.777°	32.777°
θ_4	-100.533°	-100.533°
θ_5	69.212°	69.212°
θ_6	117.649°	117.649°

Table 6.2 - Example comparison of C++ results with Excel spreadsheet

The joints class developed for use in the system calculates the kinematic solution based on an end effector target frame based at the intersection of the three wrist joint axes to simplify the development of the algorithm, and providing a universal solution for the IRB120 that would be able to be used in future applications, however, the target for the final system used for controlling the robot was based on a point at the end of the coupling mechanism as shown in Figure 6.4 as this was the equivalent mirrored position of the Polhemus Patriot sensor.

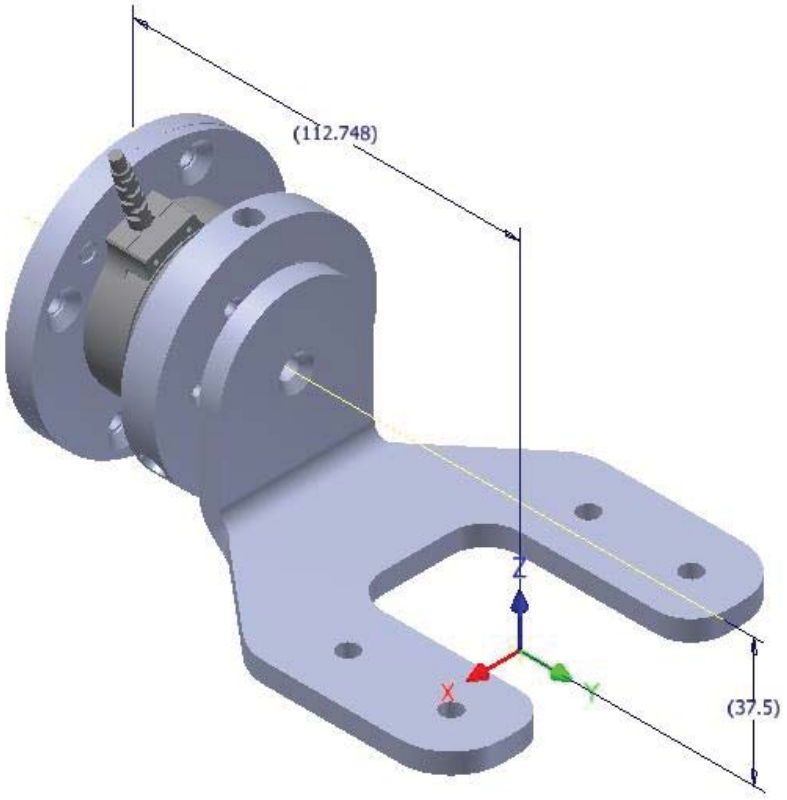

Figure 6.4 - Equivalent position of sensor frame on coupling

Therefore it was essential to add a function to the system to calculate the tool transform for the coupling mechanism. A transformation matrix was derived to determine the relative transform between the wrist joint of the IRB120, and the equivalent sensor frame position on the coupling. This transformation matrix was integrated into the joints algorithm as a means of transforming the captured frame from the motion sensor to the relative position of the wrist for the calculation of the kinematic solution for the robot.

```
//Inititalise transformation matrices
            tool[0][0]=0; tool[0][1]=1; tool[0][2]=2; tool[0][3]=3; tool[0][4]=4;
            tool[1][0]=1;
            tool[2][0]=2;
            tool[3][0]=3;

            rot[0][0]=0; rot[0][1]=1; rot[0][2]=2; rot[0][3]=3; rot[0][4]=4;
            rot[1][0]=1;
            rot[2][0]=2;
            rot[3][0]=3;

            for (n=1;n<4;n++)
                        {
                                    for (m=1;m<5;m++)
                                    {
                                                rot[n][m] = 0;
                                                tool[n][m] = 0;
                                    }
                        }

void Joints::settrans(double qt[4], double x, double y, double z) //Set transformation matrix
//Euler zyx rotation matrix
{

            tool[1][1]=(qt[0]*qt[0])+(qt[1]*qt[1])-(qt[2]*qt[2])-(qt[3]*qt[3]);
            tool[1][2]=2*((qt[1]*qt[2])-(qt[0]*qt[3]));
            tool[1][3]=2*((qt[1]*qt[3])+(qt[0]*qt[2]));

            tool[2][1]=2*((qt[3]*qt[0])+(qt[1]*qt[2]));
            tool[2][2]=(qt[0]*qt[0])-(qt[1]*qt[1])+(qt[2]*qt[2])-(qt[3]*qt[3]);
            tool[2][3]=2*((qt[2]*qt[3])-(qt[0]*qt[1]));

            tool[3][1]=2*((qt[1]*qt[3])-(qt[0]*qt[2]));
            tool[3][2]=2*((qt[1]*qt[0])+(qt[3]*qt[2]));
            tool[3][3]=(qt[0]*qt[0])-(qt[1]*qt[1])-(qt[2]*qt[2])+(qt[3]*qt[3]);

            rot[1][1]=-tool[1][3];
            rot[1][2]=tool[1][2];
            rot[1][3]=tool[1][1];

            rot[2][1]=-tool[2][3];
            rot[2][2]=tool[2][2];
            rot[2][3]=tool[2][1];

            rot[3][1]=-tool[3][3];
            rot[3][2]=tool[3][2];
            rot[3][3]=tool[3][1];

            tool[1][4]=x;
            tool[2][4]=y;
            tool[3][4]=z;

            rot[1][4]=-0.183*tool[1][1]+0.04*tool[1][3]+tool[1][4];
            rot[2][4]=-0.183*tool[2][1]+0.04*tool[2][3]+tool[2][4];
            rot[3][4]=-0.183*tool[3][1]+0.04*tool[3][3]+tool[3][4];

            printrot();

}
```

Code 6.1 - Code for the tool transform

6.2 **Motion Tracking Implementation**

Much of the implementation for the motion tracking system was reliant on the previous work completed in the testing and evaluation of the motion tracking system. The class developed for evaluating the Polhemus Patriot was implemented in the final system, as the motion control for the system. However, further development was required, as the data collected from the motion tracker was for that of the motion of the patient's unaffected arm. But for the robot targets required for control of the system, the frames from the motion tracker required manipulation to transform them to the equivalent mirror image of the original frame, mirrored through the patient's sagittal plane.

To achieve this transform, another function was added to the motion tracking class, to manipulate the frame recorded by the Polhemus Patriot sensor. By observation of the properties of a quaternion, being the three coordinates that describe the vector of a rotational axis, with a fourth dimension describing the rotation about that axis, the mirror of the quaternion can be achieved by negating one of the coordinates of the original quaternion's vector (in this case the x value), and the rotation about the axis, as shown in Figure 6.5.

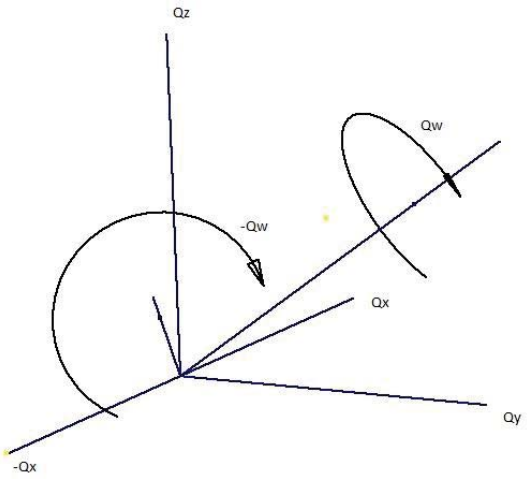

Figure 6.5 - Visualisation of a quaternion and its mirror

Taking advantage of this, the development of the function for manipulating the tracking frame was simplified, as it was not necessary to develop an algorithm to calculate the quaternion arithmetic. This also reduced the resources required by the system marginally, aiding the real time response of the system. The mirrored quaternion implementation was verified using the Robotics Toolbox in MATLAB, and the model of the IRB120 previously derived for validation of the closed form solution. Figure 6.6 shows the modelling of the IRB120 and its mirrored alternative, using the method presented above for mirroring quaternion orientation.

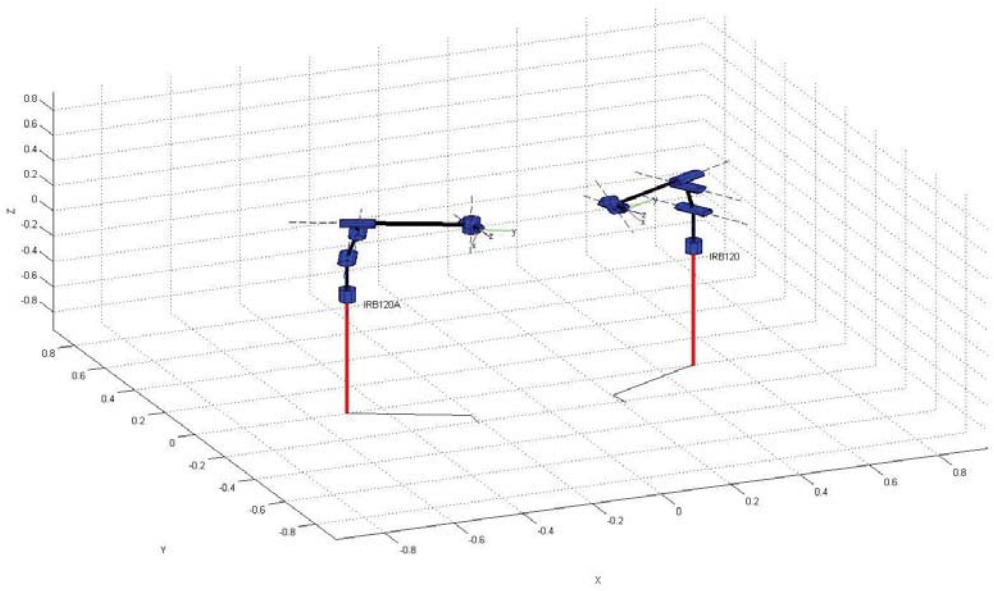

Figure 6.6 - Mirrored target frame modelled with IRB120 model in MATLAB

6.3 **Force Sensor Implementation**

Similar to the motion tracking system, the implementation of the force sensor also relied on the class developed during the validation process of the force sensor. A simple proportional control algorithm was added to the system, developed in the Rapid programming language to run on the IRC5 robot controller. This algorithm was used to provide the compliance for the system, and force monitoring to stop the system in the case of overload.

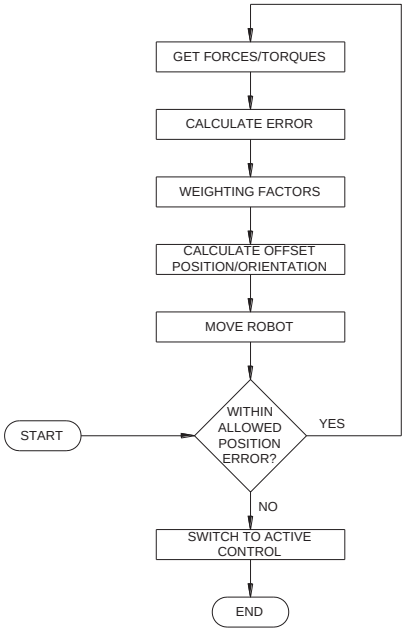

Figure 6.7 - Flow diagram for passive control

Proportional control was used for simplicity. This control algorithm was developed to read the forces and torques from the force sensor, then adjust the position and orientation of the robot's tool centre based on a proportional weighting. As the reaction time required for this was theoretically intended to be instantaneous, and the data from the force sensor was time independent, being static forces and torques, the weighting was determined experimentally. On initial experimentation of the control algorithm, it was discovered that the control algorithm required separating into two parts due to the differing force and torque readings, with the weighting for the linear forces requiring greater reaction than that of the torques to reduce the loading on the patient's arm. Code 6.2 shows the rapid functions used for implementing the proportional compliance control.

```
PROC ChckSphere()
          p10 := CRobT(\Tool:=tooldata_1 \WObj:=wobj0);
          xdif:= (p10.trans.x)-(p2.trans.x);
          ydif:= (p10.trans.y)-(p2.trans.y);
          zdif:= (p10.trans.z)-(p2.trans.z);

          if((xdif*xdif+ydif*ydif+zdif*zdif) < Sradius*Sradius) then
                    insphere:= true;
                    else
                    insphere:= false;
          endif
ENDPROC

PROC ForceTrans()
          p1.trans.x:= p1.trans.x+fortorq.rax_3*25;
          p1.trans.y:= p1.trans.y+fortorq.rax_1*25;
          p1.trans.z:= p1.trans.z+fortorq.rax_2*25;
ENDPROC

PROC ForcePos()

          var pos Torques;
          var orient rots;
          Torques.x := fortorq.rax_6;
          Torques.y := fortorq.rax_4;
          Torques.z := fortorq.rax_5;

          rots := orientZYX(Torques.z, Torques.y, Torques.x);

          p1.rot.q1 := p1.rot.q1*rots.q1-p1.rot.q2*rots.q2-p1.rot.q3*rots.q3-p1.rot.q4*rots.q4;
          p1.rot.q2 := p1.rot.q1*rots.q2+p1.rot.q2*rots.q1+p1.rot.q3*rots.q4-p1.rot.q4*rots.q3;
          p1.rot.q3 := p1.rot.q1*rots.q3-p1.rot.q2*rots.q4+p1.rot.q3*rots.q1+p1.rot.q4*rots.q2;
          p1.rot.q4 := p1.rot.q1*rots.q4+p1.rot.q2*rots.q3-p1.rot.q3*rots.q2+p1.rot.q4*rots.q1;

          p1.rot := NOrient(p1.rot);

ENDPROC
```

Code 6.2 - Rapid functions for position error and robot target due to applied loadings

6.4 System Implementation

As discussed previously, the final implementation of the system was achieved in two parts. The first part was implemented as a windows application, to run on a Windows OS (primarily Windows XP) based computer as the host that was developed to integrate the separate classes developed for the force/torque sensor and motion tracking system. This application also implemented the virtual mirror system. The specification of the host computer used were as follows – Intel® Core™ 2 Duo dual core CPU, E8400 @ 3.00 GHz with 1.94GB, 3.00GHz RAM. This computer had integrated graphics, comprising of an Intel® Q45/Q43 Express chipset.

The application utilised a multi-threading approach, allowing worker threads to maintain the operation of the different components, with the main thread collecting the data from the separate threads handling the force/torque sensor and the motion tracking system, and relaying this data to the server thread to be transferred to the robot controller.

The use of the multi-threading approach was intended to aid in the speed of operation of the system. By handling the separate components in individual processes, the individual algorithms could run in parallel, allowing the data from the sensors to be collected while the previously collected data was being transferred to the robot controller.

Communication between the individual threads was managed by the main thread with the use of pointers, passing the address of each worker thread to the main thread on initialisation, and vice versa. The implementation of the joints class for calculating the kinematic solution for the robot, which also determined whether the target was in reach, and managed singularity conditions, was also contained in the main thread. Code 6.3 shows the functions used for managing the individual threads.

```
            ServThread = CreateThread(NULL, 0, ServStart, this, 0, NULL);
            TrackThread = CreateThread(NULL, 0, TrackStart, this, 0, NULL);

            CWinThread * pSendThread = ::AfxBeginThread(sndrdymntr, (LPVOID) this, 0, 0, CREATE_SUSPENDED);
            pSendThread->m_bAutoDelete = FALSE;
            pSendThread->ResumeThread();
.
.
.
.
.
.
.
.
.
static UINT __cdecl sndrdymntr(LPVOID pParam)
{
            CDAQTest3Dlg * pThis = reinterpret_cast<CDAQTest3Dlg*>(pParam);
            VERIFY(pThis != NULL);
            VERIFY(m_pFrmRdySnd != NULL);
            CSyncObject* pWaitObjects[] = { m_pFrmRdySnd, m_pTerminateThread };
            CMultiLock MultiLock(pWaitObjects, 2L);
            while(MultiLock.Lock(INFINITE, FALSE) == WAIT_OBJECT_0)
            {
                        pThis->WrtSrvr();
                        pThis->SndSrvr();
                        pThis->frcread = false;

                        m_pRdyNwFrm->SetEvent();
            }
            // Terminate the thread
            ::AfxEndThread(0, FALSE);
            return 0;
}

DWORD __stdcall       MirrorStart(LPVOID arg)
{
            Mirror     MirFdbk;
            MirFdbk.ManipMirror();
            mirrflag = false;
            ::WaitForSingleObject(m_pTerminateThread->m_hObject, INFINITE);
            ::AfxEndThread(0, FALSE);
            return 0;
}

DWORD __stdcall       ServStart(LPVOID arg)
{
            Sock_Serv  Server;
            Sock_Serv * svr = &Server;
            CDAQTest3Dlg * dgl = reinterpret_cast<CDAQTest3Dlg*>(arg);
            dgl->PsSvr(svr);
            Server.passdlgsaddress(dgl);
            Server.Loop();
            ::WaitForSingleObject(m_pTerminateThread->m_hObject, INFINITE);
            ::AfxEndThread(0, FALSE);
            return 0;
}

DWORD __stdcall       TrackStart(LPVOID arg)
{
            Tracker parrot;
            Tracker * Patriot = &parrot;
            CDAQTest3Dlg * dgl = reinterpret_cast<CDAQTest3Dlg*>(arg);
            dgl->PsTrckr(Patriot);
            parrot.passdlgaddress(dgl);

            CSyncObject* pWaitObjects[] = { m_pRdyNwFrm, m_pTerminateThread };
            CMultiLock MultiLock(pWaitObjects, 2L);
            while(MultiLock.Lock(INFINITE, FALSE) == WAIT_OBJECT_0)
            {
                        while((((!dgl->frcread) || (!Irb.getinrange())) && dgl->Tracking)
                        {
                                    SendMessage(dgl->WnHndl, WM_forceread, 0, 0);
                                    Sleep(5);
                        }
                        if(dgl->Tracking)
                        {
                                    m_pFrmRdySnd->SetEvent();
                        }else
                        {
                                    Sleep(10);
                        }
            }
            // Terminate the thread
       ::AfxEndThread(0, FALSE);
            return 0;
}
```

Code 6.3 - Thread handling functions

The individual threads employed a polling approach, as opposed to the use of interrupts. The main algorithm developed for implementing the control of the program in the host computer would call the force sensor thread to retrieve and store the current loading information, then call the motion tracking thread to retrieve the current sensor location. The frame collected from the motion tracking system was used in the instance of the joints class to calculate the kinematic solution for the robot, monitoring whether the target was within reach of the robot.

If the target was found to be out of reach, the algorithm would return to the data collection stage, if the target was within reach, the stored force/torque loadings, the target frame information, and the kinematic solution would be passed to the socket server thread before returning to the data collection stage.

The mirror system was also handled by a dedicated thread. This thread was initialised by the main thread with control of the mirror maintained in the main thread by use of an event handler to turn the mirror on and off. The main thread also controlled the game interface, which was integrated into the mirror thread, in the same manner.

The second part of the system implementation was executed in the ABB Rapid environment to run on the IRC5 robot controller. This program handled the control of the robot, receiving the target frames, force loadings and kinematic solution from the windows application running on the host computer, and using this data to determine the correct operation of the robot.

Again, using a polling approach for the algorithm, after receiving the data form the host computer, the force loadings were checked for an overload event, and if this occurred, the robot motion would be stopped to ensure the safety of the patient. If the forces were within acceptable limits, as discussed in section 3.1, the next step was to

compare the current position of the robot with the robot target received from the host computer to determine whether the patient was achieving the exercises.

This comparison was achieved by taking the distance between the robot's current position, and comparing this with the radius of a spherical volume centred on the target frame. This radius was set at 100mm for initial trials. Finding the difference of each of the individual Cartesian coordinates between the target frame and the robot position, and using Pythagoras theorem to calculate the distance between the two frames, the resulting value was compared to the set sphere radius. This comparison was used as the switch to determine the whether the operation of the robot was to be passive, following the motion of the patient's hemiparetic arm, based on the force loading data, or to be in the active mode, driving the patient's hemiparetic arm motion. In the case of the distance between frames being less than the set sphere radius, the robot control would switch to passive control; otherwise it would switch to active control.

In passive mode, the system relied on the proportional control algorithm developed for the implementation of the force sensor, firstly determining the linear direction of motion required, and determining the amount of motion dependant on the force loading. Taking the independent force vectors in the X, Y and Z axes to determine the resultant force, a proportional weighting was used to calculate a suitable distance to move the robot in. Secondly, the amount of rotation was determined based on the resultant torque loading about the three main axes, converting these to a single quaternion, and using a second proportional weighting to determine a suitable value for the rotation about the axis of the quaternion to reduce the torque loading.

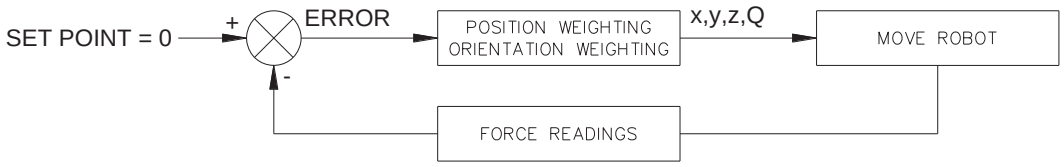

Figure 6.8 - Passive proportional control block diagram

Once the required motion was determined to reduce the force loading, and thereby follow the patient's motion, the linear motion vector, and the quaternion rotation were combined to form a new robot target for the robot to move to as shown earlier in Code 6.2.

In active mode, the frame received from the host computer was used to control the robot. This frame was converted to the robot target format required by the Rapid programming language for use with the in-built functions of the language.

In both cases, the destination robot target, determined by the various algorithms, for control of the robot were checked for singularity conditions or robot configuration errors using an in-built function (CalcjointT) that calculates the theoretical joint targets for the robot. If this function threw an error, an error handler would catch the error and use the kinematic solution received from the host computer for control of the robot instead of the robot target.

The mirror feedback was implemented using the OpenCV libraries.

6.5 **Discussion**

Development of the final Windows application was relatively straight forward, utilising Windows MFC libraries for the basis of the main program, Figure 6.9 shows the

main control window of the application. The multi-threading approach aided the operation of the system, allowing processor time to be better managed by the operating system. This meant that the sensors were constantly updating while the processes in the main thread were busy with other tasks, meaning that the system would be using the most current information available. However, delays in the system were introduced through the socket communications of the system between the host computer and the robot controller. This delay was minimal, but due to the data types used in the Rapid language, the delay in communication between the host computer and robot controller was un-necessarily increased.

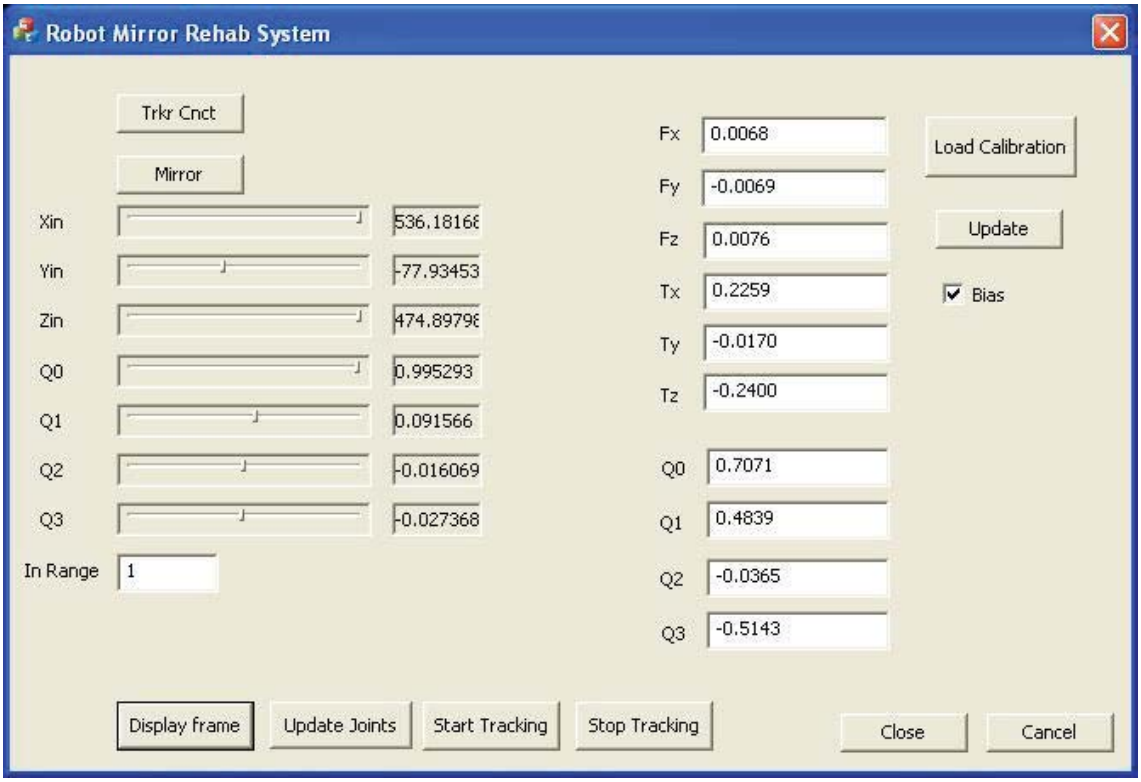

Figure 6.9 - Control window of the Windows MFC application

The Rapid language has in built functions for socket communications, simplifying the development for communication, but these were developed for receiving either string

data, or rawbytes data, with the latter intended for use with DeviceNet, ProfiBus or InterBus network protocols.

As this project relied on TCP/IP protocols, the string data type was used for communication, meaning that the information from the host PC needed to be converted to strings before transfer. Once received by the program running on the robot controller, these strings then needed to be converted to the required data types used by the Rapid language.

The function for socket communication in the Rapid language allows for a maximum string size of 80 characters, which was insufficient for the amount of data being transmitted to be transferred in one call. This meant that the data from the host computer needed to be sent in separate pieces. Initial trials of the communication approach showed that synchronisation was required between the host computer and robot controller to ensure correct data transfer. Without synchronisation, there was no guarantee that the robot control would be ready to receive the data from the host computer, and data was lost, causing program errors. This was a simple issue to solve; with a reply transmission being sent back to the host computer from the robot control after each piece of data was received and processed, with the host computer waiting for the receipt before transmitting the next piece of data. This however, added to the lag in the system. Code 6.4 & Code 6.5 show the data transmission functions of the system.

```
void Sock_Serv::sendframe(void)
{
	int n = 0;

	while (Read == true)
	{
		while (rcvd == false && skt == true)
		{
			receive();
			Sleep(10);
		}

		if(Send(ns, coordxyz) == 1)
		{
			printf("\nSend Error\n");
			break;
		}
		rcvd = false;

		while (rcvd == false && ns != INVALID_SOCKET)
		{
			if (ns == INVALID_SOCKET || n > 100)
			{
				break;
			}
			receive();
			Sleep(10);
		}

		if(Send(ns, coordq) == 1)
		{
			printf("\nSend Error\n");
			break;
		}
		rcvd = false;

		while (rcvd == false && ns != INVALID_SOCKET)
		{
			if (ns == INVALID_SOCKET || n > 100)
			{
				break;
			}
			receive();
			Sleep(10);
		}

		if(Send(ns, config) == 1)
		{
			printf("\nSend Error\n");
			break;
		}
		rcvd = false;

		while (rcvd == false && ns != INVALID_SOCKET)
		{
			if (ns == INVALID_SOCKET || n > 100)
			{
				break;
			}
			receive();
			Sleep(10);
		}

		if(Send(ns, jangles) == 1)
		{
			printf("\nSend Error\n");
			break;
		}
		rcvd = false;

		while (rcvd == false && ns != INVALID_SOCKET)
		{
			if (ns == INVALID_SOCKET || n > 100)
			{
				break;
			}
			receive();
			Sleep(10);
		}

		if(Send(ns, loads) == 1)
		{
			printf("\nSend Error\n");
			break;
		}
		rcvd = false;
		Read = false;
	}
}
```

Code 6.4 - C++ Server data send function

```
SocketSend socket1 \Str:="Send\0a\0d";
SocketReceive socket1 \str :=received_string \time :=WAIT_MAX;
if (received_string <> "") then
          ok:= StrToVal(received_string,regx);

          SocketSend socket1 \Str:="Send\0a\0d";
          SocketReceive socket1 \str:= received_string;
          ok:= StrToVal(received_string,regy);

          SocketSend socket1 \Str:="Send\0a\0d";
          SocketReceive socket1 \str:= received_string;
          ok:= StrToVal(received_string,regz);

          SocketSend socket1 \Str:="Send\0a\0d";
          SocketReceive socket1 \str:= received_string;
          ok:= StrToVal(received_string,jangles);

          SocketSend socket1 \Str:="Send\0a\0d";
          SocketReceive socket1 \str:= received_string;
          ok:= StrToVal(received_string,fortorq);
```

Code 6.5 - Rapid client data receive code

While testing the operation of the main control algorithm in the robot control, it was observed that the system wasn't switching correctly between the passive and active operations modes. The first step in investigating this issue was to examine the operation of the function making the comparison between the target position and robot position used for controlling the switch between the two operation modes. It was found that the current robot position being taken by the system was during motion of the robot, rather than at the end position of the motion, as was initially intended. This meant that the data sets being compared were in accurate for the operation of the system. The issue was solved by storing the target frame selected from the previous cycle of the algorithm (the end target for the current motion being executed) for the comparison with the new target received from the host computer in the current cycle of the algorithm. Although this corrected the operation of the switching between the operating modes, it highlighted another issue in the delay of the system operation.

Although there were delays introduced into the system by the TCP/IP communication between the host computer and robot controller, there were greater delays introduced in the robot motion control. The IRC5 robot controller separates motion control from the

main program running on the machine, allowing for faster program execution for tasks not related to the robot motion. This meant that the communications between the host computer and robot controller, as well as the algorithms used for determining force overload, operation mode and singularity handling, were able to be processed in parallel with the robot motion control. However, these processes were completed much quicker than the robot motion, meaning that the system would pause until the robot had reached the end point of the current path. This proved to be the greatest cause of lag in the system between the motion of the patient's healthy arm, and that of the hemiparetic arm.

The response time of the robot was tested by moving the sensor in a straight line over a span of 500mm at different speeds. Both the sensor and the robot were timed through the motion, and these times were compared as shown in Table 6.3 & Figure 6.10.

Test	Sensor Time	Robot Time	Difference
1	0.58	1.69	1.11
2	0.64	1.47	0.83
3	1.11	2	0.89
4	1.3	2.34	1.04
5	1.68	2.66	0.98
6	2.89	3.31	0.42
7	3.42	4.28	0.86
8	5.67	6.15	0.48
9	5.73	6.31	0.58
10	9.46	9.81	0.35

Table 6.3 - Results of time trials of system

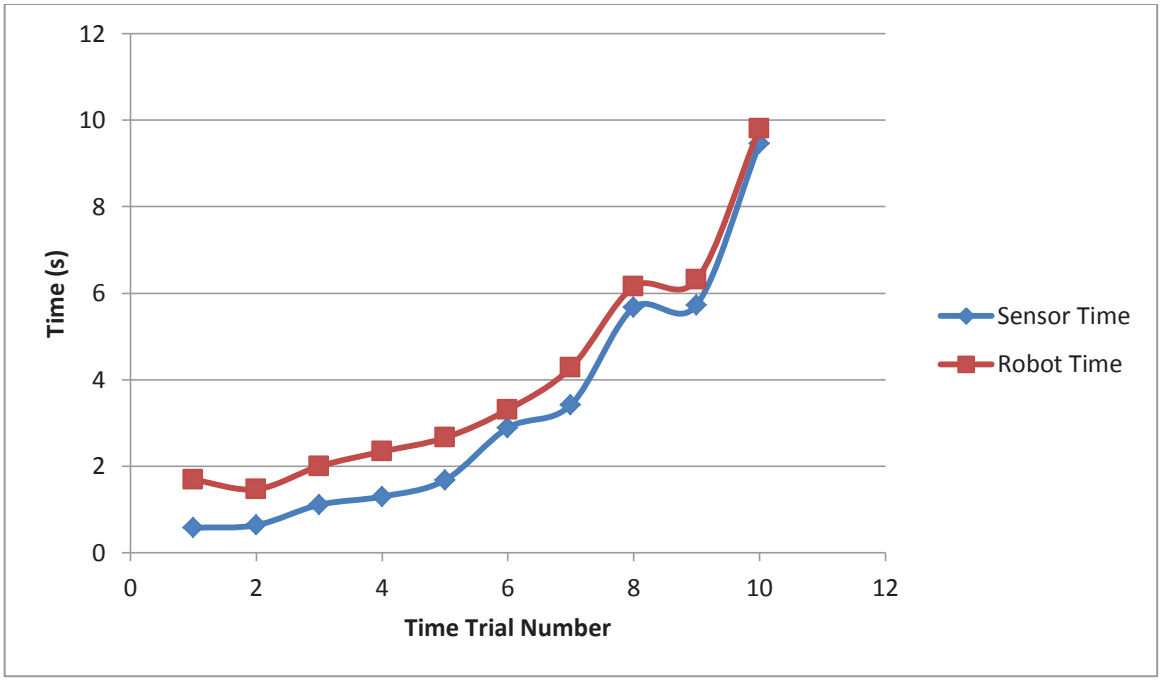

Figure 6.10 - Graphed results of time trials of system

The preferred solution for this was to interrupt the motion control when the new target was calculated and update the target for the current path to the new target. Investigation into the functions of the Rapid program, related to motion control, found that it was possible to interrupt the motion control to stop the robot's motion, which was useful for the case of a force overload condition, but it wasn't possible to alter the current path of the robot.

With further evaluation of the operation of the system, it was found that lag between the motion sensor and the robot motion could be minimised by limiting the speed of motion of the motion sensor as shown in Figure 6.10, reducing the distances between the sampled target frames, allowing the robot motion to stay in synch with these frames. This was an important discovery, as it shows a significant limitation of the current approach to the control of the system, and has a strong impact on the operation of the system.

During operation of the system, on large movements, the motion was smooth; however, when small movements were made with the motion sensor, the robot motion became jerky, stopping at every target. The Rapid language uses zone data in the functions for motion calls. The zone data is a user defined value used for “fly by” points in the path where the robot will travel past without stopping. Zone data refers to the distance from the “fly by” point the robot end effector will travel while going through a smooth corner radius from one trajectory path to the next trajectory path. On investigation of the error log from the robot controller during operation, it was discovered that on the smaller movements, the corner radius was unable to be calculated by the system, meaning that the robot was unable to travel smoothly past the “fly by” points, instead stopping at each point, causing the jerky motion.

The system was tested for singularity conditions by determining positions known to cause singularities, using the spreadsheet developed for validating the closed form solution, and placing the motion sensor in these known positions. The system responded as expected in these situations, switching to the use of the kinematic solution for the robot, calculated by the algorithm from the host computer, proving the validity of the algorithms involved.

The allowable error margin of 100mm selected for the criteria to determine the mode of operation for the system, active or passive, proved useful for testing the system. However, this was an arbitrarily chosen value for the convenience of testing the operation of the system. This was altered in the final system to be user adjustable between 0 and 200mm. This value requires evaluation under clinical trials to determine if there is an optimum value for this error margin. It is hypothesized that the optimum value for this would be dependent on the ability of the patient, with more severely affected patients

requiring a much smaller error margin providing more assistance from the system, while patients progressing through rehabilitation would require larger error margins, allowing them to complete exercises with minimal assistance, increasing the challenge of the exercise, which is supported by the work of Hee-Tae et al in their case studies using the uBot-5.

The initial proportional control algorithm used for the compliance control was tested with a single weighting for both position and orientation adjustments. This proved insufficient for control as the amount of adjustment required for the linear transfer required greater values than that of the orientation. This was due to the differing measurement scales of angular and linear measurement.

7 System Testing with Able-Bodied Participants

As an initial evaluation of the operation of the rehabilitation system developed for this project (shown in Figure 7.1), it was deemed necessary to test the system with human subjects. This provided an opportunity to observe and evaluate the performance of the different facets of the system, and give an overall impression of the system integration. This testing was also used to determine unexpected errors that may occur during operation, that would need further development, and develop a working procedure for using the system.

Item	Description
1	Motion sensor and base station
2	Mirror feedback with bubble game
3	ABB IRB120 Robot
4	Monitor with main control window

Figure 7.1 - The rehabilitation system

The testing also allowed the researcher to gain insights into the system from a user perspective, alluding to their impression of the system when experiencing it for the first

time, and a general user perception of how suitable the current system is for use with stroke patients.

7.1 **Procedure**

A small trial of 6 participants was proposed for initial testing of the system with human participants. As this was the first study in which human participants were introduced to the system, it was carried out with able-bodied individuals, aged between 20 and 40 years, screened to ensure they didn't have any health issues that may have been exacerbated by use of the system, such as heart conditions, upper body injuries, arthritis etc…

Each participant was seated comfortably with the robot spaced 500mm from their sagittal plane on the left hand side, and approximately 200mm in front of the participant. The base station for the Polhemus Patriot was placed in line with the base of the robot, 500mm to the right of the participant's sagittal plane. A computer monitor for the mirror feedback, with an attached webcam, was placed on a desk in front of the participant, positioned so that the participant's image was positioned in the centre of the screen.

Initially the participant was asked to put their right arm in the splint attached to the robot at the beginning of the test, with the splint holding the motion sensor placed on their right arm. However, it was discovered that the participants required time wearing just the left wrist splint, without their arm mounted in the robot's splint to allow them to become familiar with the operation of the system. Because of this, the procedure was altered to instruct the participant to wear just the left splint and observe the robot's behaviour, familiarising themselves with its operation. Once the participant felt confident, the test was paused, and they were instructed to place their left arm into the robot mounted splint

before continuing the test for a total of 20 minutes, playing the game that was integrated into the virtual mirror.

Once the test had reached its end, the participant was asked to complete a brief questionnaire, ranking there view of the comfort of the system, the comfort of the exercises, their confidence in the safety of the system, and their view of whether it is suitable for use with stroke patients in its current development stage. The questionnaire also gave the participant an opportunity to provide any other comments about their experience with the system.

7.2 **Results**

Participant	Male / Female	Age	Height (mm)
1	Male	32	1930
2	Male	27	1880
3	Female	32	1626
4	Female	23	1727
5	Male	28	1753
6	Male	34	1854
Average		29	1795

Table 7.1 - Participant details

During the initial tests, the participant was instructed to place both hands in the splints from the beginning of the test; the participant would make large quick movements to control the robot. This would cause the robot to behave in what appeared to be an erratic manner as it followed their movements, but with large delays as was expected from the findings in section 6.5. Figure 7.2 shows images of one of the trials, taken at 5 second intervals, to illustrate the operation of the system.

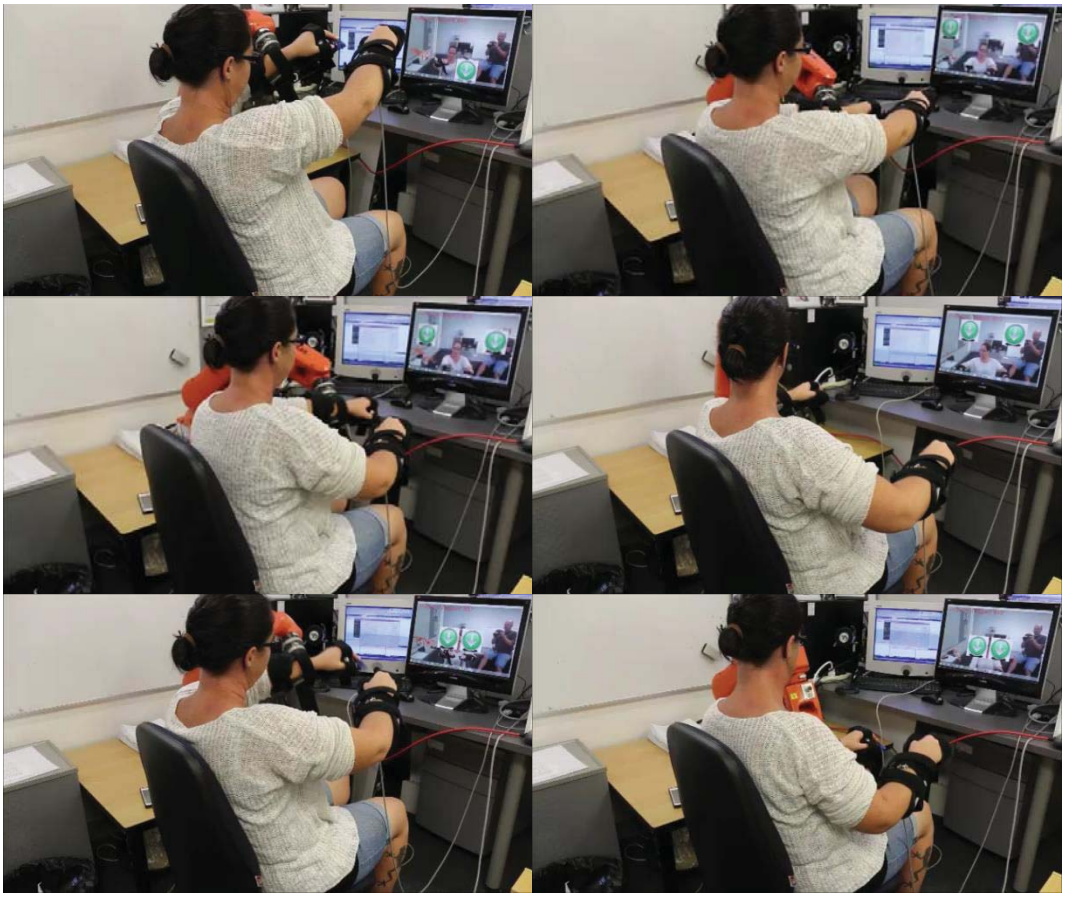

Figure 7.2 - Image sequence of trial (5 second intervals)

The large movements in these initial trials raised an unforeseen issue. As the large movements required large inertial changes, the inbuilt motion supervision system of the robot controller would trip, causing operation of the robot to halt, until manually restarted. Because of this, as mentioned before, the procedure was altered to allow the participant a period of time to become familiar with the nuances of the system, and how the robot reacts to movements of the controlling arm.

The large jerky motions of the robot in the initial trials, however, gave an opportunity to observe the operation of the passive break joint. This design proved to be affective in its operation, with the left arm breaking cleanly away from the robot when overloaded due to dynamic loadings induced by the robots motion.

The safety overload limit programmed into the system, also proved effective, stopping the system when a forces read by the force sensor exceeded the pre-determined safety limit, however, this was not as reactive as the motion supervision of the robot controller, which would react faster in the case of sudden loadings. Due to the inherent latency in the operation of the system, the safety overload limit would only react after the data had been received from the host computer.

For debugging/monitoring purposes for the supervisor of the trial, the system output data to the command window so that the data running through the system could be observed. The command window data stream, shown in Figure 7.3 primarily shows the frame captured by the motion sensor, the calculated result of the closed form solution, and a flag to indicate if the sensor was within the robots reach.

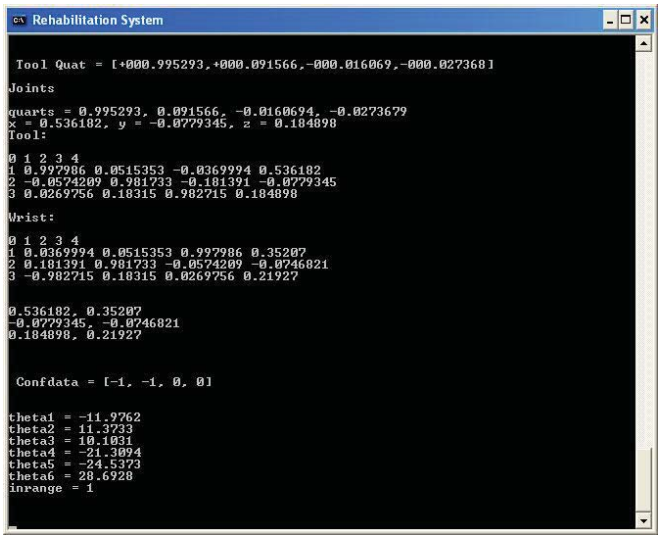

Figure 7.3 - Command window data stream snapshot

The operation of the mirror therapy component was generally as expected, with smooth motion, and the robot removed from the video stream, once the range limits for the colour selection had been adjusted. Blue tape was attached to the ends of the wrist splints to give a defined pointer for popping bubbles in the game component, which

participants engaged well with. The removal of the robot was not flawless however. With the splint attached to the robot trailed the direction robot, or with the robot in a generally stationary position, the robot's image was removed effectively, however, when the robot trailed the direction of the splint, the image used for the in-painting process would reveal artefacts of the splint at the edge of the ROI of the mask, leaving trails in the infilled region where the robot's image was removed.

Participant feedback (included in Appendix B – Participant Questionnaires) was generally positive toward the system and its operation. Participants ranked the comfort of the system and the exercises positively. Confidence in the safety of the system was also well rated, however, the general consensus from the participants' questionnaires is that the system has good potential, but is not currently suitable for use with stroke patients. Table 7.2 shows the tabulated results of the participants' rankings of the different aspects of the system. Although this is quantitative data, it gives an impression of how this small group of subjects view the current state of the system.

Participant	System Comfort (0-5)	Exercise Comfort (0-5)	Safety Rating (0-5)	Suitability for Stroke Patients (0-5)
1	3	3	3	4
2	4	3	4	2
3	3	3	2	1
4	3	4	4	3.5
5	4	4	5	2
6	3	3	4	2
Average	3.3	3.3	3.7	2.4

Table 7.2 - Tabulated participant rankings

7.3 **Discussion**

The apparent erratic behaviour observed in the first couple of trials was a result of the large, fast movements enacted by the participant who was unfamiliar with the operation of the system. This behaviour confirms the issue of lag that was illustrated during the simple evaluation of the system response time in section 6.5. Further confirmation was given in the later trials when the participants were given time to become familiar with the operation before placing their left arm in the robot mounted splint. When the participant was familiar with the operation, they tended to resist the urge to make overly fast movements, and, although still noticeably delayed, the robot was able to successfully track the motion of the participant's right arm.

When the participant suspended the movement of their right arm, allowing the robot to catch up, the motion control switched to force control as required, because the robots position was within the allowable error, set for testing at a distance of 150mm. As with the motion control, due to the bottleneck in the system caused by the communication between the host computer and the robot controller, and the delay caused by the Rapid program waiting for the motion control complete its task, the force control also suffers from delays in reaction time.

The rotational response to applied loadings was acceptable, but it was reported by participants that it felt stiff. Again, in the initial trials, the linear weighting used in the proportional control algorithm for the force control was overly sensitive for appropriate operation. Although the robot moved in the correct direction, when the participant applied what they considered medium force, the robot made large movements, pulling their arm further than they were comfortable with. The linear weighting was reduced to prevent the excessive movement, but this reduced the sensitivity to light forces to a point where they

were ineffective to provide compliant operation. From an engineering standpoint, the proportional control shows proof of concept for the control of the system, but further development is suggested with advice from a health care expert in the field of physiotherapy, to determine appropriate compliant response to loads that would be exerted by patients.

An unexpected issue arose during the trials with able bodied persons. The IRC5 robot controller comes with in-built systems to protect the hardware when overloaded, or unexpected load conditions occur, such as a collision with an object in the workspace. This feature is called Motion Supervision, and along with detecting collisions, it also monitors the inertial loadings of the robot. As this is primarily an industrial robot, it is designed for predetermined loads with known inertial loadings for the forward kinematics of the controller to accurately determine the accelerations and speeds of the robot during operation. For the current application, as the loading on the robot due to the participant's arm is constantly shifting as their arm is moved in different directions to achieve the reaching exercises of the video game interface, sometimes with the robot motion, sometimes against, meaning the resultant loading and inertial forces are unpredictable.

Because of this, in operation, when the participant caused the robot to move in large, fast motions, the motion supervision in the controller would be triggered, halting the operation of the robot, until the error was acknowledged by the supervisor of the trial. When operating in the compliant mode, being controlled by the force sensor, heavy, sudden loadings exerted by the participant would trigger the collision detection causing the robot controller to stop the robot by means of the in-built safety system, meaning that the program running in the robot controller would need resetting, and the trial would have to be restarted.

This loading condition interfered with the operation of the force overload detection in the force control of the system. If the over loading force wasn't exerted suddenly on the robot, then the system's force overload function would stop the system, however, sudden loads wouldn't be detected by the force control of the system due to the delays in the communication of the system.

The reach of the robot was also observed to be a limit on the operation of the system. It was perfectly adequate when the participant was reaching in front of them, but when the participant was required to reach toward the upper corners of the mirror image, the robot would reach the extent of its working envelope. The short reach of the robot also meant that the participant had to be seated close to the robot to ensure that it could reach their sagittal plane. The close proximity of the robot meant that the reach of the participant wasn't as free as it should ideally be.

The trials resulted in a change of protocol in using the system, as, presented previously; it was observed that the participant required time to become familiar with the operation of the system, both to learn how the robot reacted to motions of the controlling arm, and to become confident in its operation. The general feedback from participants was positive, with comfort, and confidence in the system rating well, although the feedback shows that this system is not ready for use with stroke patients.

Participants stated that their initial impression of the system was that it was daunting at first, mainly due to the jerky motion observed, that gave the impression that it would be violent, but once confident with the system, this impression was alleviated, however, the general impression was that this would scare the generally elderly patients that this system is intended for. The general overall consensus was that the participants became confident with the safety of the machine, and could see great potential of the system for

use in stroke rehabilitation, however further refinement is required. It is suggested that the system is at a stage requiring multi-disciplinary input from health care experts in the fields of physiotherapy and rehabilitation, with a broad knowledge of the rehabilitation field, to compliment the engineering contribution.

8 Conclusion and Recommendations

This project has been successful in developing a prototype to confirm the feasibility of an integrated robotic and mirror therapy rehabilitation system to be used in stroke rehabilitation for evaluating whether or not the conjunct of the two approaches would provide improved rehabilitation for stroke patients over either approach used individually.

For the operation of the system, a proportional control system may be too simplistic, and it would be advantageous in future implementations of the system to develop a PID or fuzzy logic type control algorithm for compliance control.

Although the system developed in this project has proven to be functional, it is recommended that the system undergo further development to improve the functionality and fitness for purpose before being trialled with patients in a pilot study to fully evaluate the operation of the system in the rehabilitation field.

The use of an industrial robot in this project that is not intended for this type of application was not an ideal solution. Based on the operation and complications experienced through this project, system lag in particular in regard to the real time operation required, it is recommended that a purpose built robotic platform be designed for use in later systems. The working envelope of the robotic platform should also be reviewed in light of the difficulties encountered during testing with able bodied subjects, namely the issue of the participants moving outside the robots reach during the reaching exercises required to engage with the game interface. To simplify the kinematics of the system, in the aid of improving real time operation, a Cartesian style robot is suggested in place of the articulated platform used in this project. The cuboid working envelope of a Cartesian robot may also be more appropriate for this application than the spherical working envelope of an articulated robotic arm. However, the use of an articulated arm

with a larger reach would also improve this issue, such as the preferred option of the Fanuc LR Mate 200iC discussed in chapter 5, if the project budget would allow this option.

Separating the control of the system between two computers also proved disadvantageous due to the required communication between the systems. For control of the system, a single computer would be advantageous to remove the complication involved with communication between the computer platforms used in this project. This would also involve the development of new robot motion control algorithms with application specific functions that would allow for path modification while in motion, and improved compliant behaviour.

Research into motion prediction to develop algorithms to predict the patient's healthy arm motions for use in aid of the robot control to improve real time response would also be advantageous. To this end, further research into the use of EMG signals for robot control may also be useful.

References

[1] Health_Ministry, "A Portrait of Health - Key Results of the 2006/2007 New Zealand Health Survey ", M. o. Health, Ed., ed. Wellington: New Zealand Government, 2008.

[2] "Know Stroke: Know the Signs, Act in Time," in *Stroke Sourcebook*, J. B. Shannon, Ed., First ed Detroit: Omnigraphics, 2003, pp. 3-6.

[3] H. S. Jorgensen, H. Nakayama, H. O. Raaschou, J. Vivelarsen, M. Stoier, and T. S. Olsen, "Outcome and Time-Course of Recovery in Stroke 2. Time-Course of Recovery - The Copenhagen Stroke Study," *Archives of Physical Medicine and Rehabilitation*, vol. 76, pp. 406-412, May 1995.

[4] L. A. Gilman, *Coping with Cerebral Palsy*, First ed. New York: The Rosen Publishing Group, 2001.

[5] J. Fisher, E. Morling, and F. Murray, *Supporting Children with Cerebral Palsy*. London: David Fulton Publishers Ltd, 2006.

[6] F. Miller, "Therapy, Education, and Other Treatment Modalities," in *Physical Therapy of Cerebral Palsy*, K. Dabney and M. Alexander, Eds., ed New York: Springer Science+Business Media, LLC, 2007, pp. 107-136.

[7] W. H. Oertel and N. P. Quinn, "Parkinsonism," in *Neurological Disorders: Course and Treatment*, T. Brandt, L. R. Caplan, J. Dichgans, H. C. Diener, and C. Kennard, Eds., ed San Diego: Academic Press, 1996, pp. 715 - 772.

[8] S. E. Starkstein and M. Merello, *Psychiatric and Cognitive Disorders in Parkinson's Disease*. Cambridge: Cambridge University Press, 2002.

[9] G. Kernohan, F. Hasson, and D. Hardyway, "Palliative Nursing Care in Other Neurological Conditions - Parkinson's Disease," in *Palliative Nursing: Across the Spectrum of Care*, E. Stevens, S. Jackson, and S. Milligan, Eds., ed Chichester: Blackwell Publishing Ltd, 2009, pp. 181 - 194.

[10] A. Picelli, S. Tamburin, M. Passuello, A. Waldner, and N. Smania, "Robot-assisted arm training in patients with Parkinson's disease: a pilot study," *Journal of Neuroengineering and Rehabilitation*, vol. 11, p. 4, Mar 2014.

[11] H. I. Krebs, B. T. Volpe, M. L. Aisen, W. Hening, S. Adamovich, H. Poizner, *et al.*, "Robotic applications in neuromotor rehabilitation," *Robotica*, vol. 21, pp. 3-11, Jan-Feb 2003.

[12] M. Filbin, L. M. Lee, B. L. Shaffer, and A. B. Caughey, "Osteoarthritis," in *Pathophysiology: Pulmonary, Gastrointestinal, and Rheumatology*, A. B. Caughey, Ed., ed Massachusetts: Blackwell Publishing, 2004, pp. 143 - 146.

[13] F. Desmeules, C. E. Dionne, E. Belzile, R. Bourbonnais, and P. Fremont, "Waiting for total knee replacement surgery: factors associated with pain, stiffness, function and quality of life," *Bmc Musculoskeletal Disorders,* vol. 10, p. 10, May 2009.

[14] (2009, 13/05/2010). *New Zealand National Joint Register*. Available: http://www.cdhb.govt.nz/njr/

[15] C. Ferguson, "Palliative Nursing Care in Other Neurological Conditions - Motor Neurone Disease," in *Palliative Nursing: Across the Spectrum of Care*, E. Stevens, S. Jackson, and S. Milligan, Eds., ed Chichester: Blackwell Publishing Ltd, 2009, pp. 164 - 175.

[16] (2006, 13/05/2010). *Motor Neurone Disease Association NZ: General Information*. Available: http://www.mnda.org.nz/index.html

[17] R. Warner, "Palliative Nursing Care in Other Neurological Conditions - Multiple Sclerosis," in *Palliative Nursing: Across the Spectrum of Care*, E. Stevens, S. Jackson, and S. Milligan, Eds., ed Chichester: Blackwell Publishing Ltd, 2009, pp. 175 - 181.

[18] R. Martin, R. Hohlfeld, and H. F. McFarland, "Multiple Sclerosis," in *Neurological Disorders: Course and Treatment*, T. Brandt, L. R. Caplan, J. Dichgans, H. C. Diener, and C. Kennard, Eds., ed San Diego: Academic Press, 1996, pp. 483 - 505.

[19] M. S. Society. (2008, 14/05/2010). *MS Auckland Region: News > Press Releases*. Available: http://www.msakl.org.nz/press-releases.html

[20] Statistics_New_Zealand. (2010, 15/05/2010). *National Population Estimates: March 2010 quarter*. Available: National Population Estimates: March 2010 quarter

[21] A. M. Dollar and H. Herr, "Lower Extremity Exoskeletons and Active Orthoses: Challenges and State-of-the-Art," *IEEE Transactions on Robotics,* vol. 24, pp. 144-158, 2008.

[22] C. J. Walsh, K. Endo, and H. Herr, "A quasi-passive leg exoskeleton for load-carrying augmentation," *International Journal of Humanoid Robotics,* vol. 4, pp. 487-506, 2007.

[23] H. Kazerooni, J. L. Racine, L. H. Huang, R. Steger, and Ieee, "On the control of the Berkeley Lower Extremity Exoskeleton (BLEEX)," in *2005 IEEE International Conference on Robotics and Automation*, ed New York: Ieee, 2005, pp. 4353-4360.

[24] R. Bogue, "Exoskeletons and robotic prosthetics: a review of recent developments," *Industrial Robot-an International Journal*, vol. 36, pp. 421-427, 2009.

[25] Cyberdyne_Inc. (2010, 15/05/2010). *Cyberdyne: Robot Suit HAL*. Available: http://www.cyberdyne.jp/english/robotsuithal/index.html

[26] E. Guizzo, H. Goldstein, J. Kumagai, and J. Boyd, "The RISE of the BODY BOTS," *IEEE Spectrum*, vol. 42, pp. 50-56, 2005.

[27] T. Hayashi, H. Kawamoto, and Y. Sankai, "Control method of robot suit HAL working as operator's muscle using biological and dynamical information," in *Intelligent Robots and Systems, 2005. (IROS 2005). 2005 IEEE/RSJ International Conference on*, 2005, pp. 3063-3068.

[28] G. Mone, "Building the Real Iron Man," *Popular Science*, vol. 272, pp. 44-55, 2008.

[29] M. Ishii, K. Yamamoto, and K. Hyodo, "Stand alone wearable power assisting suit (development and availability)," *Nihon Kikai Gakkai Ronbunshu, C Hen/Transactions of the Japan Society of Mechanical Engineers, Part C*, vol. 72, pp. 857-864, 2006.

[30] "A Brief History of Exoskeletons," *Popular Science*, vol. 272, pp. 50-52, 2008.

[31] R. Steger, K. Sung Hoon, and H. Kazerooni, "Control scheme and networked control architecture for the Berkeley lower extremity exoskeleton (BLEEX)," in *Robotics and Automation, 2006. ICRA 2006. Proceedings 2006 IEEE International Conference on*, 2006, pp. 3469-3476.

[32] C. J. Walsh, D. Paluska, K. Pasch, W. Grand, A. Valiente, and H. Herr, "Development of a lightweight, underactuated exoskeleton for load-carrying augmentation," in *Robotics and Automation, 2006. ICRA 2006. Proceedings 2006 IEEE International Conference on*, 2006, pp. 3485-3491.

[33] J. E. Pratt, B. T. Krupp, C. J. Morse, and S. H. Collins, "The RoboKnee: an exoskeleton for enhancing strength and endurance during walking," in *Robotics and Automation, 2004. Proceedings. ICRA '04. 2004 IEEE International Conference on*, 2004, pp. 2430-2435 Vol.3.

[34] C. G. Burgar, P. S. Lum, P. C. Shor, and H. F. M. Van der Loos, "Development of robots for rehabilitation therapy: The Palo Alto VA/Stanford experience," *Journal of Rehabilitation Research & Development*, vol. 37, p. 663, 2000.

[35] N. Hogan, H. I. Krebs, J. Charnnarong, P. Srikrishna, and A. Sharon, "MIT - Manus - A Workstation for Manual Therapy and Training 1," *Ieee International Workshop on Robot and Human Communication : Proceedings*, pp. 161-165, 1992.

[36] R. Rao, S. K. Agrawal, and J. P. Scholz, "A robot test-bed for assistance and assessment in physical therapy," *Advanced Robotics*, vol. 14, pp. 565-578, 2000.

[37] J. Stein, H. I. Krebs, W. R. Frontera, S. E. Fasoli, R. Hughes, and N. Hogan, "Comparison of two techniques of robot-aided upper limb exercise training after stroke," *American Journal of Physical Medicine & Rehabilitation*, vol. 83, pp. 720-728, Sep 2004.

[38] R. Banz, M. Bolliger, S. MÃ¼ller, C. Santelli, and R. Riener, "A method of estimating the degree of active participation during stepping in a driven gait orthosis based on actuator force profile matching," *IEEE Transactions on Neural Systems and Rehabilitation Engineering*, vol. 17, pp. 15-22, 2009.

[39] G. Colombo, M. Joerg, R. Schreier, and V. Dietz, "Treadmill training of paraplegic patients using a robotic orthosis," *Journal of Rehabilitation Research and Development*, vol. 37, pp. 693-700, 2000.

[40] J. Hidler and N. Neckel, "Inverse-dynamics based assessment of gait using a robotic orthosis," *Conference proceedings : ... Annual International Conference of the IEEE Engineering in Medicine and Biology Society. IEEE Engineering in Medicine and Biology Society. Conference*, vol. 1, pp. 185-188, 2006.

[41] S. K. Agrawal, S. K. Banala, K. Mankala, V. Sangwan, J. P. Scholz, V. Krishnamoorthy, *et al.*, "Exoskeletons for gait assistance and training of the motor-impaired," in *2007 IEEE 10th International Conference on Rehabilitation Robotics, ICORR'07*, Noordwijk, 2007, pp. 1108-1113.

[42] S. K. Agrawal, S. K. Banala, A. Fattah, V. Sangwan, V. Krishnamoorthy, J. P. Scholz, *et al.*, "Assessment of motion of a swing leg and gait rehabilitation with a gravity balancing exoskeleton," *IEEE Transactions on Neural Systems and Rehabilitation Engineering*, vol. 15, pp. 410-420, 2007.

[43] S. K. Banala, S. H. Kim, S. K. Agrawal, and J. P. Scholz, "Robot assisted gait training with active leg exoskeleton (ALEX)," *IEEE Transactions on Neural Systems and Rehabilitation Engineering*, vol. 17, pp. 2-8, 2009.

[44] R. Ekkelenkamp, J. Veneman, and H. van der Kooij, "LOPES: a lower extremity powered exoskeleton," in *Robotics and Automation, 2007 IEEE International Conference on*, 2007, pp. 3132-3133.

[45] M. Girone, G. Burdea, M. Bouzit, V. Popescu, and J. E. Deutsch, "A stewart platform-based system for ankle telerehabilitation," *Autonomous Robots*, vol. 10, pp. 203-212, Mar 2001.

[46] J. E. Deutsch, J. Latonio, G. C. Burdea, and R. Boian, "Post-stroke rehabilitation with the Rutgers Ankle system: A case study," *Presence-Teleoperators and Virtual Environments,* vol. 10, pp. 416-430, Aug 2001.

[47] G. Q. Liu, J. L. Gao, H. Yue, X. J. Mang, G. D. Lu, and Ieee, "Design and kinematics simulation of parallel robots for ankle rehabilitation," Luoyang, PEOPLES R CHINA, 2006, pp. 1109-1113.

[48] J. Yoon, J. Ryu, and K. B. Lim, "Reconfigurable ankle rehabilitation robot for various exercises," *Journal of Robotic Systems,* vol. 22, pp. S15-S33, 2006.

[49] H. I. Krebs, N. Hogan, B. T. Volpe, M. L. Aisen, L. Edelstein, and C. Diels, "Overview of clinical trials with MIT-MANUS: A robot-aided neuro- rehabilitation facility," *Technology and Health Care,* vol. 7, pp. 419-423, 1999.

[50] S. E. Fasoli, H. I. Krebs, J. Stein, W. R. Frontera, and N. Hogan, "Effects of robotic therapy on motor impairment and recovery in chronic stroke," *Archives of Physical Medicine and Rehabilitation,* vol. 84, pp. 477-482, Apr 2003.

[51] M. Ferraro, J. J. Palazzolo, J. Krol, H. I. Krebs, N. Hogan, and B. T. Volpe, "Robot-aided sensorimotor arm training improves outcome in patients with chronic stroke," *Neurology,* vol. 61, pp. 1604-1607, Dec 2003.

[52] L. R. MacClellan, D. D. Bradham, J. Whitall, B. Volpe, P. D. Wilson, J. Ohlhoff, *et al.,* "Robotic upper-limb neurorehabilitation in chronic stroke patients," *Journal of Rehabilitation Research and Development,* vol. 42, pp. 717-722, Nov-Dec 2005.

[53] S. Mazzoleni, L. Buono, P. Dario, and F. Posteraro, "Upper limb robot-assisted therapy in subacute and chronic stroke patients: Preliminary results on initial exposure based on kinematic measures," in *Biomedical Robotics and Biomechatronics (2014 5th IEEE RAS & EMBS International Conference on*, 2014, pp. 265-269.

[54] S. Mazzoleni, M. Filippi, M. C. Carrozza, F. Posteraro, L. Puzzolante, and E. Falchi, "Robot-aided therapy on the upper limb of subacute and chronic stroke patients: A biomechanical approach," in *Rehabilitation Robotics (ICORR), 2011 IEEE International Conference on*, 2011, pp. 1-6.

[55] P. S. Lum, C. G. Burgar, M. Van der Loos, P. C. Shor, M. Majmundar, and R. Yap, "MIME robotic device for upper-limb neurorehabilitation in subacute stroke subjects: A follow-up study," *Journal of Rehabilitation Research and Development,* vol. 43, pp. 631-642, Aug-Sep 2006.

[56] P. S. Lum, C. G. Burgar, P. C. Shor, M. Majmundar, and M. Van der Loos, "Robot-assisted movement training compared with conventional therapy techniques for the

rehabilitation of upper-limb motor function after stroke," *Archives of Physical Medicine and Rehabilitation,* vol. 83, pp. 952-959, 2002.

[57] P. S. Lum, C. G. Burgar, and P. C. Shor, "Evidence for improved muscle activation patterns after retraining of reaching movements with the MIME robotic system in subjects with post-stroke hemiparesis," *IEEE Transactions on Neural Systems and Rehabilitation Engineering,* vol. 12, pp. 186-194, Jun 2004.

[58] C. G. Burgar, P. S. Lum, A. M. E. Scremin, S. L. Garber, H. F. M. Van der Loos, D. Kenney, *et al.*, "Robot-assisted upper-limb therapy in acute rehabilitation setting following stroke: Department of Veterans Affairs multisite clinical trial," *Journal of Rehabilitation Research and Development,* vol. 48, pp. 445-458, 2011 2011.

[59] G. N. Lewis and E. J. Perreault, "An Assessment of Robot-Assisted Bimanual Movements on Upper Limb Motor Coordination Following Stroke," *Neural Systems and Rehabilitation Engineering, IEEE Transactions on,* vol. 17, pp. 595-604, 2009.

[60] J. J. Summers, F. A. Kagerer, M. I. Garry, C. Y. Hiraga, A. Loftus, and J. H. Cauraugh, "Bilateral and unilateral movement training on upper limb function in chronic stroke patients: A TMS study," *Journal of the Neurological Sciences,* vol. 252, pp. 76-82, 2007.

[61] M. H. Mudie and T. A. Matyas, "Can simultaneous bilateral movement involve the undamaged hemisphere in reconstruction of neural networks damaged by stroke?," *Disability and Rehabilitation,* vol. 22, pp. 23-37, Jan 2000.

[62] S. McCombe Waller and J. Whitall, "Fine motor control in adults with and without chronic hemiparesis: baseline comparison to nondisabled adults and effects of bilateral arm training," *Archives of Physical Medicine and Rehabilitation,* vol. 85, pp. 1076-1083, 2004.

[63] C. M. Stinear, P. A. Barber, J. P. Coxon, M. K. Fleming, and W. D. Byblow, "Priming the motor system enhances the effects of upper limb therapy in chronic stroke," *Brain,* vol. 131, pp. 1381-1390, May 2008.

[64] J. Whitall, S. M. Waller, K. H. C. Silver, and R. F. Macko, "Repetitive bilateral arm training with rhythmic auditory cueing improves motor function in chronic hemiparetic stroke," *Stroke,* vol. 31, pp. 2390-2395, Oct 2000.

[65] S. Hesse, G. Schulte-Tigges, M. Konrad, A. Bardeleben, and C. Werner, "Robot-assisted arm trainer for the passive and active practice of bilateral forearm and wrist movements in hemiparetic subjects," *Archives of Physical Medicine and Rehabilitation,* vol. 84, pp. 915-920, 2003.

[66] L. E. Kahn, P. S. Lum, W. Z. Rymer, and D. J. Reinkensmeyer, "Robot-assisted movement training for the stroke-impaired arm: Does it matter what the robot does?," *Journal of Rehabilitation Research and Development,* vol. 43, pp. 619-629, Aug-Sep 2006.

[67] S. Coote and E. K. Stokes, "Effect of robot-mediated therapy on upper extremity dysfunction post-stroke - a single case study," *Physiotherapy,* vol. 91, pp. 250-256, 2005.

[68] G. Rosati, P. Gallina, and S. Masiero, "Design, Implementation and Clinical Tests of a Wire-Based Robot for Neurorehabilitation," *IEEE Transactions on Neural Systems and Rehabilitation Engineering,* vol. 15, pp. 560-569, 2007.

[69] A. Toth, G. Fazekas, G. Arz, M. Jurak, and M. Horvath, "Passive robotic movement therapy of the spastic hemiparetic arm with REHAROB: Report of the first clinical test and the follow-up system improvement," *2005 Ieee 9th International Conference on Rehabilitation Robotics,* pp. 127-130, 2005.

[70] T. Nef and R. Riener, "ARMin - Design of a novel arm rehabilitation robot," *2005 Ieee 9th International Conference on Rehabilitation Robotics,* pp. 57-60, 2005.

[71] A. J. Doornebosch, H. J. M. Cools, M. E. C. Slee-Turkenburg, M. G. van Elk, and M. Schoone-Harmsen, "Robot-mediated ACtive REhabilitation (ACRE2) for the hemiplegic upper limb after a stroke: A pilot study," *Technology & Disability*, vol. 19, pp. 199-203, 2007.

[72] M. Avraam, M. Horodinca, P. Letier, and A. Preumont, "Portable smart wrist rehabilitation device driven by rotational MR-fluid brake actuator for telemedecine applications," in *Intelligent Robots and Systems, 2008. IROS 2008. IEEE/RSJ International Conference on*, 2008, pp. 1441-1446.

[73] Y. L. Fu, P. Wang, S. G. Wang, H. S. Liu, and F. X. Zhang, "Design and development of a portable exoskeleton based CPM machine for rehabilitation of hand injuries," *2007 Ieee International Conference on Robotics and Biomimetics, Vols 1-5*, pp. 1476-1481, 2007.

[74] J. Rosen, J. C. Perry, N. Manning, S. Burns, and B. Hannaford, "The human arm kinematics and dynamics during daily activities - Toward a 7 DOF upper limb powered exoskeleton," *2005 12th International Conference on Advanced Robotics,* pp. 532-539, 2005.

[75] J. C. Perry, J. Rosen, and S. Bums, "Upper-limb powered exoskeleton design," *Ieee-Asme Transactions on Mechatronics,* vol. 12, pp. 408-417, 2007.

[76] E. E. Cavallaro, J. Rosen, J. C. Perry, and S. Burns, "Real-time myoprocessors for a neural controlled powered exoskeleton arm," *IEEE Transactions on Biomedical Engineering*, vol. 53, pp. 2387-2396, 2006.

[77] P. Deegan, B. J. Thibodeau, and R. Grupen, "Designing a self-stabilizing robot for dynamic mobile manipulation," DTIC Document2006.

[78] J. Hee-Tae, J. Baird, C. Yu-Kyong, and R. A. Grupen, "Upper-limb exercises for stroke patients through the direct engagement of an embodied agent," in *Human-Robot Interaction (HRI), 2011 6th ACM/IEEE International Conference on*, 2011, pp. 157-158.

[79] J. Hee-Tae, J. Baird, C. Yu-Kyong, and R. A. Grupen, "Upper extremity physical therapy for stroke patients using a general purpose robot," in *RO-MAN, 2011 IEEE*, 2011, pp. 270-275.

[80] J. C. Perry, J. Rosen, and S. Burns, "Upper-Limb Powered Exoskeleton Design," *Mechatronics, IEEE/ASME Transactions on*, vol. 12, pp. 408-417, 2007.

[81] J. C. Perry and J. Rosen, "Design of a 7 Degree-of-Freedom Upper-Limb Powered Exoskeleton," in *Biomedical Robotics and Biomechatronics, 2006. BioRob 2006. The First IEEE/RAS-EMBS International Conference on*, 2006, pp. 805-810.

[82] M. Simkins, H. Kim, G. Abrams, N. Byl, and J. Rosen, "Robotic unilateral and bilateral upper-limb movement training for stroke survivors afflicted by chronic hemiparesis," *IEEE ... International Conference on Rehabilitation Robotics : [proceedings]*, vol. 2013, p. 6650506, 2013 2013.

[83] G. Narang, A. Narang, S. Singh, and J. Lempiainen, "Use of unobtrusive human-machine interface for rehabilitation of stroke victims through robot assisted mirror therapy," in *Technologies for Practical Robot Applications (TePRA), 2013 IEEE International Conference on*, 2013, pp. 1-6.

[84] M. Shahbazi, S. F. Atashzar, and R. V. Patel, "A framework for supervised robotics-assisted mirror rehabilitation therapy," in *Intelligent Robots and Systems (IROS 2014), 2014 IEEE/RSJ International Conference on*, 2014, pp. 3567-3572.

[85] V. S. Ramachandran and E. L. Altschuler, "The use of visual feedback, in particular mirror visual feedback, in restoring brain function," *Brain*, vol. 132, pp. 1693-1710, Jul 2009.

[86] K. Funase, T. Tabira, T. Higashi, N. Liang, and T. Kasai, "Increased corticospinal excitability during direct observation of self-movement and indirect observation with a mirror box," *Neuroscience Letters*, vol. 419, pp. 108-112, May 2007.

[87] K. Sathian, A. I. Greenspan, and S. L. Wolf, "Doing it with mirrors: A case study of a novel approach to neurorehabilitation," *Neurorehabilitation and Neural Repair*, vol. 14, pp. 73-76, 2000.

[88] E. L. Altschuler, S. B. Wisdom, L. Stone, C. Foster, D. Galasko, D. M. E. Llewellyn, *et al.*, "Rehabilitation of hemiparesis after stroke with a mirror," *Lancet*, vol. 353, pp. 2035-2036, Jun 1999.

[89] J. A. Stevens and M. E. P. Stoykov, "Simulation of Bilateral Movement Training Through Mirror Reflection: A Case Report Demonstrating an Occupational Therapy Technique for Hemiparesis," *Topics in Stroke Rehabilitation*, vol. 11, pp. 59-66, 2004.

[90] J. A. Stevens and M. E. P. Stoykov, "Using motor imagery in the rehabilitation of hemiparesis," *Archives of Physical Medicine and Rehabilitation*, vol. 84, pp. 1090-1092, Jul 2003.

[91] S. Sutbeyaz, G. Yavuzer, N. Sezer, and B. F. Koseoglu, "Mirror therapy enhances lower-extremity motor recovery and motor functioning after stroke: A randomized controlled trial," *Archives of Physical Medicine and Rehabilitation*, vol. 88, pp. 555-559, May 2007.

[92] G. Yavuzer, R. Selles, N. Sezer, S. Sutbeyaz, J. B. Bussmann, F. Koseoglu, *et al.*, "Mirror therapy improves hand function in subacute stroke: A randomized controlled trial," *Archives of Physical Medicine and Rehabilitation*, vol. 89, pp. 393-398, Mar 2008.

[93] C. D. Murray, E. Patchick, S. Pettifer, F. Caillette, and T. Howard, "Immersive virtual reality as a rehabilitative technology for phantom limb experience: A protocol," *Cyberpsychology & Behavior*, vol. 9, pp. 167-170, Apr 2006.

[94] K. Eng, E. Siekierka, P. Pyk, E. Chevrier, Y. Hauser, M. Cameirao, *et al.*, "Interactive visuo-motor therapy system for stroke rehabilitation," *Medical & Biological Engineering & Computing*, vol. 45, pp. 901-907, Sep 2007.

[95] M. Palmke, H. von Piekartz, C. Zalpour, T. Schuler, and K. Morisse, "A new perspective for Virtual Mirror Therapy Developing a low-cost-high-convenient environment utilising the Wiimote," in *Virtual Rehabilitation International Conference, 2009*, 2009, pp. 197-197.

[96] K. Matthys, M. Smits, J. N. Van der Geest, A. Van der Lugt, R. Seurinck, H. J. Stam, *et al.*, "Mirror-Induced Visual Illusion of Hand Movements: A Functional Magnetic

Resonance Imaging Study," *Archives of Physical Medicine and Rehabilitation*, vol. 90, pp. 675-681, Apr 2009.

[97] X. Yang, X. Wu, Z. Zhao, and Y. Li, "Hand tele-rehabilitation in haptic virtual environment," in *2007 IEEE International Conference on Robotics and Biomimetics, ROBIO*, Yalong Bay, Sanya, 2008, pp. 145-149.

[98] U. Dreifaldt, D. Goude, and M. Rydmark, "A home-based virtual reality system for stroke rehabilitation," *2007 Virtual Rehabilitation*, pp. 87-87, 2007.

[99] A. S. Merians, E. Tunik, G. G. Fluet, Q. Qiu, and S. V. Adamovich, "Innovative approaches to the rehabilitation of upper extremity hemiparesis using virtual environments," *European Journal of Physical and Rehabilitation Medicine*, vol. 45, pp. 123-133, Mar 2009.

[100] K. Eng, E. Siekierka, P. Pyk, E. Chevrier, Y. Hauser, M. Cameirao, *et al.*, "Interactive visuo-motor therapy system for stroke rehabilitation," *Medical & Biological Engineering & Computing*, vol. 45, pp. 901-907, Sep 2007.

[101] U. Feintuch, M. Tuchner, A. Lorber-Haddad, Z. Meiner, and S. Shiri, "VirHab - A virtual reality system for treatment of chronic pain and disability," in *Virtual Rehabilitation International Conference, 2009*, 2009, pp. 83-86.

[102] S. H. You, S. H. Jang, Y. H. Kim, Y. H. Kwon, I. Barrow, and M. Hallett, "Cortical reorganization induced by virtual reality therapy in a child with hemiparetic cerebral palsy," *Developmental Medicine and Child Neurology*, vol. 47, pp. 628-635, Sep 2005.

[103] W. Huapeng, L. Junhong, H. Handroos, B. Miraftabi, A. Heinonen, S. Peurala, *et al.*, "Virtual reality based robotic therapy for stroke rehabilitation: An initial study," in *Mechatronics and Automation (ICMA), 2011 International Conference on*, 2011, pp. 1196-1200.

[104] F. Nocchi, S. Gazzellini, C. Grisolia, M. Petrarca, V. Cannata, P. Cappa, *et al.*, "Brain network involved in visual processing of movement stimuli used in upper limb robotic training: an fMRI study," *Journal of Neuroengineering and Rehabilitation*, vol. 9, p. 12, Jul 2012.

[105] R. Kikuuwe, T. Yamamoto, and H. Fujimoto, "A Guideline for Low-Force Robotic Guidance for Enhancing Human Performance of Positioning and Trajectory Tracking: It Should Be Stiff and Appropriately Slow," *Systems, Man and Cybernetics, Part A: Systems and Humans, IEEE Transactions on*, vol. 38, pp. 945-957, 2008.

[106] G. T. Desmoulin and G. S. Anderson, "Method to investigate contusion mechanics in living humans," *Journal of Forensic Biomechanics,* vol. 2, pp. 1-10, 2011.

[107] K. R. Nash and D. J. Sheridan, "Can one accurately date a bruise? State of the science," *Journal of Forensic Nursing,* vol. 5, pp. 31-37, 2009.

[108] C. E. Clauser, J. T. McConville, and J. W. Young, "WEIGHT VOLUME AND CENTER OF MASS OF SEGMENTS OF THE HUMAN BODY," *U S Air Force Technical Documentary Report AMRL-TDR,* vol. 69, pp. 1-101, 1969 1969.

[109] R. J. van Beers, A. C. Sittig, and J. J. van der Gon Denier, "How humans combine simultaneous proprioceptive and visual position information," *Experimental Brain Research,* vol. 111, pp. 253-261, 1996.

[110] R. Maini and H. Aggarwal, "Study and comparison of various image edge detection techniques," *International Journal of Image Processing (IJIP),* vol. 3, pp. 1-11, 2009.

[111] J. J. Craig, "Introduction to Robotics," 2005.

[112] S. Kucuk and Z. Bingul, "The inverse kinematics solutions of industrial robot manipulators," in *Mechatronics, 2004. ICM '04. Proceedings of the IEEE International Conference on*, 2004, pp. 274-279.

[113] P. Corke, "A robotics toolbox for MATLAB," *Robotics & Automation Magazine, IEEE,* vol. 3, pp. 24-32, 1996.

[114] R. K. Y. Tong, W. W. F. Leung, X. L. Hu, and R. Song, "Interactive robot-assisted training system using continuous EMG signals for stroke rehabilitation," presented at the Proceedings of the 3rd International Convention on Rehabilitation Engineering \& Assistive Technology, Singapore, 2009.

[115] D. A. Gabriel, "Shoulder and elbow muscle activity in goal-directed arm movements," *Experimental Brain Research,* vol. 116, pp. 359-366, Sep 1997.

[116] A. Albu-Schaffer, C. Ott, U. Frese, and G. Hirzinger, "Cartesian impedance control of redundant robots: recent results with the DLR-light-weight-arms," in *Robotics and Automation, 2003. Proceedings. ICRA '03. IEEE International Conference on*, 2003, pp. 3704-3709 vol.3.

[117] D. J. Braun and M. Goldfarb, "A Control Approach for Actuated Dynamic Walking in Biped Robots," *Robotics, IEEE Transactions on,* vol. 25, pp. 1292-1303, 2009.

Appendix A – Robot Selection

A range of robot suppliers were considered, who supply robot arms with suitable specifications for the project. Table A.1 shows the range of robot arms that were considered.

Manufacturer	Model	DOF	Payload	Reach	Powersupply	Unit Weight	Controller Weight
Kuka	KR5 sixx R650/850	6	5kg	650/850mm	3x400V, 50-60Hz	28kg/29kg	185kg (without transformer)
ABB	IRB120	6	3kg	580mm	1x220/230V, 50-60Hz	25kg	27.5kg (panel mount)
ABB	IRB140	6	6kg	810mm	1x220/230V, 50-60Hz	98kg	27.5kg (panel mount)
Fanuc	LR Mate 200iC	6	5kg	704/892mm	1x200/230V, 50-60Hz	27kg/29kg	55kg
Kawasaki	FS03N	6	3kg	700mm	1x200-240V, 50-60Hz	20kg	45kg (with transformer)
Kawasaki	FS06N	6	6kg	1002mm	3x440V, 50-60Hz	165kg	155kg
Motoman	HP5	6	5kg	701mm	3x240V, 50-60Hz	47kg	150-250kg
Motoman	MH5	6	5kg	706mm	3x240V, 50-60Hz	27kg	250kg
Nachi	VS05E	6	5kg	653mm	3x430V, 50-60Hz	28kg	165kg

Table A.1 - List of robot arms showing relevant selection specifications

As Table A.1 shows, there were a reasonable range of robot arms available on the market, however, the majority requiring 3-phase power. Converters from 3-phase to single phase power are available, and have been considered for use in this project. The availability of these converters made the power requirements of the robot less important, yet the inclusion of a power converter in the system is undesirable as it adds further complication in the setup of the system, and further cost.

These robots also meet the payload requirement, although the higher 5kg and 6kg units hold more risk of injury to the patient, and would require more consideration with regard to the safety of the patient. The unit weights of many of the robot arms are reasonable when considering transportation of the final system. However, the weight of the controller for the 3-phase units makes them unsuitable for this project.

When considering the range of motion, these units all have a reasonable reach, meeting, or exceeding the estimated 500mm requirement.

After all aspects were considered, the Fanuc LR Mate 200iC was the preferred choice, with the Kawasaki FS03N and ABB IRB120 both viable options. Both new and used units were considered for purchase; so price and availability were checked for both new and used units of all three viable robots. Used units had a major draw-back in availability, as the requirements for this project were unusual when compared to industrial applications, especially in regard to the power requirements. Price comparisons of the various options are shown in Tables A.2 and A.3.

New Robot Prices						
Manufacturer	Model	Controller	Freight	Quoted Price		Price Approx (NZD)
ABB	IRB120	IRC5 Compact		30,000	NZD	$30,000
Fanuc	LR Mate 200iC	R-30iA Mate	Included	37,862	AUD	$47,480
Fanuc	LR Mate 200iC5L	R-30iA Mate	Included	41,367	AUD	$51,875
Fanuc	LR Mate 200iC5L c/w FS-10iA	R-30iA Mate	Included	54,746	AUD	$68,653
Kawasaki	FS03N	D76	Ex Works - JMP	54,700	NZD	$54,700

Table A.2 - List of price for new units

Used Robot Prices						
Manufacturer	Model	Controller	Freight	Quoted Price		Price Approx (NZD)
Fanuc	LR Mate 200iB	R-J3iB Mate	Not included	16,900	USD	$22,790
Fanuc	LR Mate 200i	Rj3 Mate	Not included	9,000	EUR	$17,650

Table A.3 - List of prices for used units

As explained previously, tables A.2 and A.3 show the price and availability of the suitable units and the lack of availability of used units, with the used Fanuc robots listed including an older, heavier 3-phase controller. When the budget requirements of the project were taken into consideration, the ABB IRB120 was selected.

Appendix B – Participant Questionnaires

MASSEY UNIVERSITY
COLLEGE OF SCIENCES
TE WĀHANGA PŪTAIAO

An Integrated Robotic and Virtual Mirror Therapy System for Stroke Rehabilitation

PARTICIPANT QUESTIONNAIRE

Please rate the comfort of the rehabilitation system

Uncomfortable — Comfortable

1 2 (3) 4 5

Please rate the comfort of the exercise process of the rehabilitation system

Uncomfortable — Comfortable

1 2 (3) 4 5

Please rate your confidence in the safety of the rehabilitation system

Not confident — Very confident

1 2 (3) 4 5

How suitable do you feel this rehabilitation system is for use with stroke patients?

Not suitable — Very suitable

1 2 3 (4) 5

Please give feedback on your experience of the rehabilitation system (use reverse side if necessary).

Need to minimise sudden movement of the robot arm.

Page 1 of 1

Te Kunenga ki Pūrehuroa
School of Engineering and Advanced Technology
Private Bag 102904, North Shore City 0745, Auckland, New Zealand T +64 9 443 9734 F +64 9 443 9774 www.massey.ac.nz

MASSEY UNIVERSITY
COLLEGE OF SCIENCES
TE WĀHANGA PŪTAIAO

An Integrated Robotic and Virtual Mirror Therapy System for Stroke Rehabilitation

PARTICIPANT QUESTIONNAIRE

Please rate the comfort of the rehabilitation system

Uncomfortable				Comfortable
1	2	3	(4)	5

Please rate the comfort of the exercise process of the rehabilitation system

Uncomfortable				Comfortable
1	2	(3)	4	5

Please rate your confidence in the safety of the rehabilitation system

Not confident				Very confident
1	2	3	(4)	5

How suitable do you feel this rehabilitation system is for use with stroke patients?

Not suitable				Very suitable
1	(2)	3	4	5

Please give feedback on your experience of the rehabilitation system (use reverse side if necessary).

I am a doctor at Auckland Hospital, I have dealt with stroke patients & have been involved in their rehabilitation. This system has the potential to be of huge benefit to the patients, however it is ~~not~~ in its initial stages in my opinion. The movements are not yet precise enough & smooth enough to gain patient confidence. The machine does pull & push the arm quite forcefully & is scary to begin with. I trust the safety cut off systems in place & they worked which was reassuring. All this system needs, in my opinion prior to testing on stroke patients, is fine tuning the movements so that they are smoother & less forceful.

F.T.O.

Te Kunenga ki Pūrehuroa
School of Engineering and Advanced Technology
Private Bag 102904, North Shore City 0745, Auckland, New Zealand T +64 9 443 9734 F +64 9 443 9774 www.massey.ac.nz

I think that stroke patients would greatly benefit from this technology in future as it will retrain neuronal pathways through mirror therapy.

MASSEY UNIVERSITY
COLLEGE OF SCIENCES
TE WĀHANGA PŪTAIAO

An Integrated Robotic and Virtual Mirror Therapy System for Stroke Rehabilitation

PARTICIPANT QUESTIONNAIRE

Please rate the comfort of the rehabilitation system

Uncomfortable — Comfortable

1 2 (3) 4 5

Please rate the comfort of the exercise process of the rehabilitation system

Uncomfortable — Comfortable

1 2 (3) 4 5

Please rate your confidence in the safety of the rehabilitation system

Not confident — Very confident

1 (2) 3 4 5

How suitable do you feel this rehabilitation system is for use with stroke patients?

Not suitable — Very suitable

(1) 2 3 4 5

Please give feedback on your experience of the rehabilitation system (use reverse side if necessary).

Was worried that the robotic arm would be quite violent, which it wasn't. Although it was very jerky. Good to see there are safety features and that they work, although it was alarming when the arm detached itself with my arm strapped in it. Overall a much less daunting experience than I thought it would be.

Te Kunenga ki Pūrehuroa
School of Engineering and Advanced Technology
Private Bag 102904, North Shore City 0745, Auckland, New Zealand T +64 9 443 9734 F +64 9 443 9774 www.massey.ac.nz

MASSEY UNIVERSITY
COLLEGE OF SCIENCES
TE WĀHANGA PŪTAIAO

An Integrated Robotic and Virtual Mirror Therapy System for Stroke Rehabilitation

PARTICIPANT QUESTIONNAIRE

Please rate the comfort of the rehabilitation system

Uncomfortable — Comfortable

1 2 (3) 4 5

Please rate the comfort of the exercise process of the rehabilitation system

Uncomfortable — Comfortable

1 2 3 (4) 5

Please rate your confidence in the safety of the rehabilitation system

Not confident — Very confident

1 2 3 (4) 5

How suitable do you feel this rehabilitation system is for use with stroke patients?

Not suitable — Very suitable

1 2 (3)—(4) 5

Please give feedback on your experience of the rehabilitation system (use reverse side if necessary).

Can see potential, still a little hiccuppy (movements are not smooth enough for stroke patients yet). Have done research into mirror therapy in the past so understand the concept and its use as a rehabilitation tool but in practice the current machine needs work.

Te Kunenga ki Pūrehuroa
School of Engineering and Advanced Technology
Private Bag 102904, North Shore City 0745, Auckland, New Zealand T +64 9 443 9734 F +64 9 443 9774 www.massey.ac.nz

~~[illegible]~~

Once the machines movements are more fluid, there are a number of rehabilitation opportunities outside of just walking with stroke sufferers.

The bubbles that you are trying to pop should be a little smaller as the robot was popping the bubbles without actually moving.

~~Possibly~~

The issues in ~~[illegible]~~ the fluidness of the movements could be improved through a better designed robot, one that is capable of the finer movements that I suspect the robot used in the trial is not.

MASSEY UNIVERSITY
COLLEGE OF SCIENCES
TE WĀHANGA PŪTAIAO

An Integrated Robotic and Virtual Mirror Therapy System for Stroke Rehabilitation

PARTICIPANT QUESTIONNAIRE

Please rate the comfort of the rehabilitation system

Uncomfortable				Comfortable
1	2	3	(4)	5

Please rate the comfort of the exercise process of the rehabilitation system

Uncomfortable				Comfortable
1	2	3	(4)	5

Please rate your confidence in the safety of the rehabilitation system

Not confident				Very confident
1	2	3	4	(5)

How suitable do you feel this rehabilitation system is for use with stroke patients?

Not suitable				Very suitable
1	(2)	3	4	5

Please give feedback on your experience of the rehabilitation system (use reverse side if necessary).

Very cool I worry it will scare old people. the movements are a touch fast. latency is good and after a minute I was confident in the machine.

Te Kunenga ki Pūrehuroa
School of Engineering and Advanced Technology
Private Bag 102904, North Shore City 0745, Auckland, New Zealand T +64 9 443 9734 F +64 9 443 9774 www.massey.ac.nz

MASSEY UNIVERSITY
COLLEGE OF SCIENCES
TE WĀHANGA PŪTAIAO

An Integrated Robotic and Virtual Mirror Therapy System for Stroke Rehabilitation

PARTICIPANT QUESTIONNAIRE

Please rate the comfort of the rehabilitation system

Uncomfortable — Comfortable

1 2 (3) 4 5

Please rate the comfort of the exercise process of the rehabilitation system

Uncomfortable — Comfortable

1 2 (3) 4 5

Please rate your confidence in the safety of the rehabilitation system

Not confident — Very confident

1 2 3 (4) 5

How suitable do you feel this rehabilitation system is for use with stroke patients?

Not suitable — Very suitable

1 (2) 3 4 5

Please give feedback on your experience of the rehabilitation system (use reverse side if necessary).

Still needs refining of system - can see how this will benefit future rehabilitation of stroke patients.

Te Kunenga ki Pūrehuroa
School of Engineering and Advanced Technology
Private Bag 102904, North Shore City 0745, Auckland, New Zealand T +64 9 443 9734 F +64 9 443 9774 www.massey.ac.nz

Appendix C – Ethics Approval

MASSEY UNIVERSITY
TE KUNENGA KI PUREHUROA

20 March 2015

Iain Emerson
SEAT
ALBANY

Dear Iain

Re: HEC: Southern A Application – 15/06
An integrated robotic and virtual mirror therapy system for stroke rehabilitation

Thank you for your letter dated 20 March 2015.

On behalf of the Massey University Human Ethics Committee: Southern A I am pleased to advise you that the ethics of your application are now approved. Approval is for three years. If this project has not been completed within three years from the date of this letter, reapproval must be requested.

If the nature, content, location, procedures or personnel of your approved application change, please advise the Secretary of the Committee.

Yours sincerely

Mr Jeremy Hubbard, Acting Chair
Massey University Human Ethics Committee: Southern A

cc Professor Subhas Mukhopadhyay
SEAT
PN321

Prof Don Cleland, HoS
SEAT
PN456